# Localisation of Theiler's Murine Encephalomyelitis Virus non-structural proteins 2B, 2C, 2BC and 3A in BHK-21 cells, and the effect of amino acid substitutions in 2C on localisation and virus replication

**Thesis submitted in fulfilment of the requirements for the degree**

**Masters of Science (MSc)**

**At**

**Rhodes University**

**by**

**Lindsay Murray**

**November 2006**

# i Abstract

The picornavirus family includes significant human and animal viruses such as poliovirus (PV), human rhinovirus (HRV) and foot-and-mouth-disease virus (FMDV). Current disease treatment and control strategies are limited by an incomplete understanding of the interactions between the non-structural, replicative picornavirus proteins and host cell components. To investigate these interactions, Theiler's murine encephalomyelitis virus (TMEV) 2B, 2C, 2BC and 3A proteins were transiently expressed in BHK-21 cells and detected by indirect immunostaining and laser-scanning or epifluorescence microscopy. The signal of the 2B protein overlapped with that of the ER marker protein, ERp60, as well as that of the peripheral Golgi marker protein, β-COP. The 2C protein overlapped with ERp60 in a faint reticular stain, and localised to large punctate structures that partially overlapped with β-COP at higher levels of expression. The 2BC protein located to large perinuclear structures that overlapped exclusively with β-COP. The TMEV 3A protein signal overlapped with both ERp60 and β-COP stains, in addition in cells expressing the 3A protein the ER appeared swollen and bulbous while the Golgi was dispersed in some cells. 2C and 2BC proteins with C-terminal deletions localised in the same manner as the wild type proteins indicating that the localisation signals that determine subcellular localisation of the proteins are within the N-terminal 60 amino acids of the 2C protein.

The significance of the high degree of conservation of the N-terminal domain of the 2C protein throughout the *Picornaviridae* was investigated through the introduction of amino acid substitution mutations at highly conserved residues in the N-terminal domain of 2C into the viral cDNA. Upon transfection of the viral RNA into BHK-21 cells, it was observed that substitution of amino acid residues 8, 18 and 29 abolished the ability of TMEV to induce cytopathic effect (CPE), while substitution of residues 4, 14 and 23 only attenuated the ability of TMEV to induce CPE.

To determine whether amino acid substitution mutations would affect the localisation of the 2C protein, 2C proteins with substitution mutations at amino acids 4, 8, 14, 18, 23 and 29 were transiently expressed in BHK-21 cells and detected by indirect immunostaining and examination by laser-scanning confocal and epifluorescence microscopy. The 2C mutant 4, 8 and 29 proteins showed slightly altered localisation patterns compared to the wild type

protein with a significant portion of the proteins localising in a perinuclear stain suggesting possible localisation to the nuclear envelop. The 2C mutant 14 and 18 proteins localised to a diffuse pattern in BHK-21 cells while the 2C mutant 23 protein located to small punctate structures that partially overlapped with the ERp60 stain but were completely separate from the β-COP stain.

Finally, a hydrophilic, antigenic region of the 2C protein was expressed in frame with an N-terminal GST tag and was successfully purified on a pilot-scale and detected by Western analysis. This 2C178 peptide will be used to generate antibodies against the 2C and 2BC proteins for use in future studies. This study has furthered our knowledge of the localisation of the picornavirus 2B, 2C, 2BC and 3A proteins in host cells and identified a possible link between this localisation and an ability of TMEV to replicate in BHK-21 cells.

**Declaration**

I, Lindsay Susan Murray, declare that this MSc dissertation is my own unaided work completed in fulfilment of the requirements for the degree Masters of Science at Rhodes University.

Signature: ..... Date: .....

# ii Table of contents

# iii List of Figures

**Figure 2.4.10.** Transient expression of TMEV 2C60 protein in BHK-21 cells stained with antibodies against a marker protein for the ER.

**Figure 2.4.11.** Transient expression of TMEV 2C60 protein in BHK-21 cells stained with antibodies against a marker protein for the Golgi apparatus.

**Figure 2.4.12.** Transient expression of TMEV 2BC60 protein in BHK-21 cells stained with antibodies against a marker protein for the ER.

**Figure 2.4.13.** Transient expression of TMEV 2BC60 protein in BHK-21 cells stained with antibodies against a marker protein for the Golgi apparatus.

**Figure 2.4.14.** Kyte and Doolittle hydrophobicity/ hydrophilicity plot of the amino acid sequence of the 326 amino acids of the TMEV strain GDVII 2C protein created by the Internet based software program ProtScale.

**Figure 2.4.15.** The coding sequence for the 2C178 peptide inserted into the bacterial expression vector pGEX-2T.

**Figure 2.4.16** Purification of GST-2C178 peptide and GST protein from *E. coli* BL-21 cell lysate.

**Figure 2.4.17** Autoradiograph of the immunodetection of the GST-2C178 fusion and GST peptides following SDS-PAGE and Western analysis of samples derived from the GST-specific affinity chromatography purification procedure performed on the cell lysate of pilot-scale *E. coli* BL-21 cultures.

**Figure 3.3.1.** Diagrammatic representation of the overlap PCR procedure used to engineer specific point mutations into the cDNA genome of TMEV.

**Figure 3.3.2.** Insertion of cDNA genomes of TMEV strain GDVII into the pBlueScript® II Phagemid vector subsequent to the creation of single amino acid substitution mutations in the 2C coding region by overlap PCR.

**Figure 3.4.1.** Multiple sequence alignment of the N-terminal amino acids of various picornavirus 2C proteins using Blastp internet-based software (NCBI, 2006).

**Figure 3.4.2** The development of CPE over time in BHK-21 cells infected with wild type or TME viruses obtained from the growth medium covering BHK-21 cells previously transfected with wild type or mutant TMEV RNA.

**Figure 3.4.3.** BHK-21 cells were transfected with *in vitro* transcribed RNA encoding the TMEV genome with substitution mutations at amino acids 4, 8, 14, 18, 23 or 29 on the 2C protein. RT-PCR was performed on the total RNA isolated from transfected cells.

**Figure 3.4.4.** Quantitative analysis of the effect of specific point mutations in the N-terminal domain of the 2C protein on the replication proficiency of TMEV.

**Figure 3.4.5.** Construction of recombinant vectors for the expression of mutant TMEV 2C coding regions in mammalian cells.

**Figure 3.5.6.** Subcellular localisation of TMEV mutant 4, 8 and 29 2C-V5 fusion proteins in BHK-21 cells.

**Figure 3.5.7.** Subcellular localisation of TMEV mutant 4, 8 and 29 2C-V5 fusion proteins in BHK-21 cells.

**Figure 3.5.8.** Subcellular localisation of TMEV mutant 14, 18 and 23 2C-V5 fusion proteins in BHK-21 cells.

**Figure 3.5.9.** Subcellular localisation of TMEV mutant 14, 18 and 23 2C-V5 fusion proteins in BHK-21 cells.

# iv List of Tables

# v List of Abbreviations

**Viruses:**

| | |
|---|---|
| HAV | Hepatitis A virus |
| HRV | Human rhinovirus |
| PV | Poliovirus |
| TMEV | Theiler's murine encephalomyelitis virus |
| FMDV | Foot-and-mouth disease virus |

**General acronyms:**

| | |
|---|---|
| ATP | Adenosine triphosphate |
| ATPase | Adenosine triphosphatase |
| BFA | Brefeldin A |
| BHK | Baby Hamster Kidney |
| BSA | Bovine serum albumin |
| CAP | Catabolite activator protein |
| CGN | *cis* Golgi network |
| CO2 | Carbon dioxide |
| CPE | Cytopathic effect |
| DAPI | 4,6-diamidino-2-phenylindole |
| DMEM | Dulbecco's modified eagles medium |
| DNA | Deoxyribonucleic acid |
| ER | Endoplasmic reticulum |
| FCS | Fetal calf serum |
| GST | Glutathione S-transferase |
| GTPase | Guanidine triphosphatase |
| h.p.i. | Hours post infection |
| IC | Intermediate compartment |
| IgG | Immunoglobulin |
| IPTG | Isopropyl-β-D-1-thiogalactopyranoside |
| IRES | Internal ribosome entry site |
| m.o.i. | Multiplicity of infection |
| MHC | Major histocompatibility complex |
| MCS | Multiple cloning site |
| mRNA | Messenger RNA |
| MS | Multiple sclerosis |
| NMR | Nuclear magnetic resonance |
| NTP | Nucleoside triphosphatase |
| ORF | Open reading frame |
| PBS | Phosphate-buffered saline |
| PCR | Polymerase chain reaction |
| POD | Peroxidase |
| Poly-A | Poly-adenosine |
| PSF | Penicillin/streptomycin/fungizone |
| RER | Rough endoplasmic reticulum |

| | |
|---|---|
| SDS-PAGE | Sodium dodecyl sulphate-polyacrylamide gel electrophoresis |
| SGC | Stacked Golgi cisternae |
| ssRNA | Single-stranded RNA |
| RNA | Ribonucleic acid |
| UTR | Untranslated region |
| UV | Ultra violet |

**General units and symbols:**

| | |
|---|---|
| % | percent |
| °C | degrees Celsius |
| α | Alpha |
| β | beta |
| bp | base pairs |
| $cm^3$ | cubic centimetres |
| $dH_2O$ | distilled water |
| $dddH_2O$ | triple distilled water |
| g | gram |
| kDa | kilo Daltons |
| kb | kilo base |
| l | litre |
| M | molar |
| mM | milli molar |
| mg | milligrams |
| ml | millilitres |
| mM | micromolar |
| nm | nano metres |
| nt | nucleotide |
| rpm | revolutions per minute |
| µg | micro grams |
| µl | micro Litres |
| V | volts |

# vi Acknowledgements

**My sincere thanks to the following people:**

- My supervisor, Dr Caroline Knox for her guidance, inspiration and support throughout the study.
- Professor Greg Blatch for his invaluable assistance and guidance during the writing of this dissertation.
- Professor Rosemary Dorrington for her steadfast support, guidance and inspirational teaching during my career at Rhodes University.
- Dr Graeme Bradley for his constant advice, support and creative problem solving throughout my postgraduate studies.
- Professor Edith Elliot in the Biochemistry Department at the University of Kwazulu-Natal for graciously granting me extensive time on the confocal microscope in Petermaritzburg.

**Many thanks to the following people for the kind donation of mammalian cell lines and various antibodies:**

- Dr A. Moore (University of Alabama, USA) for the BHK-21 cell line.
- Professor G Blatch (Rhodes University, South Africa) for the NIH-3T3 cell line.
- Professor R Hay, St Andrews University, UK) for the Cos-7 cell line
- Dr M Ryan (St Andrews University, UK) for the HeLa cell line.
- Dr P de Felipe (St Andrews University, UK) and Professor T. Wileman (University of East Anglia, UK) for their guidance, technical advice and the donation of the anti-Erp60 and anti-β-COP primary antibodies.

**I would like to express my gratitude to the following people for their technical and financial support:**

- Mrs Val Hodgson, Dr Vicki Longshaw and Ms Sheril Daniels for technical advice and support.
- The staff at the electron microscopy unit at the University of Kwazulu-Natal in Petermaritzburg for their endless hospitality and technical advice during my use of the confocal microscopy facility.
- Professor Botha of the Botany Department at Rhodes University for his assistance with imaging of cells using the using the Olympus BX-61 Epifluorescent Microscope.
- Mr John Gillam and Mr Anton Vorster for their tireless labouring to source funding for Zimbabweans and other foreign students in South Africa.
- The Andrew Mellon Foundation, Joint Research Council and National Research Foundation for funding.

# 1 Review of Literature

## 1.1 PICORNAVIRUSES: A GLOBAL BATTLE

The picornavirus family includes a significant number of highly virulent human and animal pathogens, notable examples being Poliovirus (PV), Human rhinoviruses (HRV) and Foot-and-mouth disease virus (FMDV). The diseases caused by these viruses have significant economical impact worldwide and consequently the picornavirus family is the most intensely studied of all the positive sense single-stranded RNA viruses. A brief description of some of the socio-economic consequences caused by picornavirus infections is given below.

As a prominent human pathogen and the cause of severe poliomyelitis worldwide, PV is the most studied virus picornavirus and is the prototypic member of the *Picornaviridae*. The severely disabling effects of poliomyelitis brought financial burden to developing countries during the 20h century leading to an aggressive vaccination program. By 2002 the occurrence of poliovirus infections had significantly decreased on a global scale (World Health Organisation, 2002). Recently however, reservoirs of PV infection have re-emerged in North West Africa.

Another significant human disease: the "common cold", is estimated to cause the loss of more working hours worldwide each year than any other single cause (US Department of Health, 2006). In the United States alone an estimated 1 billion cases of the common cold occur in the population each year (U.S. Department Of Health, 2006). Although symptoms of the common cold are known to be caused by more than 200 viruses, it is estimated that 30-35% of adult individuals diagnosed as suffering from the common cold have contracted an HRV infection (U.S. Department Of Health, 2006). To date no effective vaccine or cure has been developed against HRV infection. Although this can be largely attributed to the rapid antigenic drift observed with HRV (Savolainen *et al*, 2002), the lack of understanding of the picornavirus replication cycle on a molecular level must also be taken into account.

FMDV is a highly virulent and infectious pathogen that infects ruminant animals including domestic sheep and cattle. Despite international efforts to control the movement of cattle and sale of beef, outbreaks of this disease are still prominent in

sub-Saharan Africa and other parts of the world. If not rapidly brought under control such outbreaks can have disastrous effects. An outbreak of foot-and-mouth disease in Britain in 2001 severely damaged the British beef industry and created significant financial risks for the European agricultural community as a whole. A range of vaccines against FMDV are currently available but these are continuously challenged by the emergence of novel strains of FMDV and persistent infections in vaccinated and infected animals (Alexandersen *et al*, 2002).

In view of the substantial economic threat posed by various picornavirus infections, made more tangible by the rapid increase in global travel and trade in animal products, it is essential that more effective disease treatment and control strategies be developed. To this end, we propose that a more detailed understanding of the interactions formed between host cell components and picornavirus proteins will ultimately lead to the identification of possible drug targets for the treatment of picornavirus infections.

## 1.2 PICORNAVIRUS GENOME ORGANISATION AND REPLICATION STRATEGY

The *Picornaviridae* are highly diverse, comprising seven genera with over two hundred known serotypes that infect a wide range of mammalian hosts, including humans and livestock (Table 1.2.1).

**Table 1.2.1. The genera of the *Picornaviridae* (adapted from Bedard and Semler, 2004)**

| Genus | Example of member species | Clinical disease |
|---|---|---|
| Aphthovirus | Foot-and-mouth disease virus | Foot-and-mouth disease in ruminants |
| Cardiovirus | Theiler's murine encephalomyelitis virus | Mouse encephalomyelitis |
| Enteroviruses | Poliovirus | Poliomyelitis |
| Hepatoviruses | Hepatitis A virus | Liver disease |
| Parechoviruses | Human parechovirus | Chronic meningoencephalitis, neonatal carditis |
| Rhinoviruses | Human rhinoviruses | Common cold |
| Teschovirus | Porcine teschovirus | Teschen-Talfan neurological disease |

Picornaviruses possess a positive-sense single-stranded RNA (ssRNA) genome of 7.2 kb – 8.5 kb that encodes the viral proteins in a single open reading frame (ORF). Picornavirus genomes are characterised by a 5′ VPg and a 3′ poly-A tail (Reviewed in Bedard and Semler, 2004, Figure 1.2.1). The 5′ VPg is necessary for the initiation of viral RNA replication and it is thought that the 3′ poly-A tail lends stability to the viral RNA (Bedard and Semler, 2004).

Following the uncoating of the virus particle in the cytoplasm of an infected cell the VPg is cleaved from the viral genome by a cellular enzyme and the single open reading frame is translated as a polyprotein of 2100-2400 amino acids (reviewed in Bedard and Semler, 2004). The full-length polyprotein is not observed in infected cells as it undergoes co- and post-translational cleavage by virus-encoded proteinases,

$2A^{pro}$, $3C^{pro}$ and $3CD^{pro}$, to give a range of mature protein products and precursor polyproteins (Figure 1.2.1) which exist independently in infected cells (Harris *et al*, 1990; Wimmer *et al*, 1993; Ypma-Wong *et al*, 1998). Although the precise cleavage patterns do vary between picornaviruses the genome can be broadly divided into three regions: P1, P2 and P3 (Figure 1.2.1). P1 encodes the viral coat proteins while P2 and P3 encode the non-structural proteins involved in facilitating virus replication (Wimmer *et al*, 1993) through the modification of the intracellular environment, the assembly of the virus replication complex and the replication of viral RNA.

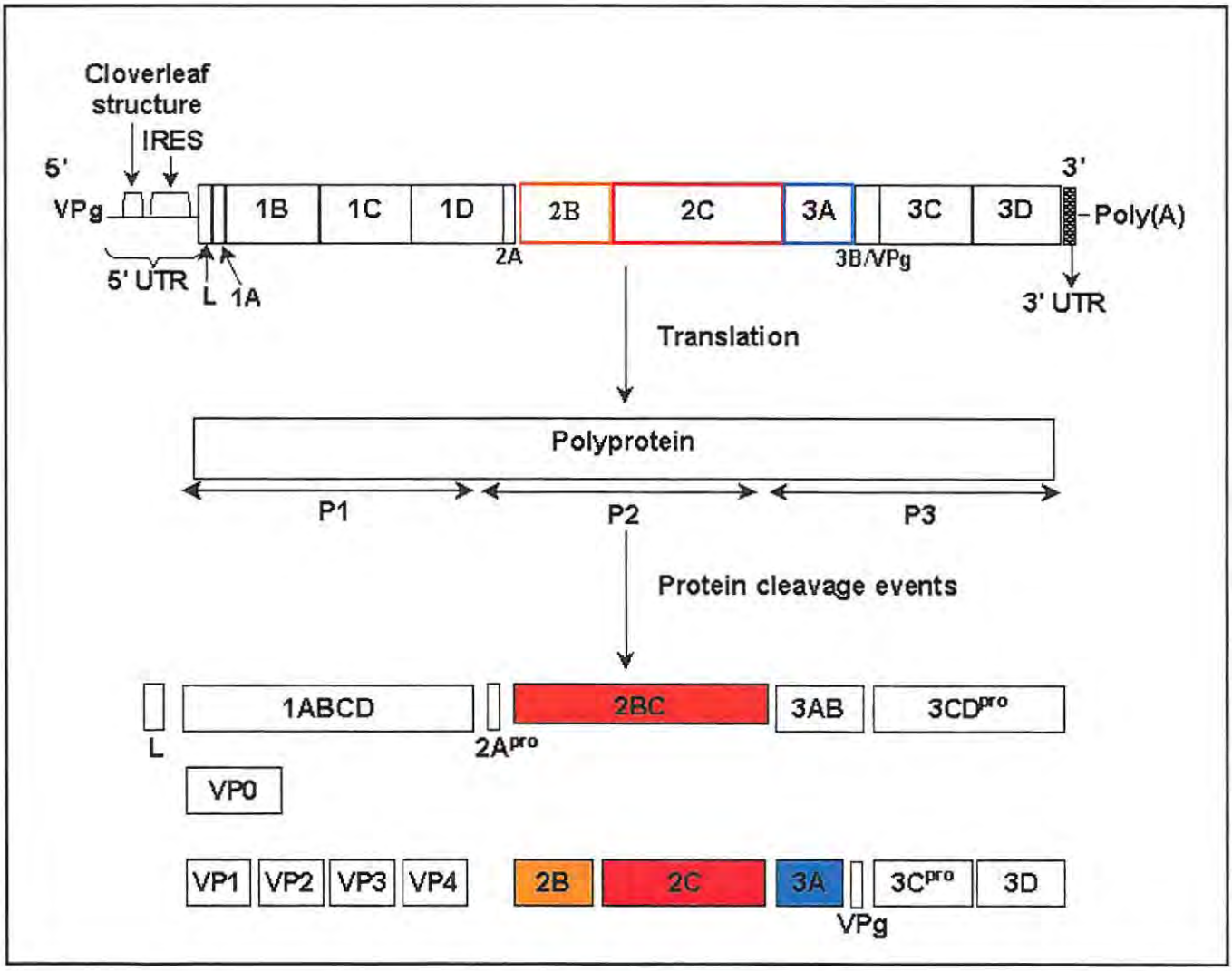


**Figure 1.2.1.** Schematic representation of PV genome organisation and protein expression. The single ORF is flanked by a 5' UTR comprising a cloverleaf structure and IRES, which mediate the initiation of CAP-independent translation, a 3' UTR and poly-A tail. The ORF is translated as a polyprotein that is co- and post-translationally cleaved to yielding four structural proteins (VP1-4) from the P1 domain, which are incorporated into nascent viral capsids, and numerous non-structural replicative proteins derived from the P2 and P3 domains (adapted from Bedard and Semler, 2004).

In addition to VPg, the 5′ terminus of the picornavirus genome is further characterised by an untranslated region (5′ UTR) that contains a cloverleaf structure required for positive-sense viral RNA replication (Andino *et al*, 1990) and an internal ribosome entry site (IRES) (Figure 1.2.1) that facilitates catabolite activator protein (CAP)-independent translation (Pelletier and Sonenberg, 1988). CAP-independent translation facilitates the translation of the viral genome while host translation is shut down during infection (Bedard and Semler, 2004). The 5′ cloverleaf structure forms a ribonucleoprotein complex with the viral protein $3CD^{pro}$ and a 36 kDa ribosome-associated cellular protein (Harris *et al*, 1994; Andino *et al,* 1993). The 3′ UTR is also known to associate with $3CD^{pro}$ as well as 3AB in the absence of other viral proteins and possesses a stem-loop structure that is required during RNA replication (Harris *et al*, 1994). However the precise role it plays during viral RNA replication is unknown (reviewed in Bedard and Semler, 2004). It is thought that 3AB may be the immediate precursor of VPg at the site of viral RNA replication (Giachetti and Semler, 1991).

Subsequent to virus protein translation and multiple cleavage events the virus replication complex is assembled and is the site of viral RNA replication. The positive-sense viral RNA of the infecting virion is used as a template for negative-sense RNA replication, mediated by the viral RNA-dependent RNA polymerase $3D^{pol}$ (Flanegan and Baltimore, 1977; Tuschall *et al*, 1982; Van Dyke and Flanegan, 1980; Van Dyke *et al*, 1982). The negative-sense viral RNA possesses a 3′ cloverleaf structure that is possibly anchored to the replication complex through binding of the vesicle-bound 2C protein (Banerjee *et al*, 1997; Banerjee and Dasgupta, 2001).

The negative-sense viral RNA is in turn used as a template for the production of nascent positive-sense RNA molecules that are translated to yield additional nascent viral proteins and are later incorporated into progeny virions (Barton and Flanegan, 1997). Nascent viral RNA synthesis occurs asymmetrically with far more positive strands being made than negative strands as the negative strands only serve as templates for positive strands, which are later incorporated into nascent virions (Barton and Flanegan, 1997).

Picornavirus capsids consist of 60 protomers, which each comprise one of each of the four polypeptides (VP1-4, Figure 1.2.1) encoded by the P1 region. The protomers are tightly packed in an icosahedral arrangement to form particles of 27-30nm in size (Internet 1). The genomic RNA is densely packed into the capsid together with sodium or potassium ions, which serve to stabilise the particle by counteracting the negative charge conferred by the phosphate groups on the genomic RNA (Internet 1).

Despite extensive investigation, the mechanisms of picornavirus RNA translation initiation and RNA replication and the cellular proteins involved in these events are not fully understood. This is a serious hindrance in the development of novel drug therapy strategies for the treatment of diseases caused by picornaviruses.

## 1.3 PICORNAVIRUS INFECTION: EFFECT ON HOST MEMBRANES

### 1.3.1 Effects on host cell ultrastructure by positive sense ssRNA virus infection

To date all investigated positive-sense ssRNA viruses are known to induce the modification of specific host cell membranes and the proliferation of membranous vesicles that support the virus replication complex, the site of viral RNA replication (Doedens and Kirkegaard, 1995; Aldabe and Carasco, 1995; Bienz *et al*, 1987; Bienz *et al*, 1990; Bienz *et al*, 1992; Cho *et al*, 1994; Schlegel *et al*, 1996; Mackenzie *et al*, 1999; Miller and Ahlquist, 2002). A variety of organelles are targeted by different viruses, with some viruses modifying the membranes of more than one organelle during the replication cycle (Schlegal *et al*, 1996; Rust *et al*, 2001). It is interesting to note that, unlike many enveloped viruses that also utilise host membranes, positive-sense ssRNA viruses lack a membranous envelope.

Some positive-sense ssRNA viruses target membranes of the secretory pathway, i.e. the Golgi apparatus (Doedens and Kirkegaard, 1995), intermediate compartment (IC) (Mackenzie *et al*, 1999), endoplasmic reticulum (ER) (Aldabe and Carasco, 1995; Bienz *et al*, 1987; Bienz *et al*, 1990; Bienz *et al*, 1992; Cho *et al*, 1994; Schlegel *et al*, 1996; Mackenzie *et al*, 1999), lysosomes and endosomes (Magliano *et al*, 1998),

while others have been shown to target the mitochondrial membrane (Miller and Ahlquist, 2002). Although extensive studies have been conducted on various viral proteins that localise to specific membranes, no conserved virus protein organelle-targeting sequences have been identified to date. However, a number of different mechanisms through which viral proteins interact with host cell membranes have been identified (Schmidt-Mende *et al*, 2001, Magliano *et al*, 1998, Mackenzie *et al*, 1999, Miller and Ahlquist, 2002).

### 1.3.2 Picornavirus infection: modification of host membranes

*(i) Picornavirus infection: targeting the secretory pathway*

During picornavirus infection non-structural proteins of the P2 and P3 genomic domains (Figure 1.2.1) target and modify membranes of the secretory pathway (Schlegel *et al*, 1996). However, the observed modifications to these membranes and the specific involvement of the different non-structural proteins vary between different viruses (Doedens *et al*, 1997; Neznanov *et al*, 2001; Moffat *et al*, 2005). This is not unexpected as non-structural proteins of different picornavirus proteins vary in size and sequence, indicating that while certain features of viral replication may be ubiquitous throughout the *Picornaviridae*, the interactions formed between the different viral proteins and host cell components may vary (Moffat *et al*, 2005).

Characteristic of infection by some picornaviruses, such as PV and FMDV, is the inhibition of anterograde protein trafficking in infected cells (Moffat *et al*, 2005; Doedens *et al*, 1997; Neznanov *et al*, 2001). Although it is possible that this phenomenon is of no consequence to viral replication and pathogenesis it has been suggested that in addition to providing membranes for the proliferation of virus-induced vesicles (Sandoval and Carasco, 1997), the modification of secretory pathway membranes may promote an evasion of the host immune response (Doedens and Kirkegaard, 1995; Dodd *et al*, 2001; Neznanov *et al*, 2001; Deitz *et al*, 2000). The host immune response to viral infections is in part reliant on the presentation of viral antigens on the surface of the infected cell by major histocompatibility complexes

(MHCs). Thus the inhibition of protein trafficking would block the transport of MHC class 1 to the cell surface (Doedens and Kirkegaard, 1995). Inhibition of protein secretion is not vital for viral replication as mutant polioviruses that do not inhibit ER-to-Golgi trafficking do not show inhibited replication ability in tissue culture (Dodd *et al*, 2001; Doedens *et al*, 1997).

Modified host membranes derived from the secretory pathway are incorporated into virus-induced vesicles prior to the assembly of the virus replication complex and the initiation of viral RNA replication (Sandoval and Carasco, 1997). The secretory pathway is a suitable target as it provides a rich supply of transport vesicle membranes to support viral replication (Sandoval and Carasco, 1997).

*(ii) Picornavirus infections: effects on membranes of the secretory pathway*

As the prototypic member of the *Picornaviridae*, PV is the most extensively investigated picornavirus with respect to virus-host membrane interactions. The origin of PV-induced membranous vesicles remains uncertain. Rust *et al* (2001) demonstrated that PV-induced vesicles are initially derived from COPII coated vesicles budding from the ER but later in infection they colocalise with Golgi marker proteins. An alternative study conducted by Schlegel *et al* (1996) showed that PV-induced vesicles contain ER, Golgi and lysosomal marker proteins thus demonstrating that the vesicles are in fact derived from membranous compartments throughout the secretory pathway. Schlegel *et al* (1996) suggested that the apparent ER origin and the double-membraned morphology of PV-induced vesicles indicated that they were of an autophagic origin. However, PV infection has been shown to induce increased lipid synthesis, thus signifying that a proportion of virus-induced vesicle membranes may be synthesised *de novo* (Guinea and Carrasco, 1990).

PV RNA replication is intricately linked to the vesiculation of host membranes as demonstrated by the localisation of viral RNA replication to the cytoplasmic surface of virus-induced double-membraned vesicles arranged in rosette-like configurations (Schlegel *et al*, 1996; Suhy *et al*, 2000; Bienz *et al*, 1992; Egger *et al*, 1996). Evidence supporting the dependency of PV replication on the virus-induced vesiculation of host cells includes the immunolocalisation of PV RNA replication to

the surface of the ER (Pfister *et al*, 1992; Troxler *et al*, 1992), the capacity of the PV 2C protein to bind viral RNA and membranes (Bienz *et al*, 1992, Bienz *et al*, 1994), the copurification of PV non-structural proteins 2B, 2C, 3A and 3AB with the vesicle rosettes (Bienz *et al*, 1994), the presence of ER and Golgi marker proteins in PV-induced vesicles (Schlegel *et al*, 1996) and the observation that the secretory pathway is disrupted in PV infected cells (Barco and Carasco, 1998; Deitz *et al*, 2000; Dodd *et al*, 2001; Doedens *et al*, 1997; Doedens and Kirkegaard, 1995; Neznanov *et al*, 2001; Sanz-Parra *et al*, 1998; van Kuppeveld *et al*, 1997).

Brefeldin A (BFA) acts as an inhibitor of ER-to-Golgi transport by blocking the formation of COPII coated vesicles (Fujiwara *et al*, 1988). The inhibition of PV replication by BFA further demonstrates the dependency of PV replication on the functioning membranes of the secretory pathway (Irurzun *et al*, 1992; Maynell *et al*, 1992). Additional evidence for the link between the secretory pathway and PV replication is provided by the inhibition of the characteristic disassembly of the Golgi complex during PV infection by Ro, a flavonoid compound that inhibits retrograde but not anterograde protein transport from the Golgi apparatus (Sandoval and Carasco, 1997).

In addition to the disassembly of the Golgi complex and the proliferation of membranous vesicles, cells infected with PV display an enlarged perinuclear space and swelling of the ER cisternae (Sandoval and Carasco, 1997; Bienz *et al*, 1987; Troxler *et al*, 1992). As PV infection progresses the coating normally situated at the sites of vesicle budding on ER cisternae becomes broadly distributed over the surface of the cisternae and the vesicles induced by PV infection are often associated with an electrodense membrane material (Bienz *et al*, 1987; Troxler *et al*, 1992). Both these features are indicative of an inhibition of protein transport (Sandoval and Carasco, 1997).

An accumulation of electrodense material is also observed in the lumen of the stacked Golgi cisternae (SGC) and adjacent vesicles prior to the disruption of the CGN and the dispersion of these elements throughout the cytosol as evidenced by the distribution of β-COP (Sandoval and Carrasco, 1997), a component of COP1 coats

and marker protein of the peripheral Golgi (Duden *et al*, 1991). Later the SGC are dispersed in thread-like structures and the SGC marker protein $GMP_{c-1}$ locates to a reticulum-like pattern with some punctate structures (Sandoval and Carasco, 1997). The microtubules and intermediate filaments of PV infected cells are radically modified, however it has been shown that the disassembly of the Golgi complex is a direct result of PV infection and not a secondary effect of the remodelling of the cytoskeleton (Sandoval and Carasco, 1997). The disassembled Golgi elements could possibly be assimilated into the ER, contributing to the extensive swelling observed in ER cisternae (Sandoval and Carasco, 1997).

FMDV infection affects the host cell in a slightly different manner to PV (Monaghan *et al*, 2004). Firstly, the disassembled Golgi apparatus and rough ER accumulate to one side of the nucleus with the newly formed membranous vesicles. This is distinctly different to the seemingly random dispersal of the Golgi apparatus in PV infected cells (Sandoval and Carasco, 1997; Monaghan *et al*, 2004). The FMDV-induced vesicles are fewer in number than those induced by PV infection and do not aggregate into rosette-like clusters. Finally, a large proportion of the FMDV-induced vesicles do not possess a double membrane (Monaghan *et al*, 2004). These differences suggest that while there may be many common features of picornavirus infection the mechanisms through which host cell membranes are modified and virus-induced vesicles generated may vary between individual viruses.

In addition, FMDV and not PV, is able to establish persistent infection in vaccinated and infected animals, unlike many other picornaviruses, suggesting that FMDV possesses an ability to evade innate and acquired host immune responses. It is possible that this ability is linked to the effect of FMDV infection on host protein secretion (Alexandersen *et al*, 2002).

To gain a broader understanding of the effects of different picornavirus infections on host cell membranes the roles played by the various non-structural picornavirus proteins in the modification of the host cell environment and the replication of viral RNA require further investigation.

### 1.3.3 The picornavirus 2B protein

The sequence of the 2B protein is not highly conserved throughout the *Picornaviridae* (Moffat *et al*, 2005) and it is therefore not surprising that the interactions formed between 2B and host cell membranes differ between different picornaviruses.

Transient expression of PV 2B in Vero cells causes the complete disassembly of the Golgi complex (Doedens and Kirkegaard, 1995) suggesting that this protein may be solely responsible for the phenomena observed by Sandoval and Carasco (1997), described above in *Section 1.3.*2. This hypothesis is supported by the observation that cells transiently expressing the PV 2C, 2BC and 3A proteins do not show disruption of the Golgi apparatus except after extensive expression times where any damage to the Golgi could be attributed to nonspecific cell damage as a result of the extreme vacuolation observed in the cells at this stage (Doedens and Kirkegaard, 1995). It is interesting to note that modifications to host cell membranes caused by individually expressed viral proteins are often more profound than those induced by viral infection (Suhy *et al*, 2000).

In addition to its effects on the integrity of the Golgi apparatus, expression of PV 2B has been shown to block protein secretion (Doedens and Kirkegaard, 1995). This characteristic can be linked with the disassembly of the Golgi complex by 2B as this protein has been shown to inhibit protein secretion `causing the retention of Ap1PI molecules with mannose oligosaccharide chains in the Golgi cisternae (Doedens and Kirkegaard, 1995).

The essential role played by picornavirus protein 2B in viral replication was verified when mutations in the 2B region of the PV genome were found to cause noncomplementable defects in viral RNA replication (Bernstein *et al*, 1986; Johnson and Sarnow, 1991). This could reflect a necessity for the presence of 2B or 2BC at the site of RNA replication or a disruption of the structure of the viral RNA causing defective RNA synthesis (Bernstein *et al*, 1986; Johnson and Sarnow, 1991). Alternatively these mutations may have affected the proliferation of virus-induced vesicles by altering the ability of 2B to modify Golgi membranes.

Membrane fractionation and immunolocalisation studies of transiently expressed FMDV 2B protein in Vero cells revealed that 2B is membrane associated and that it localises to a reticular stain closely aligned with that of the ER marker protein ERp57, suggesting that unlike PV 2B, FMDV 2B associates with ER membranes (Moffat *et al*, 2005). Later stages of 2B expression revealed modification of ER membranes into honeycomb structures adjacent to the nucleus (Moffat *et al*, 2005).

Aside from its role in the disassembly of the Golgi complex, the 2B protein has been shown to alter membrane permeability (van Kuppeveld *et al*, 1997; Aldabe *et al*, 1996; Doedens and Kirkegaard, 1995). This suggests that it may play a role in the anchorage of the replication complex to the virus-induced vesicles. Using a yeast two-hybrid approach Cuconati *et al* (1998) demonstrated that homomultimers form between PV proteins 2B and 2BC and heteromultimers are formed between proteins 2B: 2BC and 2C: 2BC *in vivo*. de Jong *et al* (2002) revealed similar results for Coxsakie B3 virus (CBV3) P2 proteins using a mammalian two-hybrid system. The multimerisation reactions were found to be mediated by the hydrophobic regions of the amphipathic α-helix and the second hydrophobic domain located on the 2B protein (de Jong *et al*, 2002) and these same domains have been shown to be responsible for the permeabilisation of the modified host membranes (Barco and Carrasco, 1998; Doedens and Kirkegaard, 1995; van Kuppeveld *et al*, 1997). However, the actual mechanism through which membrane permeability is increased is unknown. It has been hypothesised that aqueous pores may form in the targeted membranes through the formation of integral homo- or heteromultimers of the 2B and 2BC proteins, arranged with the hydrophilic regions of their amphipathic α-helices facing each other (de Jong *et al*, 2002).

In summary, the picornavirus 2B protein is implicated in the modification of host membranes (Doedens and Kirkegaard, 1995) prior to the assembly of the replication complex. Evidence also suggests that this protein plays a role in viral RNA replication (Bernstein *et al*, 1986; Johnson and Sarnow, 1991) and the alteration of host membrane permeability (van Kuppeveld *et al*, 1997; Aldabe *et al*, 1996; Doedens and Kirkegaard, 1995).

### 1.3.4 The picornavirus 2C protein

The 2C protein is very highly conserved throughout the *Picornaviridae,* indicating that it plays a vital role in the replication cycle of picornaviruses. Although the tertiary structure for any picornavirus 2C protein is yet to be solved, the occurrence of conserved α-helices and β-sheets in the secondary structure of the 2C protein have been identified. In addition, the existence of several functional domains has been established. Figure 1.3.1 is a schematic representation of the secondary structure and the functional domains identified in several picornavirus 2C proteins (Banerjee *et al*, 2004).

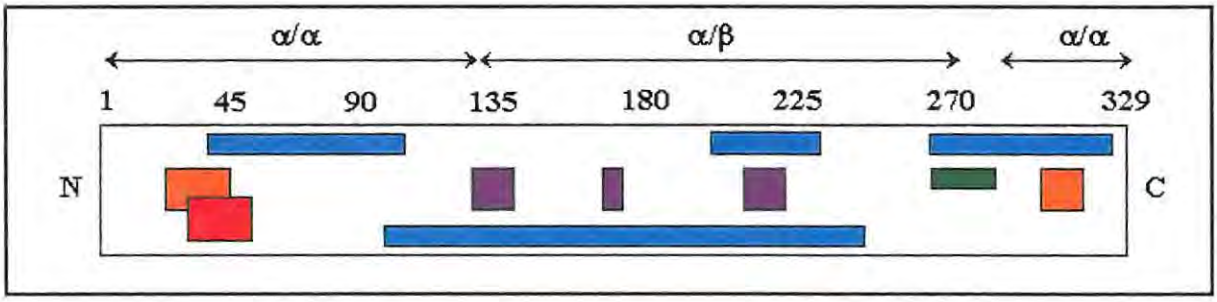


**Figure 1.3.1.** Schematic representation of the putative domain structure identified to date of the PV 2C protein (adapted from Banerjee *et al*, 2004). The structural features of the picornavirus 2C protein include: two RNA binding domains ( ), a membrane binding domain ( ), three NTP-binding domains ( ), three regions with serpin homology ( ) and a cysteine-rich zinc finger ( ).

*(i) Membrane association characteristics of 2C*

The 2C protein is membrane associated and is implicated in the proliferation of virus-induced membranous vesicles in infected cells. The PV 2C protein localises to the RER during PV infection where it stimulates the formation of smooth membranous vesicles that bud off the ER membranes and later support the virus replication complex (Aldabe and Carasco, 1995; Bienz *et al*, 1987; Bienz *et al*, 1990; Bienz *et al*, 1992; Cho *et al*, 1994; Schlegel *et al*, 1996). In addition to induction of vesiculation, the PV 2C protein has also been shown to cause extensive tubulation of ER membranes resulting in "myelin-like swirls of ER derived membrane" (Aldabe *et al*, 1996; Cho *et al*, 1994; Teterina *et al*, 1997).

Transiently expressed FMDV 2C is also membrane associated but its subcellular localisation is different to PV 2C. Like PV 2C, FMDV 2C localises to the RER and colocalises with the ER marker protein ERp57 (Moffat *et al*, 2005). In addition to the reticular localisation, FMDV 2C also locates to punctate structures adjacent to the nucleus that show the same distribution as, but do not colocalise with, the Golgi marker protein β-COP. This suggests that the FMDV protein associates with Golgi membranes but excludes some cellular proteins, including β-COP, from these membranes (Moffat *et al*, 2005).

Knox *et al* (2005) observed that at early stages of FMDV infection 2C locates to a diffuse punctate pattern to one side of the nucleus and is concentrated into larger structures adjacent to the nucleus at later stages. In addition α-mannosidase II (Man II), an enzyme located in the medial Golgi cisternae, was dispersed in the region of, but did not colocalise with, the 2C-containing structures at later stages of infection suggesting that the medial Golgi membranes are targeted by FMDV 2C but that the 2C protein excludes the Man II protein from these membranes (Knox *et al*, 2005). Further investigations by Knox *et al* (2005) using immunolocalisation techniques and marker proteins from the various membrane compartments showed that the FMDV 2C protein does not colocalise with marker proteins of the ER, intermediate compartment, trans-Golgi network or lysosomal membranes. The most likely explanation for the lack of host organelle marker proteins in the membranes supporting the FMDV replication complex is that the host proteins are efficiently excluded from the membranes during the virus-induced vesicle proliferation process (Knox *et al*, 2005). However it is possible that a proportion of virus induced vesicles are synthesised *de novo* (Guinea and Carrasco, 1990) or that other membranes such as the nuclear envelope are exploited.

The precise mechanism by which the 2C protein interacts with host membranes is unclear. However, the putative class A amphipathic helix located towards the N-terminus of the protein (Figure 1.3.1) has been implicated in mediating the membrane binding and rearranging abilities of 2C (Paul *et al*, 1994; Echeverri and Dasgupta, 1995; Echeverri *et al*, 1998) and the N-terminal 72 amino acids of the PV 2C protein have been shown to mediate membrane targeting to the ER membranes (Echeverri *et*

*al*, 1998). Class A amphipathic helices comprise a hydrophobic face separated from a basic hydrophilic face by acidic amino acid residues and are a common feature of membrane-associated viral proteins (Saier and McCaldon, 1988). They are thought to insert the hydrophobic face halfway into the phospholipid monolayer while the hydrophilic face aligns along the aqueous interface (Segrest *et al*, 1994). An alternative mechanism whereby 2C binds a cellular membrane protein has also been suggested (Echeverri *et al*, 1998) but no such interaction has yet been described. A second amphipathic α-helix on the C-terminal of the 2C protein has also been implicated in membrane binding (Teterina *et al*, 1997).

*(ii) 2C binds viral RNA: involvement in RNA replication*

In addition to the membrane-binding activities of 2C, the protein is able to interact with viral RNA (Banerjee and Dasgupta, 2001; Banerjee *et al*, 1997; Rodriguez and Carasco, 1995; Rodriguez and Carasco, 1993). PV 2C has two RNA-binding motifs: an N-terminal region (located at amino acids 21-54) and a C-terminal region (located at amino acids 312-319) (Rodriguez and Carasco, 1995).

The PV, Hepatitis A virus (HAV) and HRV 2C proteins specifically bind the 3' cloverleaf structure of negative sense viral RNA but do not bind the corresponding 5' cloverleaf structure of the positive sense viral RNA (Banerjee *et al*, 1997; Banerjee and Dasgupta, 2001). This ability appears to be unique to the 2C protein as it has been shown that the picornavirus proteins 2A, 2B, 3CD and 3C do not bind negative sense PV RNA (Banerjee *et al*, 1997).

In view of the membrane and RNA-binding capabilities of 2C it has been suggested that the 2C protein plays a role in anchoring the negative-sense viral RNA to the surface of virus-induced vesicles at the site of the replication complex. This could allow viral proteins, such as 3CD or 3AB, or host proteins such as the eukaryotic translation initiation factor, p36, to transfer from the 5' cloverleaf structure of the positive RNA strand to the 3' end of the negative strand, thus facilitating the initiation of nascent positive-sense viral RNA synthesis (Andino *et al*, 1993; Xiang *et al*, 1995; Harris *et al*, 1994). In addition, 2C is thought to possess RNA helicase activity which

would, along with $3D^{pol}$, enable the protein to facilitate the unwinding of double-stranded RNA structures occurring during the elongation of nascent positive-sense viral RNA (Haenni and Kadare, 1997). The helicase activity is however, yet to be demonstrated and is thought to require other viral or cellular proteins (Haenni and Kadare, 1997). Thus, 2C plays two important roles in viral RNA replication: a *cis*-acting function during the initiation of RNA replication and a *trans*-acting function during RNA elongation (Aldabe and Carasco, 1995; Li and Baltimore, 1988; Mirzayan and Wimmer, 1992).

The PV 2Cprotein possesses ATPase and GTPase activity (Rodriguez and Carasco, 1992, Mirzayan and Wimmer, 1994, Teterina *et al*, 1992). PV replication and specifically the initiation of negative sense RNA replication are inhibited by millimolar concentrations of guanidine hydrochloride (Pfister and Wimmer, 1999; Barton and Flanegan 1997). The 2C protein has three nucleoside triphosphatase (NTP) binding domains (Figure 1.3.1), all of which are necessary for the ATPase activity of the protein (Pfister and Wimmer, 1999). The function of 2C NTPase activity in virus replication is poorly understood. It has been suggested that it may play a part in the stabilisation or organisation of the replication complex on the surface of virus-induced vesicles, the modification of host membranes during the virus-induced vesicle proliferation stage or even the uncoating or assembly of picornavirus virions (Pfister and Wimmer, 1999). 2C has previously been implicated in both the uncoating (Li and Baltimore, 1990) and encapsidation (Vance *et al*, 1997) of picornaviruses. However it is more likely that the NTPase activity is linked to viral RNA replication as lethal mutations to the NTP-binding domains of PV 2C inhibited RNA replication *in vivo*, while no translational defects were detected (Teterina *et al*, 1992).

*(iii) 2C has protease inhibition activity*

In addition to its involvement with viral RNA replication and the proliferation of membranous vesicles in infected cells 2C has also been implicated in the control of viral protease activities (Banerjee *et al*, 2004). Multiple alignment of 2C sequences with protease inhibitors revealed that 2C possesses three putative serine protease

inhibitor motifs (Figure 1.3.1), suggesting that 2C plays a regulatory role in viral or host protease activity (Banerjee *et al*, 2004). It was also discovered that the PV 2C protein coimmunoprecipitates with the viral protease $3C^{pro}$ and is able to inhibit the protease activity of $3C^{pro}$ both *in vitro* and *in vivo* through a physical interaction that occurs either in the cytoplasm or at the membrane-bound replication complex (Banerjee *et al*, 2004). It is yet to be shown whether this regulatory activity of 2C extends to $3CD^{pro}$ (Banerjee *et al*, 2004). The biological significance of the serine protease inhibitory activity of 2C is not fully understood although it has been suggested that the inhibition of viral proteases would increase the proportion of viral polyproteins in infected cells (Banerjee *et al*, 2004). The 2C protein may also play a role in the inhibition of cellular serine proteases, thus inhibiting apoptosis in infected cells (Banerjee *et al*, 2004).

In summary, the 2C protein is a highly conserved picornavirus protein that has been implicated to perform an extensive range of functions at several stages of the picornavirus replication cycle. However, the mechanisms through which 2C is involved in the assembly of the viral replication complex, RNA replication and viral encapsidation are poorly understood.

### 1.3.5 The picornavirus 2BC protein

The picornavirus 2BC polyprotein is a membrane associated precursor of the 2B and 2C proteins that exists separately to its cleavage products (Cho *et al*, 1994; Moffat *et al*, 2005). Like many of the non-structural picornavirus proteins, PV 2BC is located within the viral replication complex on the surface of virus-induced vesicles (Cho *et al*, 1994). Transiently expressed PV 2BC protein is capable of inducing the proliferation of membranous vesicles in transformed yeast cells (Barco and Carasco, 1995) and in transfected HeLa cells (Cho *et al*, 1994). ATPase activity has also been detected with the PV 2BC protein (Pfister and Wimmer, 1999) but as with the 2C protein, the biological significance of this activity remains obscure.

The distribution of FMDV 2BC in transiently expressing Vero cells does not resemble that of either the 2B or 2C proteins (Moffat *et al*, 2005). 2BC was located in large

elements adjacent to the nucleus as well as being distributed throughout the cytoplasm in small punctate structures. Expression of FMDV 2BC resulted in the redistribution of the ER marker protein ERp57 to areas in close proximity to but not fully colocalising with 2BC (Moffat *et al*, 2005). Through immunolocalisation studies, Rust *et al* (2001) found that the PV 2BC protein in cells infected with PV or transiently expressing the protein also associated with ER membranes. The PV 2BC protein localised to small punctate structures in the cytoplasm that colocalised with ER-derived membranes containing the marker protein COPII (Rust *et al*, 2001). PV 2BC was also observed to localise to the sites of vesicle budding on the ER membranes and to vesicles containing the sec13 protein, a component of the COPII complex that is involved in vesicle budding during ER-to-Golgi protein transport (Barlowe *et al*, 1994).

PV 2BC showed some ability to inhibit ER-to-Golgi transport (Doedens and Kirkegaard, 1995). As the PV 2C protein does not affect anterograde protein transport when expressed in isolation from other viral proteins it is thought that the 2B segment of the 2BC protein, which is known to arrest protein traffic in the Golgi, is responsible for this inhibitory activity transport (Doedens and Kirkegaard, 1995). In the same study, the FMDV 2BC protein and not the 2B, 2C or 3A proteins inhibited protein transport to the plasma membrane (Moffat *et al*, 2005). 2BC modified the ER cisternae into distinct punctate structures that retained protein normally transported to the plasma membrane in the absence of 2BC (Moffat *et al*, 2005).

In summary, the picornavirus 2BC protein appears to play an integral role in the modification of host cell membranes and the proliferation of membranous vesicles prior to the assembly of the viral replication complex (Cho *et al*, 1994) and possibly affects anterograde protein trafficking in host cells (Doedens and Kirkegaard, 1995). No evidence has been presented to date to suggest that this protein plays any role in viral RNA replication or encapsidation.

### 1.3.6 The picornavirus 3A protein

The 3A protein is a membrane associated protein (Doedens *et al*, 1997; Neznanov *et al*, 2001; Moffat *et al*, 2005; O'Donnell *et al*, 2001; Pevear *et al*, 1988; Monteyne *et al*, 1997) and is the cleavage product of the 3AB protein, which is associated with the 3′ UTR along with $3CD^{pro}$ (Harris *et al*, 1994). Only the structure of the 59 N-terminal amino acids has been elucidated by nuclear magnetic resonance (NMR) (Strauss *et al*, 2003). The first 14 N-terminal amino acids were unstructured and it was discovered that 3A exists as a dimer, with monomers adjoining between helical hairpin loops from each monomer (Strauss *et al*, 2003). The PV 3A protein is not able to induce vesiculation when transiently expressed in isolation from other viral proteins. However, co-expression of PV 3A and 2BC proteins induces the formation of membranous vesicles with similar morphology to those observed in PV-infected cells (Suhy *et al*, 2000).

Transiently expressed PV 3A has been shown to specifically inhibit ER-to-Golgi protein trafficking, causing the accumulation of proteins otherwise destined for secretion and the ensuing distortion and extreme swelling of the ER cisternae (Doedens *et al*, 1997; Neznanov *et al*, 2001). Unlike PV 2B, PV 3A inhibits protein secretion at an early stage in the anterograde pathway, as demonstrated by the retention of the secretory protein Ap1PI in the ER and inhibition of the processing of mannose oligosaccharide chains into complex carbohydrates (Doedens and Kirkegaard, 1995).

FMDV 3A is partially associated with membranes while a significant proportion of the protein is distributed throughout the cytoplasm in transiently expressing cells (Moffat *et al*, 2005). Membrane-bound FMDV 3A is associated with ER membranes containing the ER marker protein calreticulin (Moffat *et al*, 2005; O'Donnell *et al*, 2001). However, unlike PV 3A, FMDV 3A does not affect ER-to-Golgi membrane trafficking (Moffat *et al*, 2005).

An extensive study by Choe *et al* (2005) investigated the ability of the 3A proteins of several picornaviruses to inhibit ER-to-Golgi protein transport. Of the viruses investigated only the 3A proteins from the closely related viruses: PV serotype 1, PV

serotype 1 and coxsakievirus B3 inhibited anterograde protein transport from the ER (Choe *et al*, 2005). There was no evidence of inhibition of ER-to-Golgi trafficking in cells expressing 3A proteins of rhinovirus 14, hepatitis A virus and enterovirus 71 (Choe *et al*, 2005). In addition expression of the 3A proteins of both the virulent GDVII strain and the non-virulent BeAn strain of TMEV did not alter anterograde protein transport (O'Donnel *et al*, 2001; Pevear *et al*, 1988). Choe *et al* (2005) found that only one conserved N-terminus amino acid, Lys9, appeared to be linked to the ability of picornavirus 3A proteins to inhibit ER-to-Golgi protein transport and suggested that the unstructured 14 N-terminal amino acids are likely to be involved in 3A-host protein interactions.

As the 3A protein is not highly conserved throughout the *Picornaviridae* it is not surprising that proteins from different picornaviruses interact with host cell components in different ways. The consequences of these differences on the pathology of different picornaviruses are unknown. A lack of inhibition of anterograde protein transport would enable infected cells to display viral antigens with MHCs on the cell surface triggering, among other immune responses, an inflammatory response (Choe *et al*, 2005). It has been suggested that a functioning secretory pathway may be advantageous for viruses, such as rhinovirus 14, who's spread from cell to cell is enhanced by inflammation (Choe *et al*, 2005). The PV 3A protein is known to inhibit several characteristics of host immune responses, namely the presentation of viral antigens with MHC class 1 molecules (Deitz *et al*, 2000), the inhibition of the secretion of antiviral cytokines (e.g. IL-6, IL-8) and interferon-β from poliovirus-infected cells (Dodd *et al*, 2001). Various mutations created in the 3A proteins of both FMDV and hepatitis A virus have been linked with changes in viral pathogenesis (Beard and Mason, 2000; Nunez *et al*, 2001; Beneduce *et al*, 1995), further linking the activity of the 3A protein with the evasion of host immune responses.

In summary, evidence suggests that the picornavirus 3A protein, and its precursor polyprotein 3AB, are involved in several events during the picornavirus replication cycle including the modification of host membranes (Suhy *et al*, 2000), viral RNA replication (Harris *et al*, 1994) and possibly in the evasion of the host immune

responses through the inhibition of anterograde protein transport in the host cell (Doedens *et al*, 1997; Neznanov *et al*, 2001).

## 1.4 TMEV: AN AVAILABLE PICORNAVIRUS REPLICATION SYSTEM

### 1.4.1 A replication system for TMEV in BHK-21 cells

From the information above, it is clear that the non-structural picornavirus proteins have a broad range of functions, some of which involve interactions with host cell components and others that involve other viral proteins. In view of this, it is important to study the various non-structural proteins both in isolation, through transient expression in transfected cells, and in the presence of other viral proteins during infection.

Due to the health and economic risks posed by picornaviruses such as PV, FMDV, HRV and HAV, disease security regulations restrict the infection of cell cultures with these viruses to facilities with appropriate disease protection and security measures. Such facilities were not available to this study necessitating the development of an infection system of a less hazardous picornavirus in tissue culture.

TMEV is a picornavirus that belongs to the Genus Cardiovirus. Four strains are currently recorded: the virulent strains GDVII and FA and the non-virulent strains DA and BeAn. TMEV is a naturally occurring enteric pathogen in mice but poses no threat to humans or livestock, thus enabling its use in conventional tissue culture facilities.

The ability of TMEV to infect the BHK-21 cell line is previously recorded (Kong *et al*, 1994; van Pesch *et al*, 2001). This same cell line was used in this study to further our understanding of the interactions formed between the picornavirus P2 and 3A proteins and host cell components.

### 1.4.2 Pathology of TMEV infection in mice

Briefly, TMEV infects the central nervous system of mice causing either acute lethal encephalomyelitis (strains GDVII and FA) or biphasic disease whereby after mild encephalomyelitis lasting approximately two weeks the mice show chronic demyelination, similar to that seen in human multiple sclerosis patients (Monteyne *et al*, 1997). This demonstrates that despite host immune responses TMEV, like FMDV, is capable of developing persistent infections. The L protein (Figure 1.2.1) has been implicated in interfering with α/β interferon production, thus inhibiting the host immune response (van Pesch *et al*, 2001). TMEV strain GDVII is frequently used as an animal model during multiple sclerosis research. Although the causal factors of multiple sclerosis are complex, viruses have been implicated in affecting the progression of this condition (Tolley *et al*, 1999).

### 1.4.3 TMEV non-structural proteins: interactions with host cell components

As with other picornaviruses, TMEV expresses the 2B, 2C, 2BC and 3A non-structural replicative proteins. However, relatively little is known about these proteins with respect to the roles they play in modifying the host cell environment and mediating TMEV RNA replication. The subcellular localisation and membrane association characteristics of these proteins as well as their involvement in virus RNA replication and encapsidation are yet to be investigated. Additionally the effect each of these proteins and TMEV infection in general on host cell ultrastructure are also unknown.

## 1.5 IDENTIFICATION OF KNOWLEDGE GAP

An extensive range of studies has been conducted regarding the structure of the picornavirus replication complex, the replication of picornaviral RNA and the roles played by the various non-structural proteins in the viral replication cycle. Despite this, very little is known of the precise molecular mechanisms through which picornavirus proteins interact with host cell components. It is assumed that some unknown interactions between the non-structural proteins and host proteins exist and the identification and description of these interactions could provide valuable information for the design of drug therapies for picornavirus infections. For example, the development of persistent FMDV infections in cattle and sheep pose a dire threat to the agricultural industry worldwide. The development of more effective disease treatment and control strategies relies on further understanding of the mechanisms through which picornaviruses evade host immune responses.

As discussed above, these objectives can only be met through the study of picornavirus proteins in isolation through transient expression, and in the context of viral replication through infection. Consequently this study initially focussed on the subcellular localisation and membrane association of the TMEV 2B, 2C, 2BC and 3A proteins. This enabled a comparison of these characteristics of the TMEV proteins with the localisation and modification of host membranes by the corresponding proteins of PV and FMDV. Secondly, this study endeavoured to determine the effect of mutating highly conserved amino acids in the 2C protein on the subcellular localisation of the 2C protein as well as on TMEV replication.

Most of what is known about picornavirus replication is based on studies using PV proteins and replication systems. Alternative studies using FMDV and other picornaviruses have provided evidence that the non-structural proteins of different picornaviruses vary in function and interactions with host components. However, the variety of picornaviruses investigated with respect to molecular interactions with host components is limited. Thus, this study will contribute significantly to the general understanding of picornavirus biology.

## 1.6 PROBLEM STATEMENT

There is an incomplete appreciation of the interactions formed between the various non-structural picornavirus proteins and host cell components and the role that these interactions play in the virus replication cycle and the evasion of host immune responses. The characterisation of the membrane association and localisation of the 2B, 2C, 2BC and 3A protein of the relatively less studied TMEV will add to the general understanding of picornavirus replication and provide a platform for further studies involving the identification of novel interactions between picornavirus and host proteins.

## 1.7 AIMS AND OBJECTIVES

The overriding intension of this study was to increase the general understanding of the interactions formed between picornavirus non-structural proteins and host membranes through the investigation of the TMEV P2 and 3A proteins.

1. To this end we aimed to first transiently express the 2B, 2C, 2BC and 3A TMEV proteins in BHK-21 cells and determine their subcellular localisation by immunolocalisation studies.

2. Further investigations into the importance of the highly conserved N-terminal domain of the 2C protein with respect to subcellular localisation of this protein was then conducted. We aimed to first identify specific amino acids in the N-terminal domain of the 2C protein that are particularly highly conserved by the computational multiple alignment of picornavirus 2C sequences. Point mutations were created at these residues and the subcellular localisation of the mutant proteins was determined as with the wild type 2C protein above.

3. Additionally we aimed to determine the effect of these point mutations on the ability of TMEV to replicate in BHK-21 cells. This involved the transfection of BHK-21 cells with infectious RNA encoding wild type and mutant TME viruses to determine which mutations were lethal and which merely slowed the replication of the virus. Next, for the mutant viruses showing limited replication abilities, we aimed to quantify the extent to which the point mutations inhibited the rate of TMEV replication by constructing a viral replication curve of virus particles produced per unit time.

4. Finally, in view of future studies involving the identification of novel interactions between the picornavirus 2C protein and host proteins we aimed to express and purify a hydrophobic, antigenic GST- tagged fragment of the 2C protein for use in future protein pull-down assays and in the production of an antibody against the TMEV 2C and 2BC proteins.

# 2 Localisation of TMEV P2 and 3A proteins

## 2.1 INTRODUCTION

An increased understanding of the molecular interactions formed between picornavirus proteins and host cell components is essential for the development of novel disease treatment and control strategies. Prior to this study the localisation of the non-structural TMEV 2B, 2C, 2BC and 3A proteins to host membranes was unexplored.

The localisation of these viral proteins to specific cellular organelles was investigated through their transient expression in BHK-21 cells followed by indirect immunofluorescent staining of the cells with primary antibodies against epitope-tagged viral proteins and marker proteins of the ER and Golgi apparatus. Subsequent to secondary staining with fluorophore conjugated secondary antibodies, laser scanning confocal microscopy was employed to image the localisation of the viral proteins. BHK-21 cells were chosen as the cell line in which to express these proteins as later experiments involving the infection of mammalian cells with TMEV were also carried out using this cell line.

It was necessary to express the viral proteins as fusions with the C-terminal V5-epitope tag as antibodies against the TMEV proteins investigated in this study were not available. The coding regions for the TMEV 2B, 2C, 2BC and 3A proteins were subcloned into the pcDNA3.1/V5-His© TOPO® (Invitrogen) mammalian expression vector (see Appendix A). This vector was selected as the small size of the V5 epitope encoded downstream of the inserted protein coding sequence ensures that it does not interfere with the localisation of fusion proteins (Invitrogen, 2004).

Future investigations of the interactions formed between the TMEV 2B, 2C, 2BC and 3A proteins and host cell proteins as well as the ability of the individual proteins to induce host cell membrane rearrangement will require antibodies against these proteins.

Subsequent to localising to the RER during PV infection, the PV 2C protein promotes the budding of vesicles from ER membranes (Aldabe and Carasco, 1995; Bienz *et al*, 1987; Bienz *et al*, 1990; Bienz *et al*, 1992; Cho *et al*, 1994; Schlegel *et al*, 1996). In addition the PV 2BC protein has been shown to cause extensive vesiculation when transiently expressed in HeLa cells (Cho *et al*, 1994). In view of these findings with the PV proteins, future studies characterising the interactions formed between the TMEV proteins and host membranes would seek to determine the ability of firstly TMEV infection, and secondly the transient expression of the TMEV 2C and 2BC proteins to cause vesiculation of the membranes of the secretory pathway of host cells by electron microscopy and using an antibody to detect the 2C and/or 2BC proteins. An antibody against the TMEV 2C protein would also be used in future studies to identify interaction formed between the TMEV 2C or 2BC proteins and host proteins by protein pull-down assays. This study sought to express and purify a hydrophilic and antigenic region of the 2C protein to be used in the generation of such an antibody.

The cDNA coding sequence of the selected region of the TMEV 2C protein was inserted into a bacterial expression vector encoding a Glutathione S-transferase (GST)-tag on the N-terminus of the peptide. The expression of the peptide with a tag was necessary to facilitate purification by affinity chromatography. Although the GST- tag is relatively large (26kDa) compared to alternative protein tags such as a His tag (0.66 kDa) it was selected based on its ability to increase the solubility of the fusion peptide (Constans, 2002). The fusion peptide was expressed on a pilot-scale and purified by affinity chromatography. Future work will include the large-scale expression of the fusion peptide and the generation of the anti-TMEV 2C antibody in a mammal such as mice or rabbits.

## 2.2 AIMS AND OBJECTIVES

Broadly, the aims of this component of the study was to explore the membrane association of the TMEV 2B, 2C, 2BC and 3A proteins with respect to their localisation to membranes of the host secretory pathway, and secondly to identify and express a soluble region of the 2C protein against which antibodies can be raised. Specifically, the objectives were as follows:

1. To subclone the coding sequences for the TMEV 2B, 2C, 2BC and 3A proteins into the mammalian expression vector pcDNA3.1/V5-His© TOPO®.

2. To express the TMEV 2B, 2C, 2BC and 3A proteins transiently in BHK-21 cells through the transfection of this cell line with recombinant DNA encoding the proteins.

3. To immunolocalise the TMEV 2B, 2C, 2BC and 3A proteins in BHK-21 cells by the immunostaining of cells and laser scanning confocal microscopy.

4. To identify a region of the 2C protein that possesses a high degree of hydrophilicity and antigenicity and to insert the cDNA coding region for the selected peptide sequence into the bacterial expression vector pGEX-2T.

5. To express the peptide as a GST-fusion peptide in *E. coli* cells on a pilot-scale, purify by affinity chromatography and to confirm the successful expression and purification by SDS-PAGE and Western analysis.

## 2.3 METHODS AND MATERIALS

### 2.3.1 Construction of recombinant vectors for the expression of TMEV 2B, 2C, 2BC and 3A coding regions in mammalian cells

In order to transiently express the TMEV 2B, 2C, 2BC and 3A proteins in cells the coding regions for these proteins were subcloned into the mammalian expression vector pcDNA3.1/V5-His© TOPO®.

The coding regions for the TMEV 2B, 2C, 2BC and 3A proteins were PCR amplified (see Appendix C for primers used) using the high fidelity DNA-dependent DNA polymerase Expand (Promega) and pGDVII-WT DNA (see Appendix A) as a template. Subsequent to electrophoresis on a 1% agarose gel (1% wt/vol agarose in TAE buffer: 0.114 % Glacial acetic acid, 1 mM EDTA pH 8, 40 mM Tris-HCl), PCR products were excised and purified using the Wizard SV Gel and PCR Clean-up System (Promega) according to manufacturers instructions.

The purified 2B PCR product was subcloned directly into pcDNA3.1/V5-His© TOPO® (Invitrogen) using the pcDNA3.1/V5-His© TOPO® TA Expression Kit according to manufacturers instructions. Due to limited availability of the "empty" pcDNA3.1/V5-His© TOPO® vector an alternative strategy was employed to insert the coding regions for the 2C, 2BC and 3A proteins into the vector. The pCKF2C construct, comprising the coding sequence for FMDV 2C inserted into the multiple cloning site (MCS) of pcDNA3.1/V5-His© TOPO®, was subjected to restriction digestion with *Bam* H1 (Promega) and *Xba* 1 (Promega). 1 µg of each of the 2C, 2BC and 3A PCR products was subjected to the same restriction digestion and both the linearised pcDNA3.1/V5-His© TOPO® vector and the PCR products were purified using the Wizard SV Gel and PCR Clean-up System, subsequent to electrophoresis on a 1% agarose gel. The coding sequences for the 2C, 2BC and 3A proteins were subcloned into the linearised pcDNA3.1/V5-His© TOPO® vector in frame with the C-terminal V5 epitope using T4 DNA ligase (Promega) at room temperature for four hours followed by overnight incubation at 4°C.

Competent *E. coli* JM109 cells (Promega) were transformed with the recombinant vectors and spread plated on Luria agar plates (0.5 % NaCl, 0.5 % yeast extract, 1% tryptone, 2% nutrient agar) containing ampicillin (100 μg/ml) (Roche). Plates were incubated at 37°C overnight. Bacterial colonies were inoculated into 5ml Luria Broth (0.5 % NaCl, 0.5 % yeast extract, 1% tryptone) cultures containing Ampicillin (100 μg/ml) and incubated overnight at 37°C, shaking at 200 rpm. The presence of recombinant plasmids containing the correct insert in the bacterial cultures was detected by the "colony PCR" screening technique. This involved the PCR amplification of the insert of interest using 1 μl of confluent bacterial culture as a source of template DNA and the same reaction parameters and specific primers originally used to amplify the insert (see Appendix C).

Recombinant plasmids were isolated using the QIAprep ® Spin Miniprep Kit (Qiagen) and named as shown in Table 2.3.1. The presence of correct inserts was confirmed by restriction analysis with *Bam* H1 (pLMT2B) or *Bam* H1 and *Xba* 1 (pLMT2C, pLMT2BC and pLMT3A), and later by chain-termination-based sequencing (performed by Inqaba Biotechnical Industries (Pty) Ltd) using standard T7 and BGH primers (Invitrogen).

**Table 2.3.1. Recombinant vectors constructed by inserting cDNA coding sequences of the TMEV 2B, 2C, 2BC and 3A proteins into the mammalian expression vector pcDNA3.1/V5-His© TOPO®**

| Name | Forward primer | Reverse primer | Insert Size (nucleotides) | Protein encoded insert |
|---|---|---|---|---|
| pLMT2B | 2BF | 2BR | 380 | TMEV 2B |
| pLMT2C | 2CF | 2CR | 978 | TMEV 2C |
| pLMT2BC | 2BF | 2CR | 1 358 | TMEV 2BC |
| pLMT3A | 3AF | 3AR | 264 | TMEV 3A |

### 2.3.2 Construction of recombinant vectors for the expression of truncated TMEV 2C and 2BC coding regions in mammalian cells

The N-terminal 60 amino acids of the Picornavirus 2C protein are thought to include the residues responsible for membrane association and the RNA binding activity of the protein (Banerjee *et al*, 2004; Echeverri and Dasgupta, 1995). If this is true for the TMEV 2C protein it is possible that the localisation of this protein, and possibly the 2BC protein, in host cells during viral replication is controlled by signal sequences within this region. To test whether the localisation of the 2C and 2BC proteins in host cells was affected by the absence of the C-terminal regions of the 2C protein truncated coding regions of the 2C and 2BC proteins, containing only the first 180 nucleotides (and thus 60 amino acids) of the 2C coding sequence, were subcloned into the pcDNA3.1/V5-His© TOPO® vector.

The truncated coding regions for the TMEV 2C and 2BC proteins were PCR amplified as described above in *Section 2.3.1* (see Appendix C for primers used). Subsequent to purification, restriction digestion and subcloning of these truncated coding regions into the pcDNA3.1/V5-His© TOPO® vector was performed as described with pLMT2C above (*Section 2.3.1*). The truncated 2C and 2BC coding sequences will be referred to as 2C60 and 2BC60 from this point forward.

**Table 2.3.2. Recombinant vectors constructed by inserting cDNA coding sequences of the truncated TMEV 2C and 2BC proteins into the mammalian expression vector pcDNA3.1/V5-His© TOPO®**

| Name | Forward primer | Reverse primer | Insert Size (nucleotides) | Insert |
|---|---|---|---|---|
| pLMT2C60 | 2CF | 2C60R | 180 | Truncated TMEV 2C (2C60) |
| pLMT2BC60 | 2BF | 2C60R | 560 | Truncated TMEV 2BC (2BC60) |

### 2.3.3 Maintaining a BHK-21 cell line

BHK-21 cells (kind gift of Dr A. Moore, University of Alabama, USA) were used in this study as both a host for viral infection and as a platform for the transient expression of viral proteins. At all times cells were maintained in Dulbecco's Modified Eagle's Medium (DMEM) (Highveld Biological (Pty) Ltd or Cambrex) with 5% fetal calf serum (FCS) (Highveld Biological (Pty) Ltd) and 1% Penicillin/ Streptomycin/ Fungizone (PSF) (Highveld Biological (Pty) Ltd) in 25 $cm^3$ non-vented flasks (Sarstedt) and were incubated in a Series II Water Jacketed $CO_2$ Incubator (ThermoForma) at 37°C and 5% $CO_2$. At 5% $CO_2$, using non-vented culture flasks with the lids untightened, the dissolved $CO_2$ in the unbuffered media is sufficient to maintain a pH of approximately 7.4, which is ideal for mammalian cell growth. All experiments pertaining to the culture or transfection of mammalian cells were carried out in a sterile environment in a laminar flow hood.

*(i) Subculturing cells*

Confluency can be described as the percentage of the growth surface of a culture flask that is covered by the cultured cells. When cells reached 100% confluency, i.e. the growth surface was completely covered; they were subcultured into fresh culture flasks. Cell-matrix and cell-cell interactions were broken through the addition of Trypsin (Highveld Biological (Pty) Ltd). Once cells had been vigorously resuspended in 1 ml of DMEM (5% FCS, 1% PSF) to remove any remaining cell-cell interactions, approximately 1.00 x $10^6$ resuspended cells were seeded into 7 ml DMEM (5% FCS, 1% PSF) in a fresh culture flask. Flasks were incubated as described above. Using this protocol it was observed that cells reached 100% confluency after approximately 72 hours incubation and were thus subcultured at these intervals for the duration of the experiments described in this study.

*(ii) Cryopreservation of BHK-21 cells*

It is important to store reserve stocks of a cell line in case of contamination of existing cultures or incubator failure. BHK-21 cells that had reached 100% confluency in a 25 $cm^3$ culture flask were trypsinised as described above and resuspended in 1ml

cryopreservation medium (50% FCS, 39% DMEM, 10% glycerol, 1% PSF). Resuspended cells were aliquoted into cryovials (Sarstedt) and slowly cooled to -80°C overnight before long-term storage in liquid nitrogen.

### 2.3.4 Transfection of BHK-21 cells with cDNA encoding TMEV P2 and 3A proteins

*(i) Preparation of cells for transfection*

A 13 mm glass coverslip (VWR International) was placed at the bottom of each well in a 24-well plate (Greiner Bio-one) with 1 ml DMEM (5% FCS, 1% PSF). BHK-21 cells grown to 100% confluency in a 25 $cm^3$ culture flask were passaged as described above. After trypsinised cells were resuspended in 1ml DMEM (5% FCS, 1% PSF), approximately 7.50 x $10^4$ cells were aliquoted into each well and the 24-well plate was incubated at 37°C and 5% $CO_2$ for approximately 24 hours by which time cells were 70 - 90% confluent.

*(ii) Transfection of BHK-21 cells*

Recombinant plasmids were introduced into BHK-21 cells using the transfection reagent ExGen (Fermentas). According to manufacturer's instructions the recommended ratio of DNA: ExGen in a transfection reaction in a 24-well plate is 1 µg DNA: 3.3 µl ExGen and the recommended amount of DNA added to cells in each well is 1µg (Fermentas). Accordingly, transfection mixtures comprising 100 µl 150 mM NaCl, 1 µg DNA and 3.3 µl ExGen, were made up in sterile eppendorf tubes and incubated for 1 hour at room temperature (RT), vortexing at 5-minute intervals.

After overnight incubation at 37°C and 5% $CO_2$, medium was aspirated from 70% confluent BHK cells growing on coverslips in a 24-well plate and 400 µl DMEM (5% FCS, 1% PSF) was aliquoted into each well. The transfection mixtures were added drop wise to their respective wells and the 24-well plate was incubated at 37°C and 5% $CO_2$. After 4 hours incubation the medium and transfection reagents were

aspirated off the cells in each well and 500 µl of DMEM (5% FCS, 1% PSF) was added to each well and incubation continued for a further 15 hours to allow protein expression.

### 2.3.5 Indirect immunofluorescent staining of transfected cells

Transfected cells were rinsed four times in 1 × PBS (8.0 g NaCl, 1.44 g $Na_2HPO_4$, 0.2 g KCl, 0.24 g $KH_2PO_4$ in 1 000 ml $dH_2O$) (pH 7.4) before 400µl of 4% (wt/vol) paraformaldehyde (pH 7.8) was added to each well to fix the cells. The plate was incubated for 20 minutes at room temperature, shaking at 50 rpm. Fixed cells were rinsed twice in 1 × phosphate-buffered saline (PBS, pH 7.4) and permeabilised in permeabilisation buffer (10% wt/vol sucrose and 0.5% Triton X-100 (Saarchem) in 1 × PBS, pH 7.4) for 20 minutes at room temperature, shaking at 50 rpm.

Cells were stained with anti-V5 mouse monoclonal IgG antibody (1: 500) (Invitrogen) and either anti-βCOP (1: 250) (Kind gift of T. Wileman, University of East Anglia, UK) or anti-ERp60 rabbit polyclonal IgG antibody (1: 5 000) (Kind gift of T. Wileman, University of East Anglia, UK) primary antibodies diluted in permeabilisation buffer, for 1 hour 30 minutes at room temperature, shaking at 50 rpm. Cells were then washed in 1 × PBS (pH 7.4) containing 1% Tween-20 (Saarchem). Primary antibodies were detected using Texas Red® Goat anti-mouse IgG (H+L) (1: 500) (Molecular probes) and Alexa Fluor® 488 Goat anti-rabbit IgG (H+L) (1: 500) (Molecular probes) diluted in permeabilisation buffer for 20 minutes at room temperature, shaking at 50 rpm. Details of the antibodies used in the indirect immunofluorescent staining are shown below in Table 2.3.3. Cells were washed in 1 × PBS (pH 7.4) containing 1% Tween-20. DNA was stained with 10ng/ml DAPI (Roche) diluted in 1% Tween-20 in PBS for 10 minutes at room temperature, shaking at 50 rpm. Coverslips were mounted on microscope slides using Vectashield Hard Set Fluorescent Mounting Medium (Vector Laboratories).

| Table 2.3.3. Antibodies used in the indirect immunofluorescent staining of BHK-21 cells expressing TMEV P2 and 3A proteins | | | |
|---|---|---|---|
| | **Antibody** | **Target protein** | **Subcellular localisation** |
| **Primary antibodies** | **Anti-V5 mouse monoclonal IgG** | V5 antigenic tag on C-terminus of recombinant viral proteins | None |
| | **Anti-βCOP rabbit polyclonal IgG** | β-COP | Mostly membrane associated in the CGN, although some cytoplasmic distribution occurs |
| | **Anti-ERp60 rabbit polyclonal IgG** | ERp60 | Lumen of the ER |
| **Secondary antibodies** | **Alexa Fluor® 488 Goat anti-rabbit IgG (H+L)** | Anti-βCOP and anti-ERp60 rabbit polyclonal IgG primary antibodies | None |
| | **Texas Red® Goat anti-mouse IgG (H+L)** | Anti-V5 mouse monoclonal IgG primary antibody | None |

### 2.3.6 Microscopic examination of BHK-21 cells expressing TME viral proteins

Immunostained BHK-21 cells transiently expressing TMEV proteins were examined using the Zeiss LSM 510 Meta confocal microscope at the Electron Microscopy Unit at the University of Kwazulu-Natal, Petermaritzburg. The number of cells expressing the viral protein in question was counted on each sample and expressed as a percentage of the approximate total number of cells present. The distribution of the viral proteins, as indicated by red fluorescence, was also noted. Cells were imaged using the Zeiss LSM 510 Meta confocal microscope and LSM 510 software (Zeiss) at 400× magnification using the 40× oil immersion objective and laser lines at 488 nm and 543 nm. The 488 nm laser line excited the Alexa Fluor® fluorophore (Excitation/Emission: 495 nm/519 nm) conjugated to the anti-rabbit IgG causing the emission of green fluorescence, while the 543 nm laser line excited the Texas Red® fluorophore (Excitation/Emission: 596 nm/615 nm) conjugated to the anti-mouse IgG causing the emission of red fluorescence.

### 2.3.7 Identification of a hydrophobic, antigenic region of 2C

In view of the ultimate objective of expressing a soluble region of the 2C protein that could be used to raise antibodies against that protein, the hydrophobic/ hydrophilic and antigenic properties of the amino acid sequence of the 2C protein was analysed with the aim of identifying a hydrophilic region of the protein with several possible antigenic sites.

The internet-based software program ProtScale (Internet 2) was used to construct a Kyte and Doolittle plot of the amino acid sequence of the TMEV 2C protein, indicating the relative hydrophilicity/ phobicity of different regions of the protein. Likewise, the internet-based software program Emboss antigenic (Internet 3) was used to identify antigenic regions of the TMEV 2C protein. The region selected for expression will be referred to as the 2C178 peptide from this point forward.

### 2.3.8 Construction of a recombinant vector for the expression of the 2C178 region of the TMEV 2C protein in *E. coli*

In order to express the 2C178 peptide in *E. coli* cells the coding region for this peptide was inserted into the bacterial expression vector pGEX-2T (Amersham Biosciences) in frame with the coding region for the GST antigen. The coding region for the 2C178 peptide was PCR amplified (see Appendix C for primers and thermocycle reaction programs) using the high fidelity DNA-dependent DNA polymerase Expand (Promega) and pGDVII-WT DNA (see Appendix A) as a template. Subsequent to electrophoresis on a 1% agarose gel at 100 V, the PCR product was excised and purified using the Wizard SV Gel and PCR Clean-up System (Promega) according to manufacturer's instructions.

Both the 2C178 PCR product and the pGEX-2T vector were subjected to restriction digestion with *Bam* H1 and *Eco* R1, following which the digested 2C178 insert and pGEX-2T vector were purified using the Wizard SV Gel and PCR Clean-up System,

subsequent to electrophoresis on a 1% agarose gel. The coding sequences for the 2C178 peptide was subcloned into the linearised pGEX-2T vector using T4 DNA ligase (Promega) at room temperature for four hours followed by overnight incubation at 4°C.

Competent *E. coli* JM109 cells (Promega) were transformed with the ligation mix and transformed cells were spread plated on Luria agar plates containing ampicillin (100 μg/ml) (Roche). Plates were incubated at 37°C overnight. Bacterial colonies were inoculated into 5 ml Luria Broth cultures containing ampicillin (100μg/ml) and incubated overnight at 37°C, shaking at 200 rpm. The presence of recombinant plasmids containing the correct insert in the bacterial cultures was detected by colony PCR as described in *Section 2.3.1.*

The recombinant plasmid was termed pLMGT2C178 and was isolated using the QIAprep ® Spin Miniprep Kit (Qiagen). The presence of correct inserts was confirmed by restriction analysis with *Bam* H1 and *Eco* R1, and later by chain-termination-based sequencing (performed by Inqaba Biotechnical Industries (Pty) Ltd) using a standard 3' pGEX Sequencing Primer (Amersham Biosciences, see appendix C).

### 2.3.9 Expression of 2C178 in *E. coli* BL-21 cells and pilot-scale purification by affinity chromatography

*(i) IPTG-induced expression of the 2C178 peptide in E. coli BL-21 cells*

No more than 48 hours prior to the expression of the GST-2C178 peptide, 30 μl of competent *E. coli* BL-21 cells were transformed with 1 μg of either pLMGT2C178 or pGEX-2T DNA and transformed cells were spread plated on Luria agar plates containing ampicillin (100 μg/ml) and incubated at 37°C overnight.

Bacterial colonies were inoculated into 5 ml Luria broth cultures containing ampicillin (100 μg/ml) and incubated overnight at 37°C, shaking at 200 rpm. A 100 μl sample confluent bacterial culture was inoculated into 100 ml Luria broth containing

ampicillin (100 μg/ml) and incubated at 37°C, shaking at 200 rpm until bacterial growth was mid log phase and the $OD_{600}$ of the culture was 0.700. Expression of the GST-2C178 fusion peptide and GST protein was induced for 3 hours at 37°C, shaking at 200 rpm, through the addition of isopropyl-beta-D-thiogalactopyranoside (IPTG, Fermentas) to the cultures at a final concentration of 5 mM. Untransformed *E. coli* BL-21 cells grown to a confluency of $OD_{600}$= 0.7 were also subjected to IPTG-induction as a negative control.

*(ii) Purification of the 2C178 peptide by affinity chromatography*

Following IPTG-induced protein expression, bacterial cells were pelleted at 9 000 rpm at 4°C for 1 minute and resuspended in 0.5ml ice-cold Lysis buffer (5 mM phosphomethylsulfonyl fluoride (PMSF), 1% Triton ×-100 in PBS, pH 7.4). Cells were lysed by sonication at 40 Amps for 2 × 30-second bursts at 4°C. Cell debris was pelleted by centrifugation at 14 000 rpm at 4° C for 5 minutes.

Approximately 16 hours prior to the purification of the GST-2C178 fusion peptide and GST protein, 0.07 g lyophilised glutathione agarose beads (Sigma) were added to 1 ml sterile $dH_2O$ and allowed to swell at 4°C. To purify the expressed GST-2C178 fusion peptide and GST protein, 200 μl swollen glutathione agarose beads were added to 1 ml of each cell lysate and incubated at room temperature for 1 hour, rotating gently every 5 minutes. Impurities were removed from the beads by six wash steps of 1 ml ice-cold Lysis buffer added to the beads and pulse-centrifugation at 6 000 rpm. Both the GST-2C178 fusion peptide and GST protein were eluted from the glutathione agarose beads by incubation by adding 100μl ice-cold elution buffer (50 mM Tris-HCL, pH 8.0, 5 mM reduced glutathione [Sigma]) and incubating at room temperature for 10 minutes. Beads were subjected to pulse-centrifugation at 6 000 rpm. The elution step was repeated three times before pooling all 300 μl of eluent.

*(iii) SDS-PAGE electrophoresis and Western blot analysis of purified 2C178 peptide*

Immediately following purification the GST-2C178 fusion peptide and GST protein were denatured by adding 0.25 volume SDS-PAGE sample buffer and boiling for 5

minutes. Denatured isolates of the GST-2C178 fusion peptide and GST protein were subjected to SDS-PAGE electrophoresis through a 12% SDS-PAGE gel, followed by either staining with Coomassie staining solution (45% methanol, 45% water, 10% glacial acetic acid, 0.002% wt/vol Coomassie Brilliant Blue (Saarchem) or transfer onto Hybond nitrocellulose membrane at 250 A for 1 hour. Remaining protein binding sites on the membrane were blocked by incubating the membrane in BLOTTO solution (10% 1M Tris pH 7.6, 3% 5M NaCl, 5% wt/vol fat-free milk powder, 0.05% Tween 20) overnight at room temperature. GST was detected using the anti-GST Goat IgG Horse radish phosphatase (HRP)-conjugated antibody (Amersham Biosciences) and the ECL Advance ™ Western Blotting Detection Kit (Amersham Biosciences) as per manufacturer's instructions. The resulting chemiluminescence was detected by a 1 second exposure of the nitrocellulose membrane to X-ray film.

## 2.4 RESULTS AND DISCUSSION

### 2.4.1 Construction of recombinant vectors for the expression of TMEV 2B, 2C, 2BC, 3A, 2C60 and 2BC60 coding regions in mammalian cells

*(i) Restriction analysis of recombinant vectors*

The coding regions for the TMEV 2B, 2C, 2BC and 3A proteins as well as the coding regions for the truncated 2C60 and 2BC60 proteins were subcloned into the mammalian expression vector pcDNA3.1/V5-His© TOPO® as described in *Section 2.3.1*. Subsequent to purification from transformed *E. coli* JM109 cells, recombinant vectors underwent restriction analysis with *Bam* H1 (pLMT2B) or *Bam* H1 and *Xba* 1 (pLMT2C, pLMT2BC and pLMT3A) to confirm the presence of the correct insert. Figure 2.4.1 is a digital image of agarose gel electrophoresis of the digested constructs.

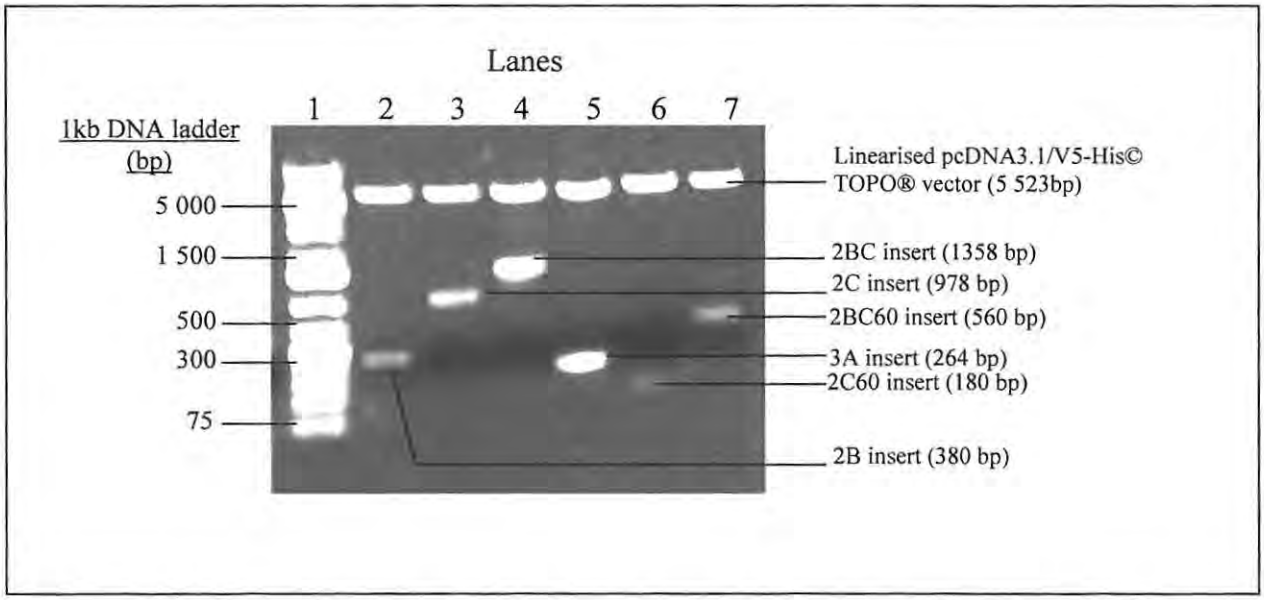


**Figure 2.4.1** Diagnostic restriction digest of recombinant plasmids encoding wild type TMEV proteins. Coding sequences for the TMEV 2B, 2C, 2BC, 3A, 2C60 and 2BC60 proteins were PCR amplified from the cDNA of the viral genome and inserted into the multiple cloning site of the mammalian expression vector pcDNA3.1/V5-His© TOPO® ®. The presence of the correct coding sequence inserts in the recombinant vectors was confirmed via restriction analysis. Digested vectors were electrophoresed through a 1% agarose gel (0.5g agarose, 50ml 1× TAE buffer, 8µl 1mg/ml O'Gene Ruler I kb DNA Ladder Plus (Fermentas), **Lane 2-** pLMT2B digested with *Bam* H1, showing an insert of 380 base pairs (bp), **Lane 3-** pLMT2C digested with *Bam* H1 and *Xba* 1, showing an insert of 978 bp, **Lane 4-** pLMT2BC digested with *Bam* H1 and *Xba* 1, showing an insert of 1357 bp, **Lane 5-** pLMT3A digested with *Bam* H1 and *Xba* 1, showing an insert of 264 bp, **Lane 6-** pLMT2C60 digested with *Bam* H1 and *Xba* 1, showing an insert of 180 bp, **Lane 7-** pLMT2BC60 digested with *Bam* H1 and *Xba* 1, showing an insert of 560 bp.

*(ii) Chain-termination-based sequencing of recombinant vectors*

Chain-termination-based sequencing was performed on the recombinant vectors shown in Figure 2.4.1 by Inqaba Biotechnical Industries (Pty) Ltd) using standard T7 and BGH primers (Invitrogen). All inserts shown in Table 2.3.1 and 2.3.2 were successfully sequenced. All coding sequences for the various TMEV proteins were compared with the sequence of the GDVII strain of TMEV (Pubmed accession number: 2251141). All sequences were in frame with no mutations except a single Glu to Lys substitution mutation located at amino acid 69 on the 2B sequence in the pLMT2B, pLMT2BC and pLMT2BC60 constructs. This mutation was later discovered to be present on the original pGDVII-WT template DNA (see Appendix B for summary of sequencing data)

### 2.4.2 Microscopic examination of BHK-21 cells expressing TME viral proteins

With the aim of characterising the subcellular distribution and effect on host membranes of the TMEV 2B, 2C, 2BC and 3A proteins, BHK-21 cells were transfected with recombinant mammalian expression vectors encoding these proteins. Protein expression progressed for 19 hours before cells were fixed with a paraformaldehyde solution and immunostained with primary antibodies recognising the V5 fusion tag on the C-terminus of the expressed viral proteins as well as primary antibodies raised against specific marker proteins of the ER or Golgi apparatus. Secondary staining was performed with fluorophore-conjugated secondary antibodies. Texas Red® Goat anti-mouse IgG (H+L) and Alexa Fluor® 488 Goat anti-rabbit IgG (H+L) recognised the anti-V5 and anti-ERp60/ anti--β-COP primary antibodies, respectively. Cells were mounted on microscope slides with Vectashield Hard Set Fluorescent Mounting Medium and examined by laser-scanning confocal microscopy. Successful expression of TMEV protein-V5 fusions in transfected and immunostained BHK-21 cells was indicated by the observation of red fluorescence when samples were excited with the 543nm laser line. Staining of organelle marker proteins was identified by green fluorescence when samples were excited with the 543nm laser line.

*(i) TMEV 2B protein transiently expressed in BHK-21 cells*

Transfection efficiency can be described as the proportion of cells in a sample that are transfected with the nucleic acid in question and in these experiments is indicated by the proportion of cells in a sample that are expressing the protein encoded by the transfecting construct. The TMEV 2B protein was successfully expressed in BHK-21 cells but at repeatedly low transfection efficiencies varying between 0.5% - 2%.

Transfection efficiencies were not improved by varying the ratio of DNA: ExGen transfection reagent, by varying the amount of DNA transfected into the cells or even using different isolates of the same plasmid samples. Transfections were also

performed on HeLa and Cos-7 cell lines with no improvement in transfection efficiency. In addition, the transfection efficiency of the recombinant vectors expressing the different TMEV proteins varied greatly despite the transfections with the different constructs being repeatedly performed in the same experiment. The reason for this phenomenon remains unknown. The only variable between cells transfected with the different constructs was the actual coding sequence of the viral protein expressed. This leads to the possibility that the number of cells expressing the viral proteins may not in fact reflect the true transfection efficiency of the experiment but may instead be dependent on the ability of the RNA encoding the viral proteins to exit the nucleus following transcription (Personal communication, Professor T. Wileman). As picornavirus RNA never enters the nucleus during the viral replication cycle it is unlikely that these RNA sequences would encode nuclear export signals. Thus although transfection of the BHK-21 cells with the DNA constructs encoding the viral proteins may have been successful, the export of transcribed viral RNA from the nucleus may have been inefficient to different extents for the different viral protein coding sequences. In future studies this problem could be avoided by cloning the coding sequences for the viral proteins into mammalian expression vectors that encode a nuclear export signal at the C-terminal of the MCS.

All cells expressing the 2B-V5 fusion showed a similar distribution of this protein. Frames A, D and G in Figure 2.4.2 shows the 2B protein located to fine reticular structures with several larger punctate structures concentrated in the perinuclear region. Some of these structures overlapped with the ERp60 stain, as indicated by the yellow signal in frames C, F and I in Figure 2.4.2, while a significant proportion of the 2B-V5 fusion remained separate. This suggests that although a proportion of the 2B protein locates to the ER, this protein may also associate with other host membranes. Although the concentration of 2B in the perinuclear region suggests a possible association with the nuclear envelope, the dispersion of this protein throughout the cytosol as far as the plasma membrane may suggest a possible association with endosomal and/or lysosomal membranes.

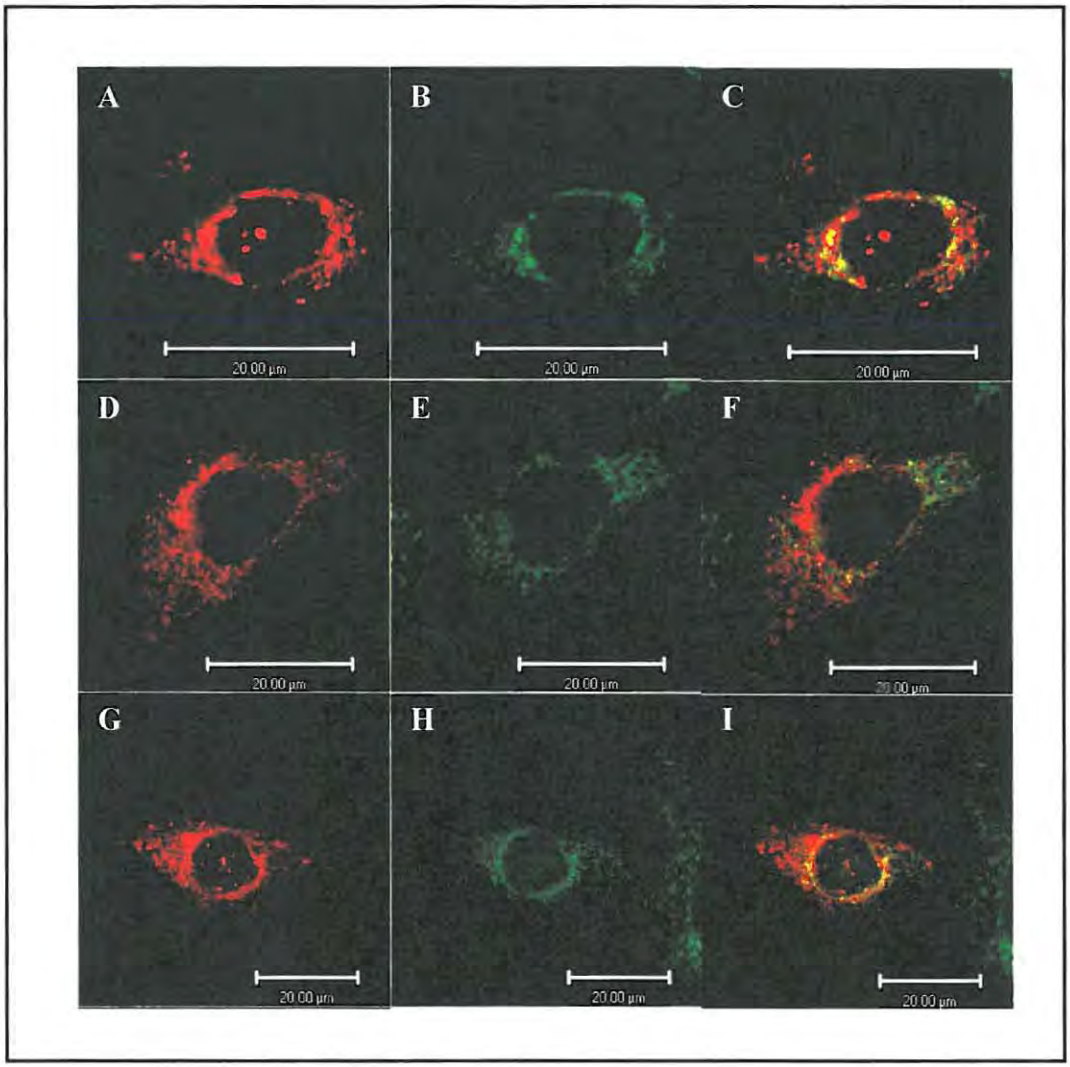


**Figure 2.4.2** Transient expression of TMEV 2B protein in BHK-21 cells stained with antibodies against a marker protein for the ER. BHK-21 cells transfected with pLMT2B and expressing the TMEV 2B-V5 fusion protein imaged using Zeiss LSM 510 Meta confocal microscope and LSM 510 software. Cells are immunostained with primary antibodies raised against the V5 tag and the ER marker protein, as well as fluorophore-conjugate secondary antibodies. Red fluorescence indicates the position of the 2B-V5 fusion protein (**Frames A, D, G**), green fluorescence indicates the ERp60 stain (**Frames B, E, H**) and yellow signal in the merged images (**Frames C, F and I**) indicates an overlap of red and green signals.

All BHK-21 cells expressing the 2B-V5 fusion and counterstained with antibodies against the Golgi apparatus marker protein β-COP (Figure 2.4.3) showed the same distribution of the 2B protein (Frames A, D and G) as those counterstained with anti-ERp60. Interestingly some of the 2B accumulated in the perinuclear region appeared to overlap with the β-COP stain indicating a possible association between TMEV 2B and membranes of the CGN.

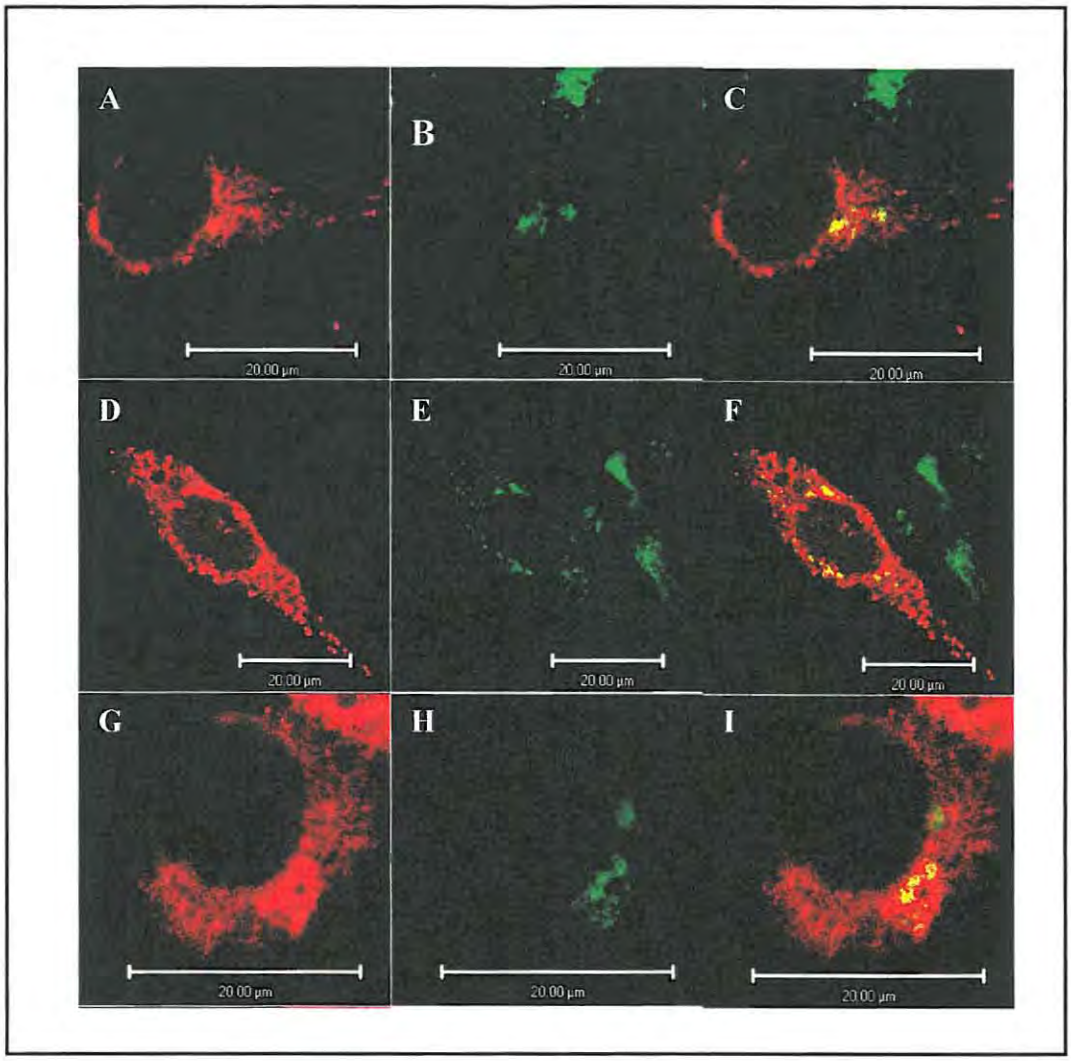


**Figure 2.4.3** Transient expression of TMEV 2B protein in BHK-21 cells stained with antibodies against a marker protein for the Golgi apparatus. BHK-21 cells transfected with pLMT2B and expressing the TMEV 2B-V5 fusion protein imaged using Zeiss LSM 510 Meta confocal microscope and LSM 510 software. Cells are immunostained with primary antibodies raised against the V5 tag and the Golgi apparatus marker protein β-COP, as well as fluorophore-conjugate secondary antibodies. Red fluorescence indicates the position of the 2B-V5 fusion protein (**Frames A, D, G**), green fluorescence indicates the β-COP stain (**Frames B, E, H**) and yellow signal in the merged images (**Frames C, F and I**) indicates an overlap of red and green signals.

As mentioned in *Section 1.3.2*, the PV 2B protein localises exclusively with the Golgi membranes causing the complete disassembly of the Golgi cisternae, consequently disrupting protein secretion through the exocytic pathway (Doedens and Kirkegaard, 1995). In contrast, the FMDV 2B protein was observed to locate to a reticular stain closely associated with that of the ERp57 protein, suggesting an association with membranes of the ER (Moffat *et al*, 2005). The distribution of the TMEV 2B protein most closely mimics that of the corresponding FMDV protein although these results

suggest that some localisation to the Golgi apparatus may also occur. No gross disassembly of the Golgi complex was observed, although this can not be confirmed without examining cells transiently expressing the 2B protein by transmission electron microscopy.

Further studies are required to conclusively determine the subcellular localisation of the TMEV 2B protein in host cells and its effect on membranes of the host cell secretory pathway. These would include further localisation studies using marker proteins for lysosomal and endosomal membranes, electron microscopic examination of cells transiently expressing the viral protein and the coimmunoprecipitation of the 2B protein and the various organelle marker proteins from membrane fractions pertaining to specific organelles. The biological significance of the possible association of the TMEV 2B protein with membranes derived from the ER and Golgi complex remains unexplored. The effect of the TMEV 2B protein on protein secretion through the exocytic pathway could be determined through the implementation of protein transport assays as described in Doedens and Kirkegaard (1995) and Moffat *et al* (2005).

*(ii) TMEV 2C protein transiently expressed in BHK-21 cells*

The 2C protein was successfully expressed in BHK-21 cells as a 2C-V5 fusion with transfection efficiencies of 1% - 5% achieved. Although higher than that observed with cells expressing the 2B-V5 fusion, this efficiency is also extremely low compared to the advertised transfection efficiency of >80% expected with the ExGen transfection reagent (Fermentas).

In expressing cells, the 2C-V5 fusion protein showed several distributions that appeared to be linked to the amount of protein expression. At low expression levels 2C located to a relatively faint reticular stain (Frames A, D and G of Figure 2.4.4) that partially overlapped with the ERp60 stain (Frames C, F and I of Figure 2.4.4). At higher levels of expression 2C was concentrated in the perinuclear region and was also located in large structures adjacent to the nucleus (Frames A, D and G of Figure 2.4.5) that overlapped with the β-COP stain (Frames C, F and I of Figure 2.4.5). Of

the cells expressing the 2C protein, an approximately equal number showed the two different protein distributions. These observations suggest that the TMEV 2C protein may localise to different regions of the host cell, possibly at different stages of protein expression. Further examination of this phenomenon through the examination of cells stably expressing the TMEV 2C protein is necessary to resolve this whether this is the case. Furthermore, in addition to colocalising with marker proteins of the ER and Golgi apparatus, the persistently evident perinuclear stain suggests that this protein may also be associated with either the nuclear envelope or the rough endoplasmic reticulum (RER) that is continuous with the nuclear envelope.

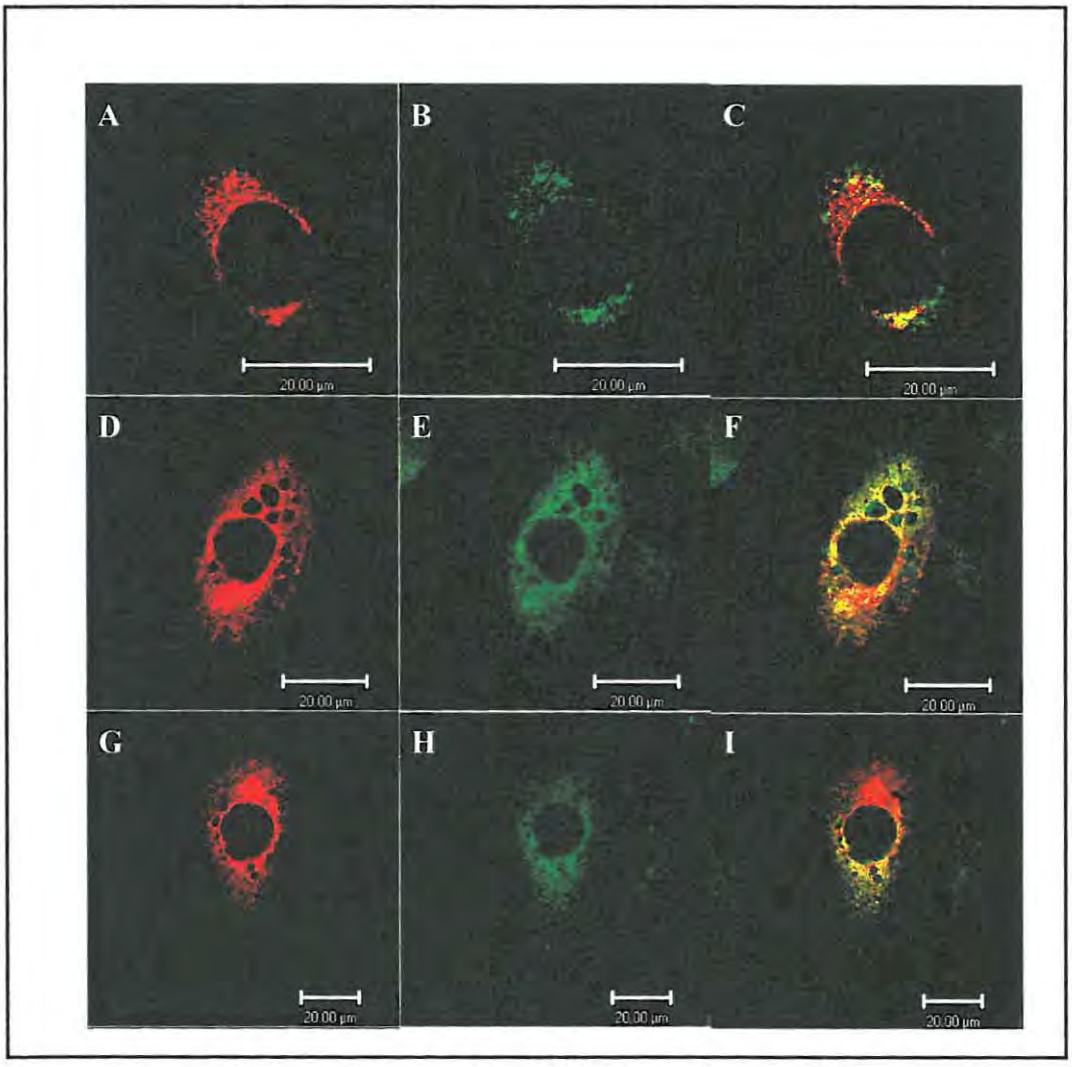


**Figure 2.4.4** Transient expression of TMEV 2C protein in BHK-21 cells stained with antibodies against a marker protein for the ER. BHK-21 cells transfected with pLMT2C and expressing the TMEV 2C-V5 fusion protein imaged using Zeiss LSM 510 Meta confocal microscope and LSM 510 software. Cells are immunostained with primary antibodies raised against the V5 tag and the ER marker protein ERp60, as well as fluorophore-conjugate secondary antibodies. Red fluorescence indicates the position of the 2C-V5 fusion protein (**Frames A, D, G**), green fluorescence indicates the ERp60 stain (**Frames B, E, H**) and yellow signal in the merged images (**Frames C, F and I**) indicates an overlap of red and green signals.

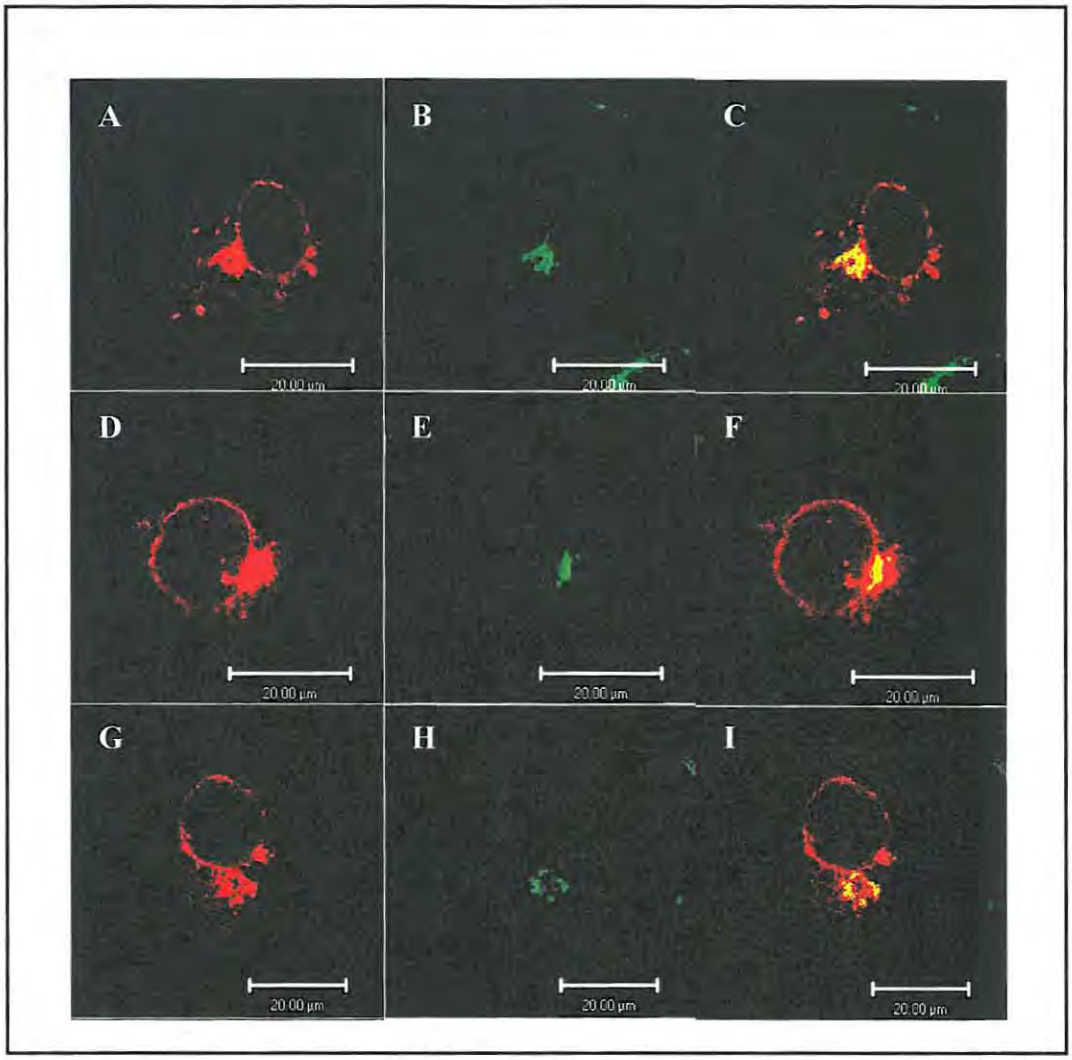


**Figure 2.4.5** Transient expression of TMEV 2C protein in BHK-21 cells stained with antibodies against a marker protein for the Golgi apparatus. BHK-21 cells transfected with pLMT2C and expressing the TMEV 2C-V5 fusion protein imaged using Zeiss LSM 510 Meta confocal microscope and LSM 510 software. Cells are immunostained with primary antibodies raised against the V5 tag and the Golgi apparatus marker protein β-COP, as well as fluorophore-conjugate secondary antibodies. Red fluorescence indicates the position of the 2C-V5 fusion protein (**Frames A, D, G**), green fluorescence indicates the β-COP stain (**Frames B, E, H**) and yellow signal in the merged images (**Frames C, F and I**) indicates an overlap of red and green signals.

As already mentioned in *Section 1.3.3*, the PV 2C protein locates to reticular-like structures and is known to associate with and modify RER membranes (Aldabe and Carasco, 1995; Bienz *et al*, 1987; Bienz *et al*, 1990; Bienz *et al*, 1992; Cho *et al*, 1994; Schlegel *et al*, 1996). The FMDV 2C protein also interacts with RER membranes but has also been shown to localise to large perinuclear structures (Moffat *et al*, 2005) similar to those observed with the transient expression of the TMEV 2C protein. In addition, Knox *et al* (2005) observed that at early stages of FMDV infection 2C locates to a diffuse punctate pattern to one side of the nucleus and is

concentrated into larger structures adjacent to the nucleus at later stages. The evidence presented in Figures 2.4.4 and 2.4.5 suggests that the TMEV 2C protein may interact with host membranes in a similar manner to the FMDV 2C protein.

As described above with the 2B protein, further studies are required to conclusively determine whether the 2C protein is membrane-associated in host cells and to explore the biological significance of the interactions formed between the 2C protein and host membranes with respect to its effects on host cell protein secretion.

*(iii) TMEV 2BC protein transiently expressed in BHK-21 cells*

Expression of the TMEV 2BC-V5 fusion protein was achieved in BHK-21 cells but transfection efficiencies were extremely low with fewer than thirty cells expressing the protein per sample, i.e. transfection efficiency varied between 0.010% - 0.015%. Consequently it was difficult to obtain a number of quality images of the subcellular distribution of the 2BC protein.

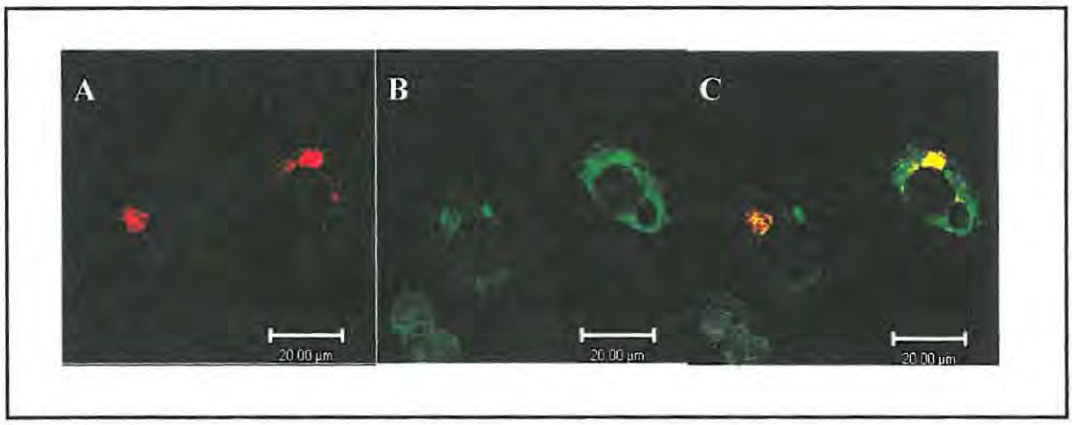


**Figure 2.4.6** Transient expression of TMEV 2BC protein in BHK-21 cells stained with antibodies against a marker protein for the ER. BHK-21 cells transfected with pLMT2BC and expressing the TMEV 2BC-V5 fusion protein imaged using Zeiss LSM 510 Meta confocal microscope and LSM 510 software. Cells are immunostained with primary antibodies raised against the V5 tag and the ER marker protein ERp60, as well as fluorophore-conjugate secondary antibodies. Red fluorescence indicates the position of the 2BC-V5 fusion protein (**Frames A, D, G**), green fluorescence indicates the ERp60 stain (**Frames B, E, H**) and yellow signal in the merged images (**Frames C, F and I**) indicates an overlap of red and green signals.

In all cells expressing the 2BC-V5 fusion protein (frame A, Figure 2.4.6) most of the 2BC protein was located to large perinuclear structures that closely overlapped with the β-COP stain (Frame C, F and I, Figure 2.4.7), suggesting that this protein localises

to the peripheral Golgi, while the remainder of the protein was distributed to small punctate structures throughout the cytoplasm (Frames A, D and G, Figure 2.4.7).

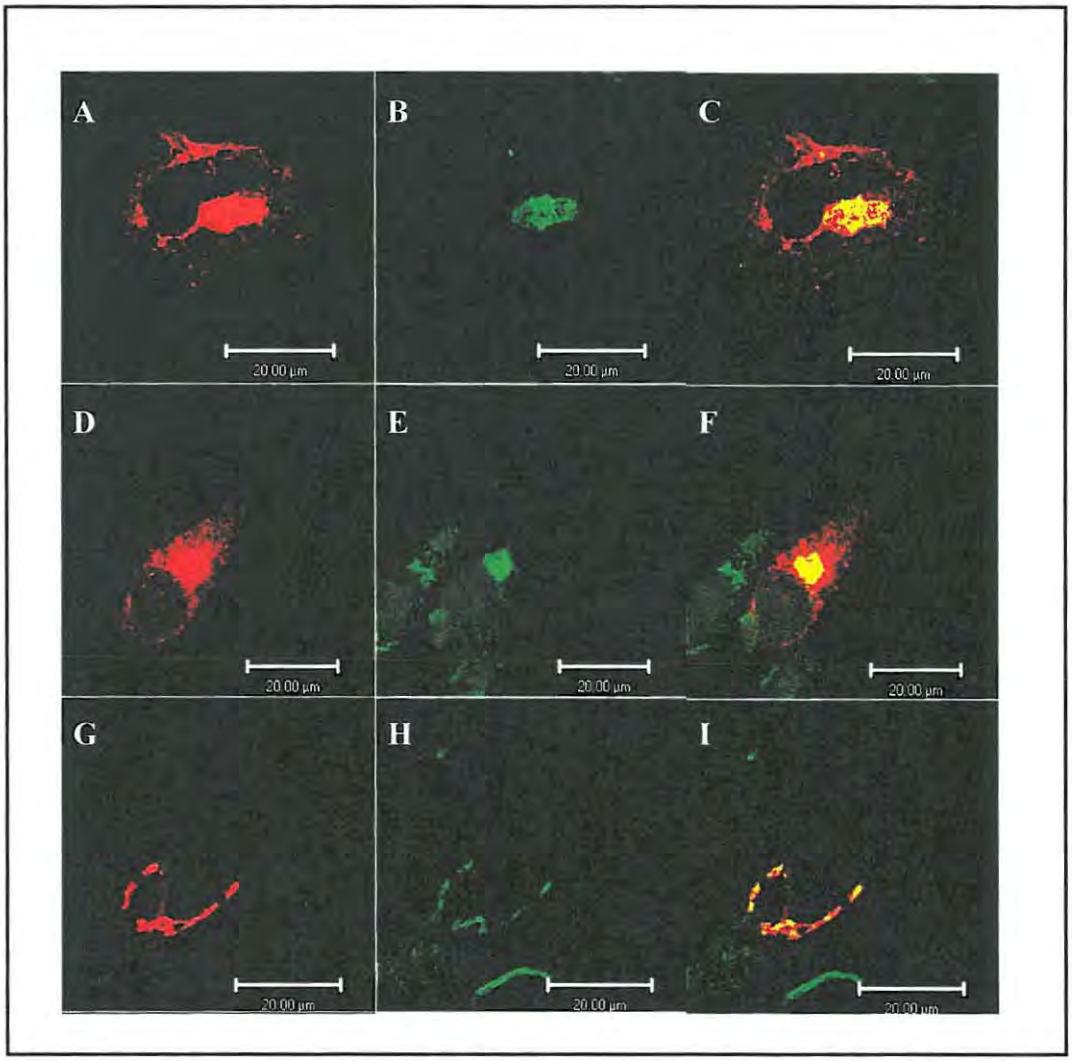


**Figure 2.4.7** Transient expression of TMEV 2BC protein in BHK-21 cells stained with antibodies against a marker protein for the Golgi apparatus. BHK-21 cells transfected with pLMT2BC and expressing the TMEV 2BC-V5 fusion protein imaged using Zeiss LSM 510 Meta confocal microscope and LSM 510 software. Cells are immunostained with primary antibodies raised against the V5 tag and the Golgi apparatus marker protein β-COP, as well as fluorophore-conjugate secondary antibodies. Red fluorescence indicates the position of the 2BC-V5 fusion protein (**Frames A, D, G**), green fluorescence indicates the β-COP stain (**Frames B, E, H**) and yellow signal in the merged images (**Frames C, F and I**) indicates an overlap of red and green signals.

These observations were reminiscent of the localisation of the FMDV 2BC protein to the Golgi apparatus determined by Moffat *et al* (2005). However, unlike with the FMDV 2BC protein, there was almost complete overlap of the β-COP stain with the 2BC-V5 stain. Interestingly, the distribution of the TMEV 2BC protein (Frames A, D

and G, Figure 2.4.7) in BHK-21 cells was similar to that of TMEV 2C in cells expressing the protein at high levels (Frames A, D and G of Figure 2.4.5) in that both proteins showed a strong overlap with the β-COP stain. The small punctate structures extended throughout the cytosol, frequently as far as the plasma membrane, suggesting a possible association with endosomal and/or lysosomal membranes.

Observation revealed that in all cells expressing the 2BC protein, the ERp60 stain was very faint compared to untransfected neighbouring cells and no clear overlap of red and green signals was observed. As ERp60 is located in the lumen of the ER membranes it is possible that the 2BC protein associates with ER membranes, effectively coating them and preventing access of the anti-ERp60 antibody to the marker protein during the immunostaining process. However, the transient expression of FMDV 2BC protein has been shown to cause the redistribution of the ER marker protein ERp57 (Moffat *et al*, 2005). There was some overlap between the transiently expressed TMEV 2BC protein and the ERp60 stain (Frame C, Figure 2.4.6), however without examining cells transiently expressing the 2BC protein by transmission electron microscopy it can not be determined whether the TMEV 2BC protein has a redistribution effect on these membranes.

Rust *et al* (2001) demonstrated the colocalisation of the PV 2BC protein with ER-derived membranes containing the marker protein COPII. In addition the FMDV 2CB protein is responsible for the inhibition of protein transport to the plasma membrane (Moffat *et al*, 2005) and the PV 2BC protein has also shown some ability to inhibit ER-to-Golgi transport (Doedens and Kirkegaard, 1995). In view of these findings with other picornavirus 2BC proteins it is not unlikely that the TMEV 2BC protein does associate with ER membranes and may affect ER-to-Golgi protein transport. These phenomena will be examined in future studies using protein transport assays in addition to electron microscopic examination of cells transiently expressing the TMEV 2BC protein, as mentioned above.

However in order to further explore the interactions of the 2BC protein with host cell components, the membrane association of this protein must first be confirmed in further studies.

The biological significance of the possible membrane association of the TMEV 2BC protein is unexplored. The PV 2BC protein is capable of inducing the proliferation of vesicles from secretory pathway membranes. In view of this, further studies may also focus on the ability of TMEV 2BC to modify membranes of the secretory pathway and cause the proliferation of membranous vesicles.

*(iv) TMEV 3A protein transiently expressed in BHK-21 cells*

Transfection of cells with the pLMT3A construct resulted in far higher transfection efficiencies than those experienced with constructs encoding the 2B, 2C and 2BC proteins. Efficiencies ranging from 5% - 10% were observed with almost all cells that expressed the 3A protein displaying very high levels of protein expression. However, despite the relative success of these transfection experiments when compared to those with pLMT2B, pLMT2C and pLMT2BC, these efficiencies are still low compared to the possible transfection efficiency of >80% with the ExGen transfection reagent (Fermentas). As mentioned above, these experiments were conducted repeatedly together with the constructs encoding the other wild type TMEV proteins.

The difference in "transfection efficiencies" thus indicates that the actual sequence of the protein coding region is somehow important for viral protein expression in mammalian cells transfected with cDNA encoding that protein. It is possible that a larger proportion of cells were successfully transfected but that expression levels in these cells was too low to be detected by immunofluorescence microscopy. However, this is unlikely as there was no significant difference observed in the transfection efficiencies of any of the plasmids encoding the TMEV proteins in cells with a 12-hour expression period compared to those with a 19-hour expression period. The transfection efficiencies experienced with the different plasmids encoding the 2B, 2C, 2BC and 3A proteins did not vary significantly when BHK-21 cells were transfected with different isolates of these plasmids, thus indicating that the variation in transfection efficiencies was not a product of varying DNA quality.

The TMEV 3A protein stain overlapped with stains of both the ER marker protein ERp60 (Figure 2.4.8) and the peripheral Golgi marker protein β-COP (Figure 2.4.9.).

The ERp60 stain was modified in cells expressing the 3A protein compared to untransfected neighbouring cells with the ER appearing distorted with large bulbous swellings that overlapped with the location of the 3A protein. In addition, the 3A protein partially overlapped with the β-COP stain in approximately 30% of the cells expressing the protein and in approximately 10% of expressing cells, at particularly high levels of 3A protein expression, the β-COP stain appeared dispersed throughout the cytoplasm.

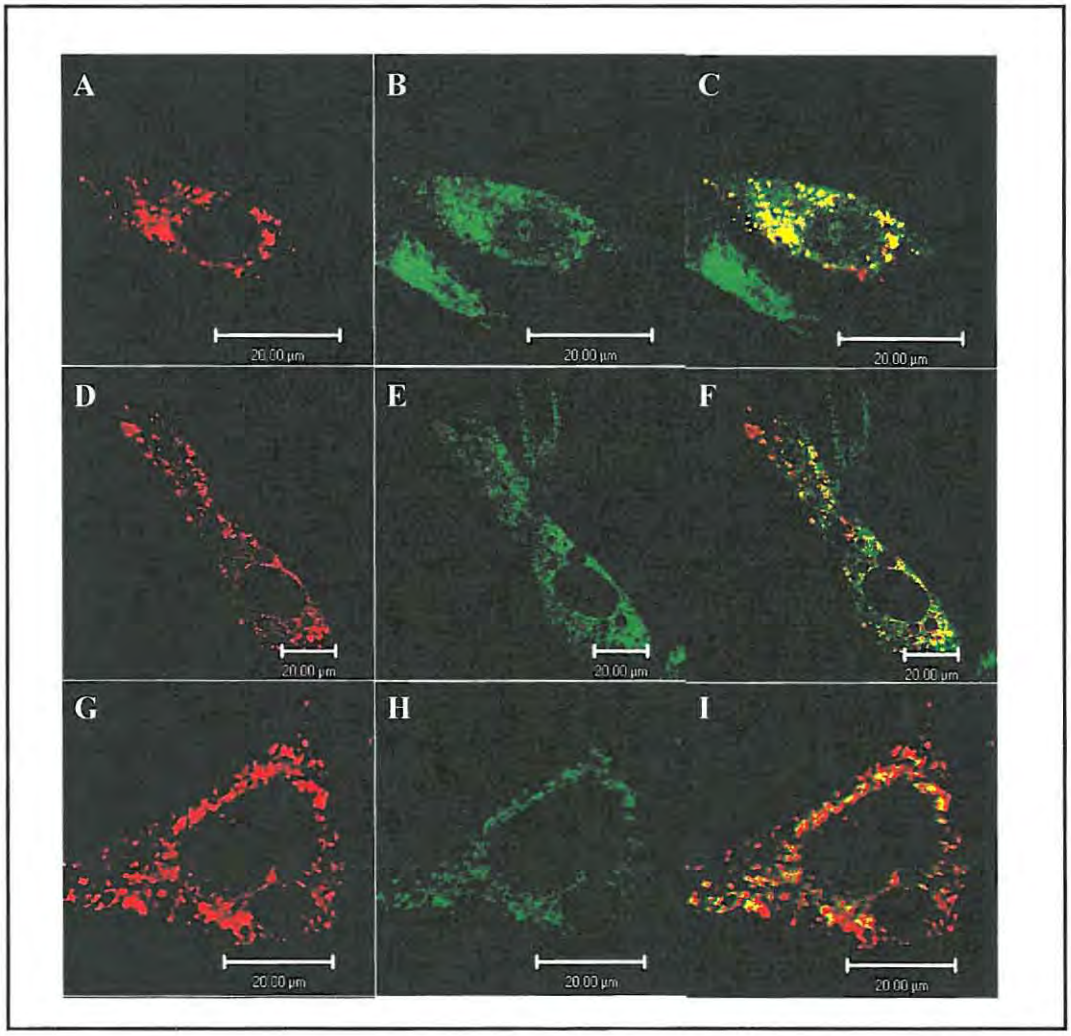


**Figure 2.4.8** Transient expression of TMEV 3A protein in BHK-21 cells stained with antibodies against a marker protein for the ER. BHK-21 cells transfected with pLMT3A and expressing the TMEV 3A-V5 fusion protein imaged using Zeiss LSM 510 Meta confocal microscope and LSM 510 software. Cells are immunostained with primary antibodies raised against the V5 tag and the ER marker protein ERp60, as well as fluorophore-conjugate secondary antibodies. Red fluorescence indicates the position of the 3A-V5 fusion protein (**Frames A, D, G**), green fluorescence indicates the ERp60 stain (**Frames B, E, H**) and yellow signal in the merged images (**Frames C, F and I**) indicates an overlap of red and green signals.

PV 3A is involved in the proliferation of virus-induced vesicles (Suhy *et al*, 2000) and inhibits ER-to-Golgi protein trafficking (Choe *et al*, 2005), causing the

accumulation of proteins otherwise destined for secretion and the ensuing distortion and extreme swelling of the ER cisternae (Doedens *et al*, 1997; Neznanov *et al*, 2001). FMDV 3A is also associated with ER membranes but does not affect ER-to-Golgi trafficking (Moffat *et al*, 2005; O'Donnell *et al*, 2001; Monteyne *et al*, 1997). As mentioned in *Section 1.3.6*, only the 3A proteins of PV and closely related serotypes are known to affect anterograde protein trafficking. The 3A proteins of rhinovirus 14, hepatitis A virus and enterovirus 71 and both the virulent GDVII strain and the non-virulent BeAn strain of TMEV do not affect protein secretion (Choe *et al*, 2005; O'Donnel *et al*, 2001).

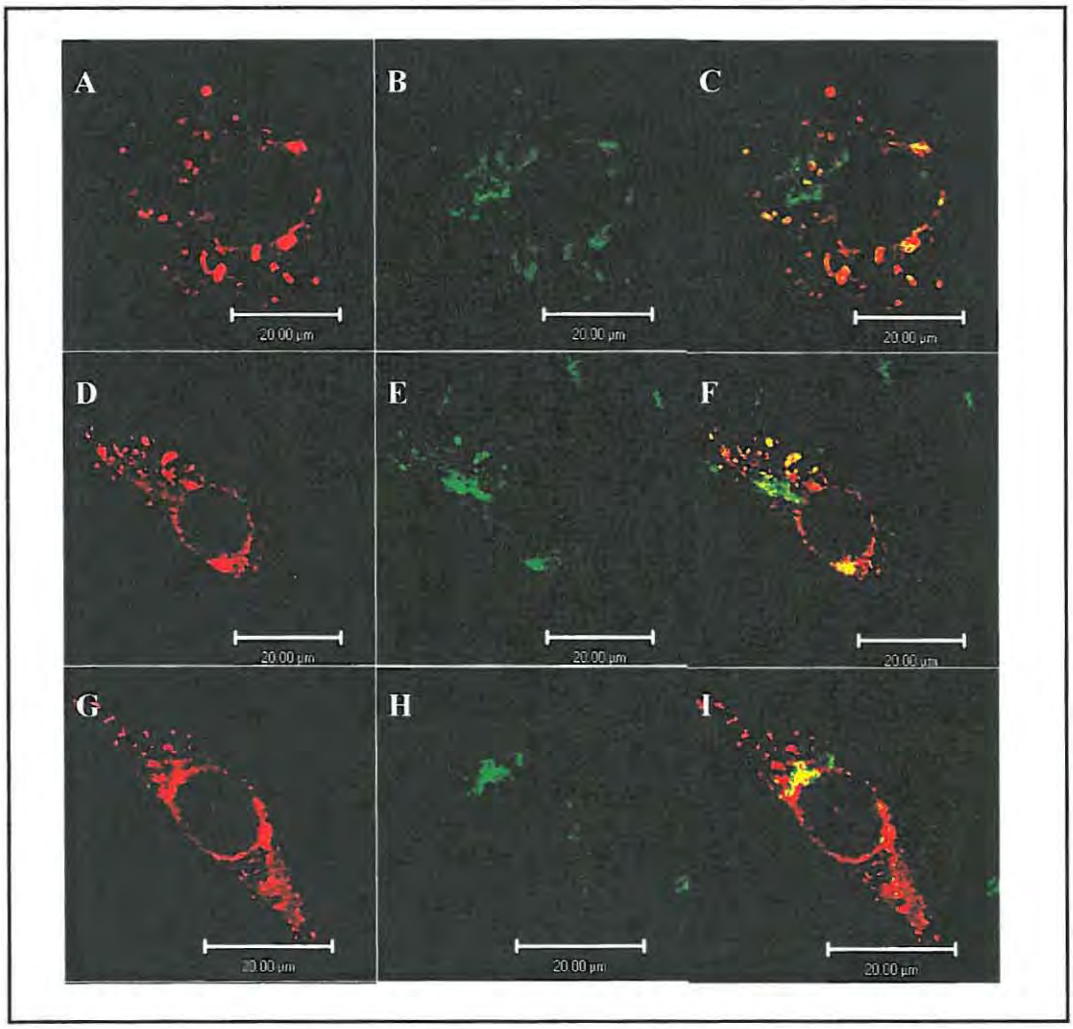


**Figure 2.4.9** Transient expression of TMEV 3A protein in BHK-21 cells stained with antibodies against a marker protein for the Golgi apparatus. BHK-21 cells transfected with pLMT3A and expressing the TMEV 3A-V5 fusion protein imaged using Zeiss LSM 510 Meta confocal microscope and LSM 510 software. Cells are immunostained with primary antibodies raised against the V5 tag and the Golgi apparatus marker protein β-COP, as well as fluorophore-conjugate secondary antibodies. Red fluorescence indicates the position of the 3A-V5 fusion protein (**Frames A, D, G**), green fluorescence indicates the β-COP stain (**Frames B, E, H**) and yellow signal in the merged images (**Frames C, F and I**) indicates an overlap of red and green signals.

Taken together the results obtained in this study and the studies mentioned above indicate that the TMEV 3A protein possibly modifies ER (and possibly Golgi apparatus) membranes for a purpose not involved in the blockage of protein secretion. Further studies may involve an investigation of the ability of this protein to bind host membranes and induce proliferation of vesicles in BHK-21 cells.

*(v) TMEV truncated 2C and 2BC proteins transiently expressed in BHK-21 cells*

The transfection efficiencies obtained through the transfection of BHK-21 cells with the pLMT2C and pLMT2BC constructs encoding the wild type TMEV 2C and TMEV 2BC proteins were excessively low. The N-terminal 60 amino acids of the picornavirus 2C protein are thought to include the residues responsible for membrane association and the RNA binding activity of the protein (Banerjee *et al*, 2004; Teterina *et al*, 1997; Echeverri and Dasgupta, 1995). In view of this it was postulated that expressing only the first 60 amino acids of the 2C protein in the 2C and 2BC coding sequences might not affect the subcellular localisation of these proteins.

The transfection of BHK-21 cells with the recombinant vectors encoding the truncated 2C and 2BC proteins resulted in transfection efficiencies ranging from 10% - 30%. This result contrasted greatly with the low transfection efficiencies observed with the wild type 2C and 2BC proteins. The reason for this increased efficiency is unknown. All transfection experiments were carried out repeatedly alongside transfections with the recombinant vectors encoding the truncated 2C and 2BC proteins, indicating once again that the efficiency of viral protein expression in transfected mammalian cells is affected by the coding sequence of the protein.

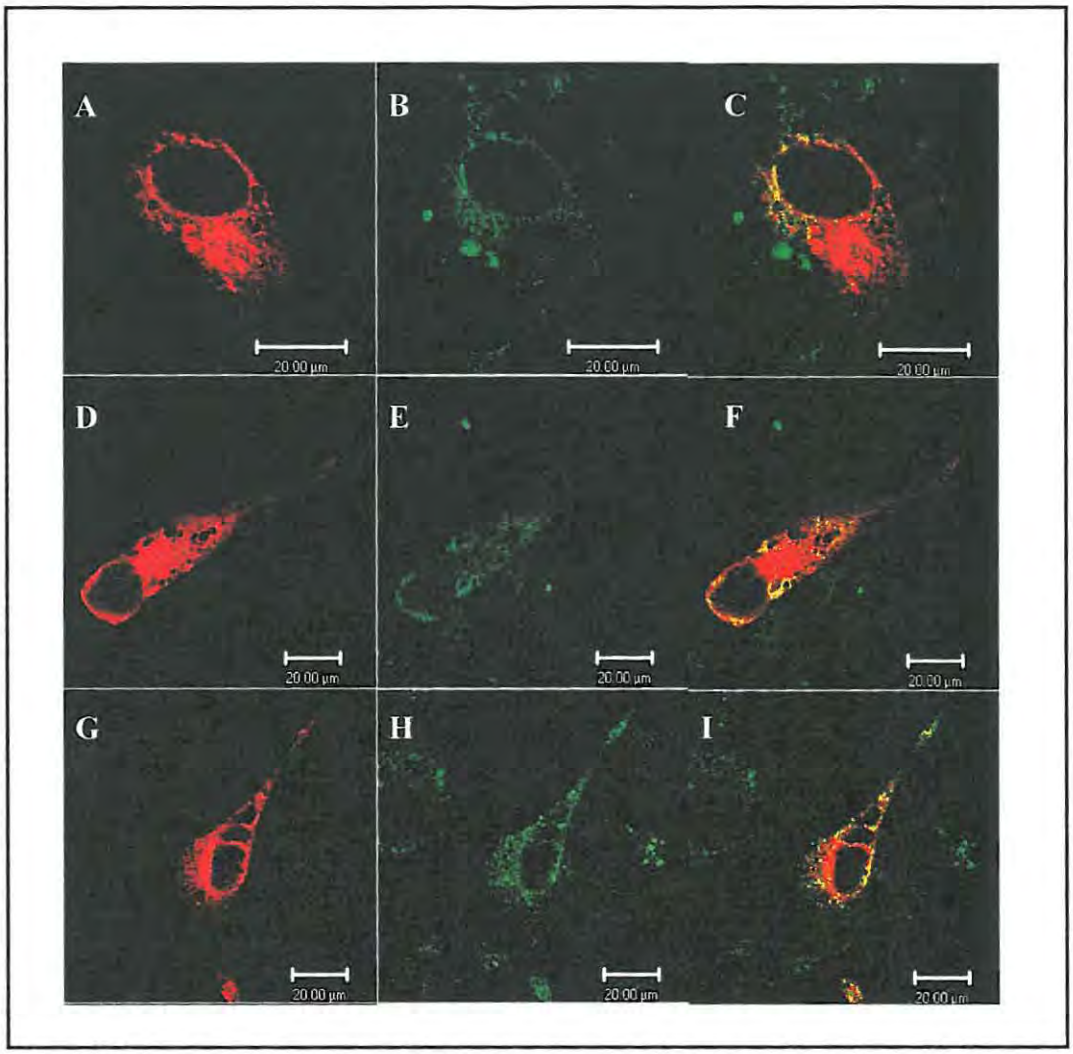


**Figure 2.4.10** Transient expression of TMEV 2C60 protein in BHK-21 cells stained with antibodies against a marker protein for the ER. BHK-21 cells transfected with pLMT2C60 and expressing the TMEV 2C60-V5 fusion protein imaged using Zeiss LSM 510 Meta confocal microscope and LSM 510 software. Cells are immunostained with primary antibodies raised against the V5 tag and the ER marker protein ERp60, as well as fluorophore-conjugate secondary antibodies. Red fluorescence indicates the position of the 2C60-V5 fusion protein (**Frames A, D, G**), green fluorescence indicates the ERp60 stain (**Frames B, E, H**) and yellow signal in the merged images (**Frames C, F and I**) indicates an overlap of red and green signals.

It is possible that the TMEV proteins are cytotoxic to varying extents resulting in the death of cells expressing these proteins and thus the apparent low transfection efficiencies. This is unlikely as there was no significant observable difference in the number of cells surviving after expression of the different wild type and truncated TMEV proteins. A possible, although unlikely, alternative explanation is that the truncation of the 2C coding sequence created a nuclear export signal on the mRNA, protecting the transcribed RNA from being degraded in the nucleus and increasing export efficiency.

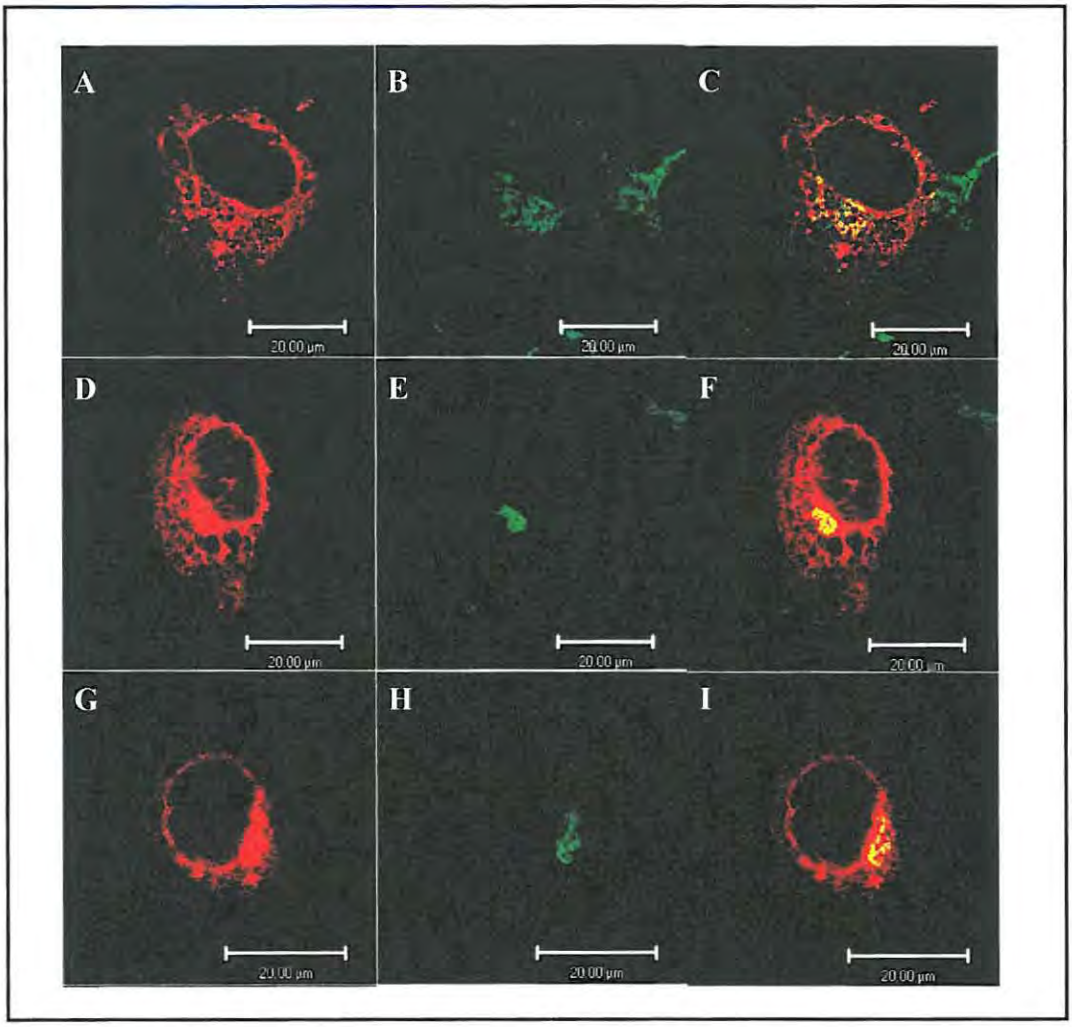


**Figure 2.4.11** Transient expression of TMEV 2C60 protein in BHK-21 cells stained with antibodies against a marker protein for the Golgi apparatus. BHK-21 cells transfected with pLMT2C60 and expressing the TMEV 2C60-V5 fusion protein imaged using Zeiss LSM 510 Meta confocal microscope and LSM 510 software. Cells are immunostained with primary antibodies raised against the V5 tag and the Golgi apparatus marker protein β-COP, as well as fluorophore-conjugate secondary antibodies. Red fluorescence indicates the position of the 2C60-V5 fusion protein (**Frames A, D, G**), green fluorescence indicates the β-COP stain (**Frames B, E, H**) and yellow signal in the merged images (**Frames C, F and I**) indicates an overlap of red and green signals.

The distribution of the truncated 2C protein (2C60) was indistinguishable from that of the wild type 2C protein. At low expression levels 2C60 was located to a reticular stain, partially overlapping with the ERp60 stain (Frames A, D and G, Figure 2.4.10), and at high levels it was located to a perinuclear stain and large structures adjacent to the nucleus that partially overlapped with the β-COP stain (Frames A, D and G, Figure 2.4.11). An approximately equal number of cells showed each of these distributions.

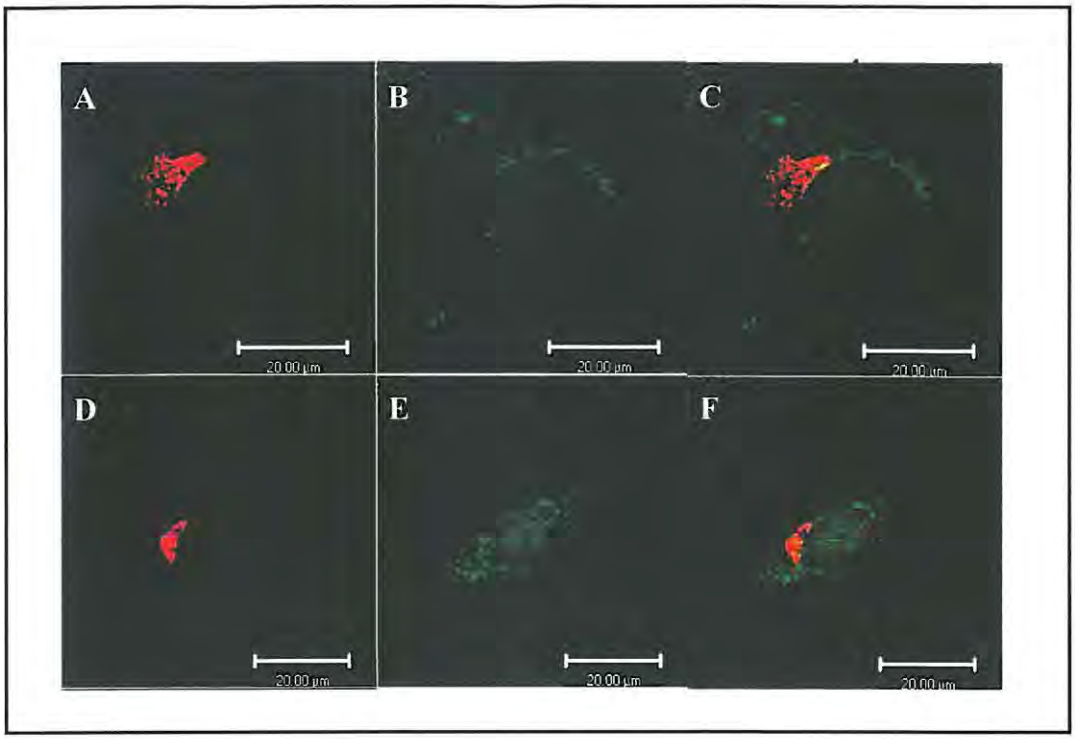


**Figure 2.4.12** Transient expression of TMEV 2BC60 protein in BHK-21 cells stained with antibodies against a marker protein for the ER. BHK-21 cells transfected with pLMT2BC60 and expressing the TMEV 2BC60-V5 fusion protein imaged using Zeiss LSM 510 Meta confocal microscope and LSM 510 software. Cells are immunostained with primary antibodies raised against the V5 tag and the ER marker protein ERp60, as well as fluorophore-conjugate secondary antibodies. Red fluorescence indicates the position of the 2BC60-V5 fusion protein (**Frames A, D, G**), green fluorescence indicates the ERp60 stain (**Frames B, E, H**) and yellow signal in the merged images (**Frames C, F and I**) indicates an overlap of red and green signals.

Similarly, the distribution of the truncated 2BC protein (2BC60) was indistinguishable from that of the wild type 2BC protein. 2BC60 was located to large structures adjacent to the nucleus that almost completely overlapped with the β-COP stain (Frames A, D and G, Figure 2.4.13). As with the wild type 2BC, smaller punctate structures were also located in the cytosol. These structures extended to the plasma membrane in a distribution not dissimilar to that of the LAMP1 (a lysosomal marker protein) stain recorded by Knox *et al*, 2005. Very little or no overlap of the 2BC60 protein and the ERp60 stain and, as with wild type 2BC, the ERp60 stain was very faint in most cells expressing the 2BC60 protein (Frames A and D, Figure 2.4.12).

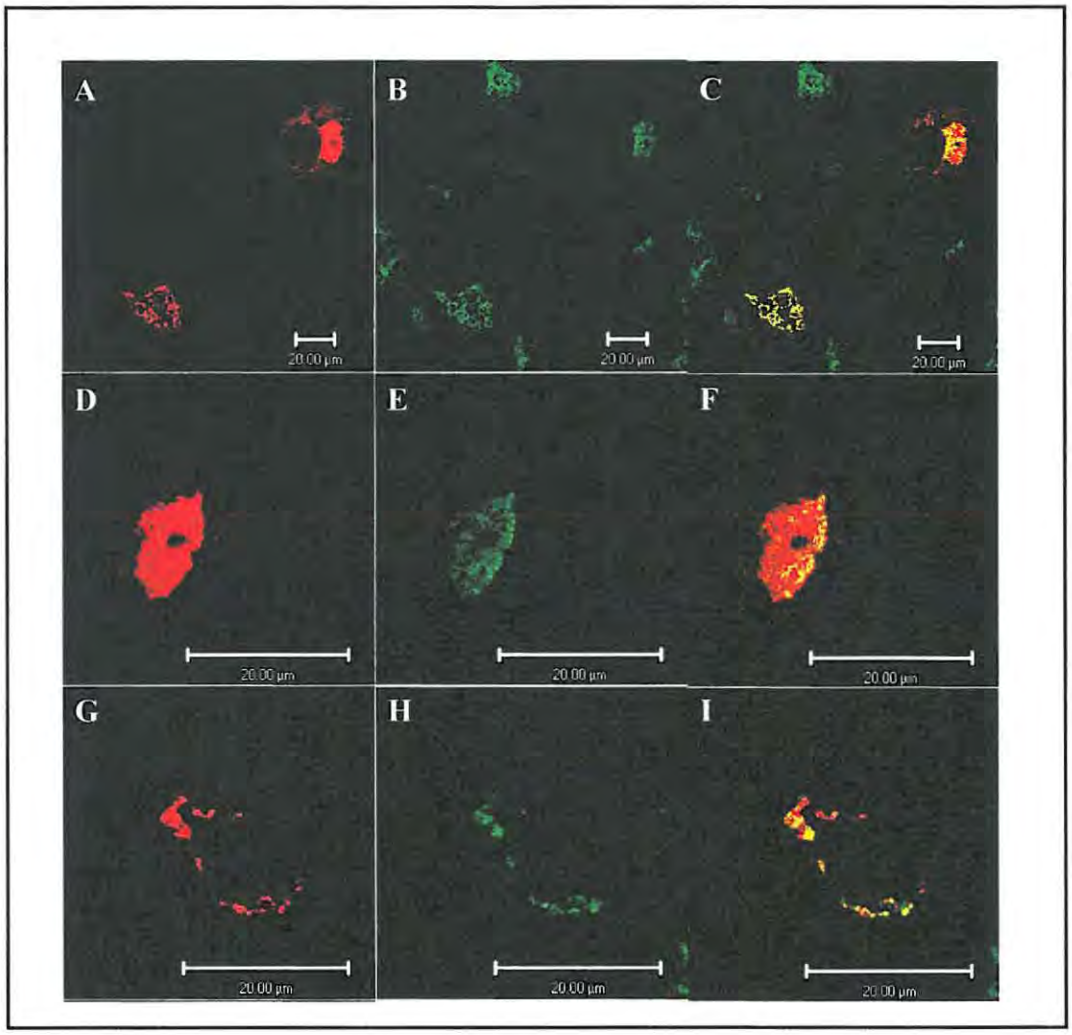


**Figure 2.4.13** Transient expression of TMEV 2BC60 protein in BHK-21 cells stained with antibodies against a marker protein for the Golgi apparatus. BHK-21 cells transfected with pLMT2BC60 and expressing the TMEV 2BC60-V5 fusion protein imaged using Zeiss LSM 510 Meta confocal microscope and LSM 510 software. Cells are immunostained with primary antibodies raised against the V5 tag and the Golgi apparatus marker protein β-COP, as well as fluorophore-conjugate secondary antibodies. Red fluorescence indicates the position of the 2BC60-V5 fusion protein (**Frames A, D, G**), green fluorescence indicates the β-COP stain (**Frames B, E, H**) and yellow signal in the merged images (**Frames C, F and I**) indicates an overlap of red and green signals.

Taken together, these results suggest that the truncated 2C60 and 2BC60 proteins localise to the same regions within the host cell as the wild type 2C60 and 2BC60 proteins, thus indicating that amino acids 61 – 326 are not important for the membrane targeting and membrane association of the TMEV 2C and 2BC proteins. This supports the findings of Banerjee *et al* (2004) who determined a putative membrane association domain in the N-terminal 45 amino acids of the PV 2C protein. Furthermore, these results suggest that when low transfection efficiencies are encountered in cells expressing viral proteins the expression of truncated proteins may

be an alternative strategy to cloning the coding sequences of viral protein into mammalian expression vectors encoding nuclear export signals in order to avoid the degradation of RNA transcribed from transfected DNA.

### 2.4.3 Identification of a hydrophobic, antigenic region of 2C

Figure 2.4.14 depicts the Kyte and Doolittle hydrophobicity/ hydrophilicity plot generated using the Internet based program Protscale (Internet 2). Values above 0 on the y-axis indicate amino acid residues with hydrophobic character while values below 0 on the y-axis indicate amino acid residues with hydrophilic character. In view of this, the region highlighted (amino acids 31-210) in Figure 2.4.14 was chosen as the region of the protein that was most hydrophilic and therefore likely to be soluble in a bacterial expression system.

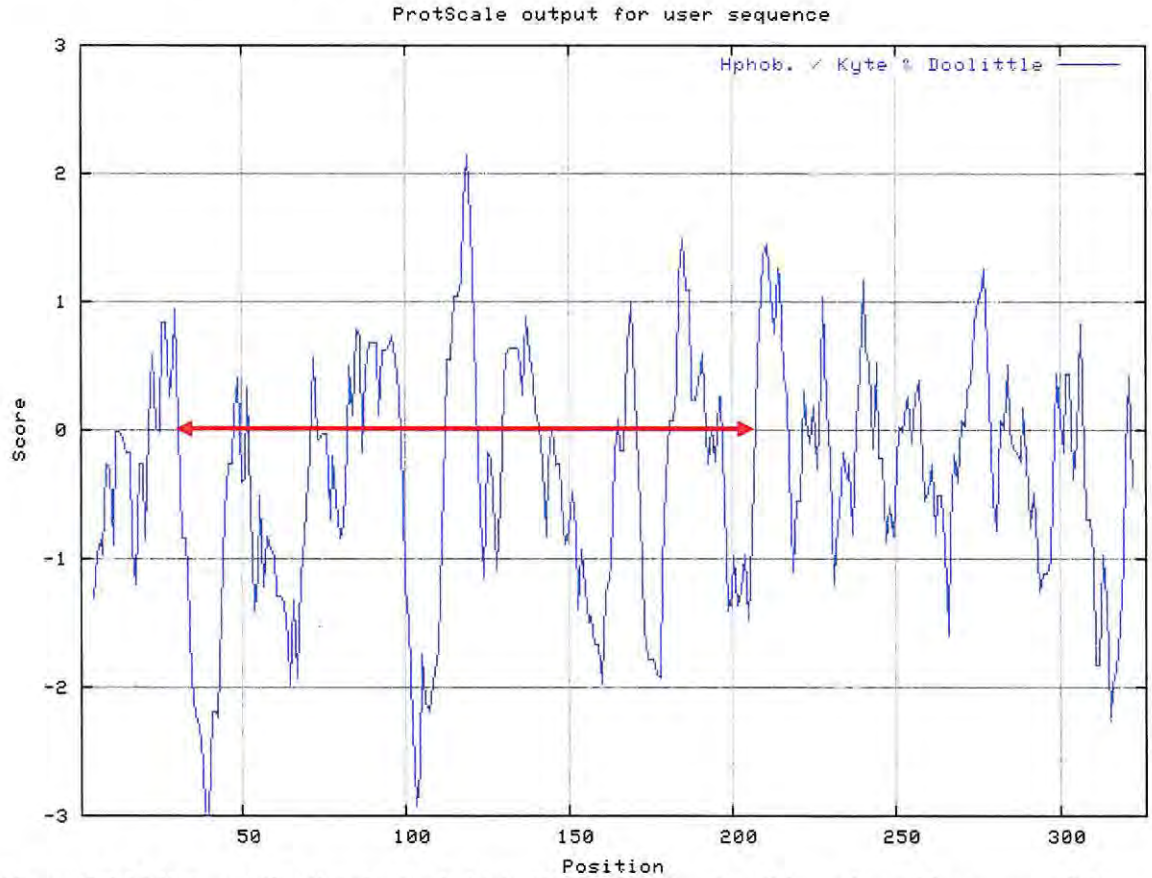


**Figure 2.4.14** Kyte and Doolittle hydrophobicity/ hydrophilicity plot of the amino acid sequence of the 326 amino acids of the TMEV strain GDVII 2C protein created by the Internet based software program ProtScale. Values above 0 on the y-axis indicate amino acid residues with hydrophobic character while values below 0 on the y-axis indicate amino acid residues with hydrophilic character. The high degree of hydrophilicity of the highlighted region (red arrow) suggests its solubility in the cytoplasm of *E. coli* cells.

The identification of antigenic regions of the 2C protein was performed by the Internet based program Emboss Antigenic (Internet 3). Of the possible 13 antigenic regions identified within this protein, 7 were located between amino acids 31-210 (Table 2.4.1). On the basis of the relatively high hydrophilicity and antigenicity of amino acids 31-210 of the 2C protein this region was selected for expression in *E. coli* cells and will be referred to as the 2C178 peptide. This peptide has a molecular mass of 36871.2g and the molecular formula $C_{1634}H_{2547}N_{447}O_{482}S_2$, as calculated by the internet-based program ProtParam (Gasteiger *et al*, 2005).

**Table 2.4.1 Antigenic regions of the 2C protein as detected by the internet based protein analysis program Emboss Antigenic**

| Amino acid residues of TMEV 2C protein | Total Nº amino acid residues | Antigenicity score * | Amino acid sequence |
|---|---|---|---|
| **106-122** | **17** | **1.246** | **DHSVTRPEPVVVVLRGA** |
| 220-235 | 16 | 1.175 | KFRPVTVAHYPAVDRR |
| **67-100** | **34** | **1.172** | **KAYCECTASFKYFDDLYNLAVTCKRIPLASLCEK** |
| **181-188** | **8** | **1.160** | **FTVFCQMV** |
| 267-285 | 19 | 1.144 | SKPQLACFSADCPLLHKRG |
| 296-306 | 11 | 1.140 | VYNLQQVVKMV |
| 239-251 | 13 | 1.116 | DFTVTAGPHCKTP |
| **128-141** | **14** | **1.113** | **SVTSQIIAQSVSKM** |
| 208-216 | 9 | 1.093 | TSSFIVATT |
| 23-30 | 8 | 1.079 | IQSIVNWL |
| **145-152** | **8** | **1.075** | **RQSVYSMP** |
| **42-58** | **17** | **1.070** | **QSKLDKLLMEFPDHCRN** |
| **164-170** | **7** | **1.051** | **QFSVIMD** |

* Antigenicity scores above 1 are proportionally representative of polypeptide regions that are likely to induce an antigenic response in mammals

** The antigenic regions detected in the 2C protein are shown in decreasing rank of antigenic potential

*** Antigenic regions located between amino acids 31-210 on the 2C protein are indicated in bold type

### 2.4.4 Construction of a recombinant vector for the expression of an antigenic, hydrophobic region of the TMEV 2C protein in *E. coli*

*(i) Restriction analysis of the* pLMGT2C178 *recombinant vector*

A pilot scale study was performed to ensure that the 2C178 peptide was expressed as a soluble protein in *E. coli*. To this end the coding region for the 2C178 peptide was inserted into the bacterial expression vector pGEX-2T, encoding a GST-tag on the N-terminus of the peptide, as described in *Section 2.3.8*. Following purification from transformed *E. coli* JM109 cells, the recombinant pLMT2C178 vector underwent restriction analysis with *Bam* H1 and *Eco* R1 to confirm the presence of the correct insert. Figure 2.4.15 below is a digital image of agarose gel electrophoresis of the digested construct.

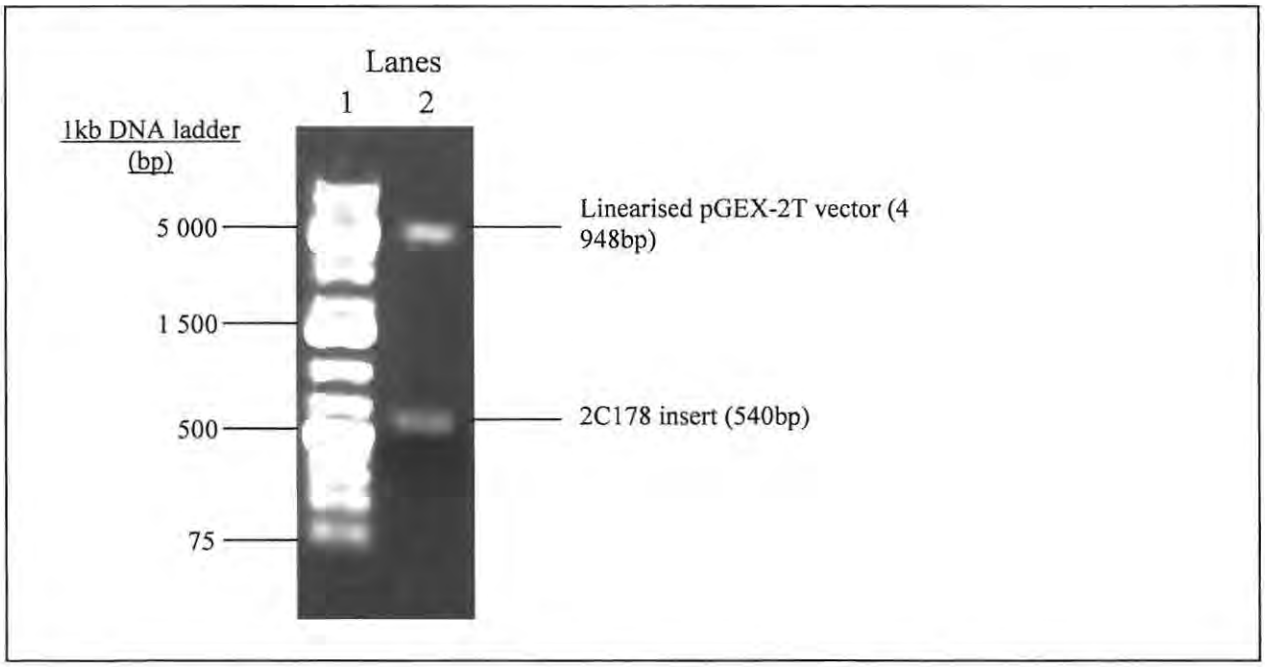


**Figure 2.4.15** The coding sequence for the 2C178 peptide inserted into the bacterial expression vector pGEX-2T. The coding sequence of the peptide was PCR amplified from the cDNA of the viral genome and inserted into the multiple cloning site of the bacterial expression vector pGEX-2T. The presence of the correct coding sequence insert in the recombinant vector was confirmed via restriction analysis. Digested vector DNA was electrophoresed through a 1% agarose gel before being imaged under UV illumination. **Lane 1-** 8µl 1mg/ml O'Gene Ruler 1 kb DNA Ladder Plus (Fermentas), **Lane 2-** pLMGT2C178 digested with *Bam* H1 and *Eco* R1, showing an insert of 534 base pairs.

*(ii) Chain-termination-based sequencing of the* pLMGT2C178 *recombinant vector*

Chain-termination-based sequencing was performed on pLMGT2C178 by Inqaba Biotechnical Industries (Pty) Ltd) using the 3' pGEX Sequencing Primer (Amersham Biosciences). The coding sequence for the 2C178 peptide was in frame with the N-terminal GST tag and no mutations were detected.

### 2.4.5 Expression of 2C178 in *E. coli* BL-21 cells and pilot-scale purification by affinity chromatography

Subsequent to the successful insertion of the coding sequence of the 2C178 peptide into the MCS of the pGEX-2T bacterial expression vector, *E. coli* BL-21 cells were transformed with the recombinant pLMGT2C178 vector and expression of the GST-2C178 fusion peptide was induced by exposure of the cells to IPTG, an artificial inducer of the *tac* promoter on the pGEX-2T vector. The GST-2C178 fusion peptide was purified by affinity chromatography, as described in *Section 2.3.9*, by exploiting the affinity of glutathione agarose beads for the N-terminal GST tag of the 2C178 peptide. Likewise the unfused GST protein was purified from *E. coli* cells transformed with the pGEX-2T vector as a positive control. The same purification and detection procedure was carried out on untransformed *E. coli* BL-21 cells as a negative control. Figure 2.4.16 shows the proteins present in the various fractions during the purification of the GST-2C178 fusion peptide and the GST protein (positive control). The fractions were electrophoresed through a 12% acrylamide SDS-PAGE gel, which was subsequently stained with Coomassie staining solution.

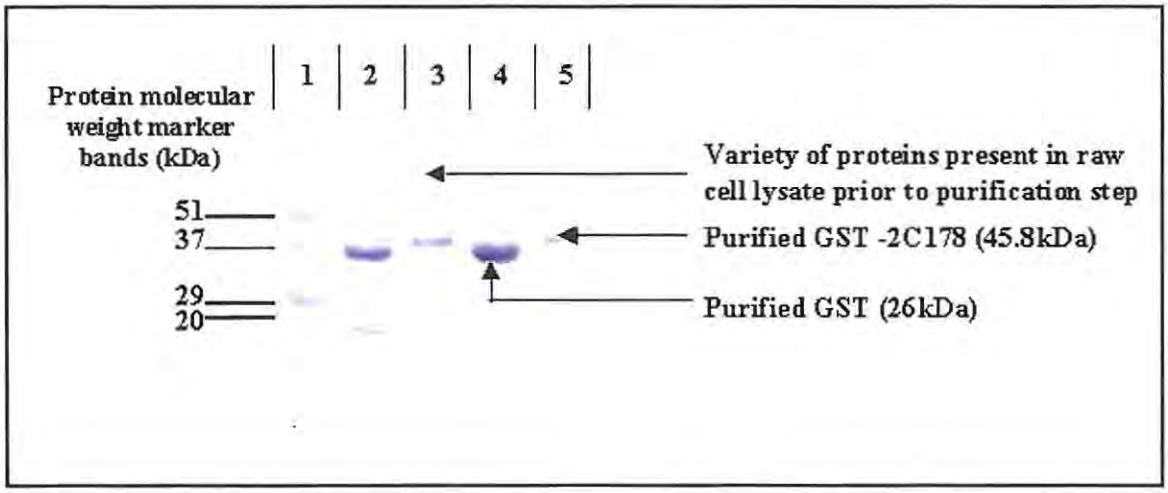


**Figure 2.4.16** Purification of GST-2C178 peptide and GST protein from *E. coli* BL-21 cell lysate. Following a four-hour IPTG-induced expression interval, cell lysates of *E. coli* BL-21 cells transformed with the pLMG2T2C178 and pGEX-2T plasmids were subjected to an affinity chromatography purification step whereby the GST-2C178 peptide and GST protein were purified using glutathione agarose beads. Samples were subjected to SDS-PAGE through a 12% acrylamide gel before staining with Coomassie staining solution. **Lane 1-** 10µl Prestained SDS-PAGE Standard Broad Range (BioRad), position and size of marker bands is indicated, **Lane 2-** 15µl unpurified *E. coli* BL-21 cell lysate containing the GST protein, **Lane 3-** 15µl unpurified *E. coli* BL-21 cell lysate containing the GST-2C178 fusion peptide, **Lane 4-** 15µl purified GST protein, **Lane 5-** 15µl purified GST-2C178 peptide.

A variety of proteins was detected in the raw bacterial lysate prior to the purification step (Lanes 2-3, Figure 2.4.16) while Lanes 4-5 of Figure 2.4.16 indicate that the affinity chromatography-based purification procedure successfully removed all proteins from the samples except the 26Da GST protein (Lane 4) and the 45.8 kDa GST-2C178 peptide (Lane 5). The bands in Lanes 4-5 of Figure 2.4.16 were identified as the GST protein and GST-2C178 peptide, respectively through the subjection of these samples to SDS-PAGE and Western blot analysis followed by immunodetection of the GST peptide (Figure 2.4.17).

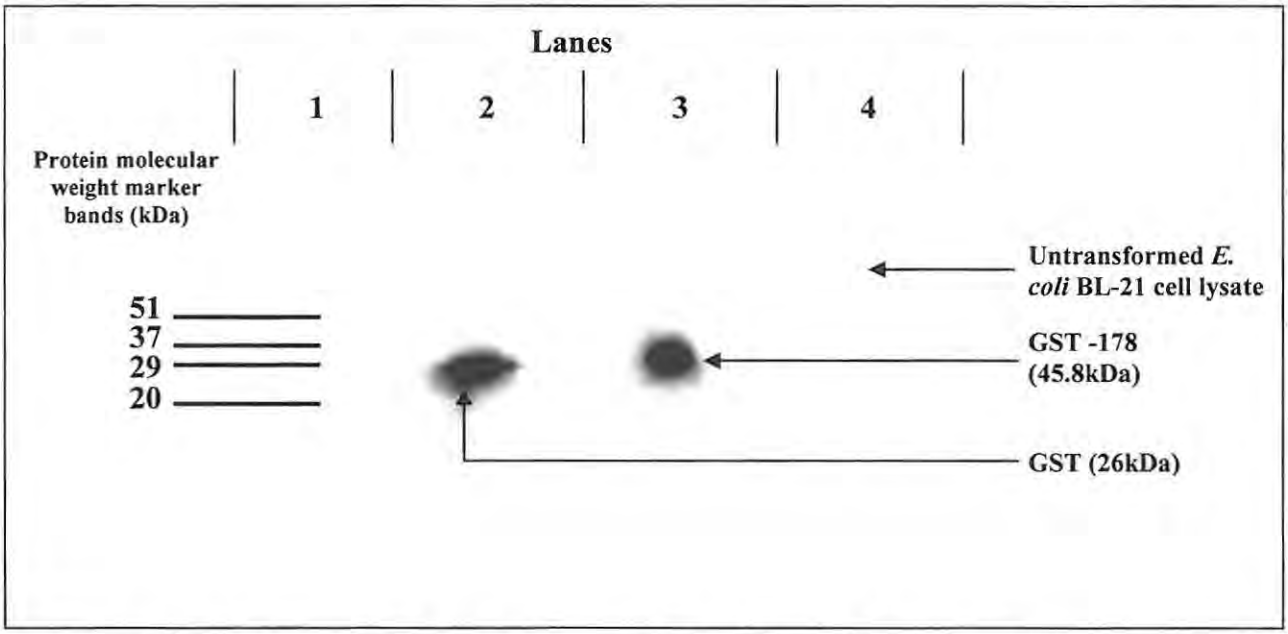


**Figure 2.4.17** Autoradiograph of the immunodetection of the GST-2C178 fusion and GST peptides following SDS-PAGE and Western analysis of samples derived from the GST-specific affinity chromatography purification procedure performed on the cell lysate of pilot-scale *E. coli* BL-21 cultures. **Lane 1-** 10µl Prestained SDS-PAGE Standard Broad Range (BioRad), position and size of marker bands is indicated, **Lane 2-** 15µl purified GST peptide, **Lane 3-** 15µl purified GST-2C178 fusion peptide and **Lane 4-** Untransformed *E. coli* BL-21 cell lysate subjected to the same purification procedure.

The GST-2C178 fusion peptide and the positive control GST peptide were successfully purified from *E. coli* BL-21 cells transformed with the pLMGT2C178 and pGEX-2T vectors, respectively, as shown in Lanes 2 and 3 of Figure 2.4.17. No protein was recognised by the antibody raised against GST in the sample derived from untransformed *E. coli* BL-21 cell lysate (Lane 4, Figure 2.4.17) indicating positive identification of the proteins detected in Lanes 2 and 3 of Figure 2.4.17 as the GST and GST-2C178 fusion peptides, respectively. Taken together these results indicate that the expression of the GST-2C178 fusion peptide was successfully induced by IPTG in *E. coli* BL-21 cells transformed with the pLMGT2C178 recombinant vector and that the fusion peptide was successfully purified on a pilot-scale by affinity chromatography.

Additionally, the successful purification of the GST-2C178 fusion peptide from the lysate of *E. coli* BL-21 cells after the removal of cell debris indicates that this peptide is indeed soluble in the cytoplasm of these bacterial cells. This feature is essential for maximum yield of the peptide during the large-scale purification of the peptide that

must precede antibody production. Due to time constraints experienced during this particular study the large-scale expression and purification of the GST-2C178 fusion peptide will be included in future work.

As described in *Section 2.1* the antibodies raised against the 2C178 peptide will be utilised in further studies for the immunodetection of the TMEV 2C and 2BC proteins in BHK-21 cells transfected with plasmids encoding the proteins as well as BHK-21 cells infected with TMEV to allow the further characterisation of the effect of these proteins on host membranes by electron microscopy. Antibodies against the 2C and 2BC proteins will also be utilised during pull-down assays to detect the interaction of these proteins with host proteins.

In addition to viral protein-host membrane interactions future studies will also seek to identify and describe interactions that form between viral and host proteins. As the 2C178 peptide comprises slightly over half of the amino acid sequence of the TMEV 2C protein it is possible that it includes regions that form interactions with host proteins. The ability of the GST tag of the GST-2C178 fusion peptide to bind a glutathione agarose matrix could be exploited to allow the use of the 2C178 peptide as "bait" during protein pull-down assays. This will be discussed in more detail in *Section 4.1*.

## 2.5 CONCLUSIONS

The insertion of the coding sequences for the TMEV 2B, 2C, 2BC and 3A proteins into the mammalian expression vector pcDNA3.1/V5-His© TOPO® and the subsequent expression of these proteins in BHK-21 cells was successfully achieved. The following conclusions were reached respecting the subcellular localisation of the TMEV 2B, 2C, 2BC and 3A proteins:

1. The TMEV 2B protein locates to fine reticular structures with several larger punctate structures concentrated in the perinuclear region. Some of the reticular structures overlapped, and therefore possibly colocalise, with the ERp60 stain, while a significant proportion of the 2B-V5 fusion remained separate. In addition some of the 2B accumulated in the perinuclear region appeared to overlap with the β-COP stain indicating a possible localisation of TMEV 2B to the peripheral Golgi. The dispersion of this protein throughout the cytosol as far as the plasma membrane suggests that the localisation of 2B to endosomal and/or lysosomal membranes must be investigated.

2. At low expression levels the TMEV 2C protein locates to faint reticular structures that overlap with ERp60 staining while at higher expression levels this protein locates to a concentrated perinuclear stain and larger structures adjacent to the nucleus that overlap with the β-COP stain. These observations indicate that this protein localises to both the ER and peripheral Golgi but that these associations may be dependent on levels of protein expression. The persistently evident perinuclear stain suggests that this protein may also be associated with either the nuclear envelope or the RER that is continuous with the nuclear envelope.

3. The TMEV 2BC protein locates to large structures adjacent to the nucleus that appear to colocalise with the β-COP stain. No overlap of 2BC with the ERp60 stain was observed. However, ERp60 staining in cells expressing this TMEV protein was very faint suggesting that 2BC may be masking the ERp60 stain.

4. The TMEV 3A protein signal overlapped with both ERp60 and β-COP stains. In cells expressing the 3A protein the ER appeared swollen and bulbous while the Golgi was dispersed in some cells.

5. The localisation of the truncated 2C60 and 2BC60 proteins in BHK-21 cells appeared indistinguishable from that of the wild type 2C and 2BC proteins. This indicated that the amino acids 61 – 326 of the 2C protein are not important for the membrane targeting and membrane association of the TMEV 2C and 2BC proteins. Secondly the transfection efficiencies achieved with these proteins were significantly greater than those achieved with the wild type proteins, suggesting that the expression of truncated viral proteins is a possible strategy for increasing poor transfection levels.

6. Further studies are required to investigate the association of the TMEV 2B, 2C, 2BC and 3A proteins with endosomal and lysosomal membranes.

7. Further studies are also required to investigate the effect of the TMEV 2B, 2C and 2BC proteins on host cell protein secretion as it has already been determined that the TMEV 3A protein does not affect exocytic protein trafficking.

The identification, expression and purification of a region of the TMEV 2C protein in *E. coli* BL-21 cells for the purpose of producing a soluble antigenic peptide for the generation of antibodies against the TMEV 2C and 2BC protein in a mammal was successful. Specifically the following conclusions were reached:

8. Amino acids 31-210 of the TMEV 2C protein were identified as possessing a predominantly hydrophilic character as well as 7 of 13 identified antigenic regions of the 2C protein. The identified peptide sequence was named 2C178.

9. The cDNA coding region for the 2C178 peptide was successfully inserted into the bacterial expression vector pGEX-2T.

10. Pilot-scale expression of the GST-2C178 fusion peptide was achieved through IPTG induction and the fusion peptide was purified by affinity chromatography with a matrix of glutathione agarose beads.

11. Immunodetection of the GST-2C178 fusion peptide, subsequent to SDS-PAGE and Western blot confirmed that the protein was successfully expressed and purified. The GST-2C178 fusion peptide was soluble as it was purified from the cell lysate of *E. coli* BL-21 cells.

# 3 Point mutations in 2C: effect on localisation and TMEV replication

## 3.1 INTRODUCTION

The 2C protein is highly conserved throughout the picornavirus family and is thought to be intricately involved in the assembly of the virus replication site as well as viral RNA replication (Aldabe and Carasco, 1995; Bienz *et al*, 1987; Bienz *et al*, 1990; Bienz *et al*, 1992; Cho *et al*, 1994; Schlegel *et al*, 1996; Banerjee *et al*, 1997; Banerjee and Dasgupta, 2001; Rodriguez and Carasco, 1995; Mirzayan and Wimmer, 1994; Rodriguez and Carasco, 1993). In view of the 2C protein's importance in the virus replication cycle it was hypothesised that the mutation of particularly highly conserved residues within the 2C protein may have an effect on the localisation of both the 2C and 2BC proteins in host cells and would therefore affect the ability of TMEV to replicate. The N-terminal domain of the 2C protein, which is thought to be involved with both the membrane association and the RNA binding activity of the protein (Paul *et al*, 1994; Echeverri and Dasgupta, 1995; Echeverri *et al*, 1998; Rodriguez and Carasco, 1995), was selected as the region for mutagenesis.

The sequences of the N-terminal domain of several picornavirus 2C proteins were aligned in order to identify particularly highly conserved amino acid residues. Point mutations were created in the cDNA of the TMEV genome and the wild type and mutant cDNA genomes were transcribed *in vitro* to produce infectious viral RNA. Infectious wild type and mutant TME viruses were obtained through the transfection of BHK-21 cells with these RNAs. Quantification of the effect of the amino acid substitution mutations on the ability of TMEV to induce CPE was expressed as the increase in viable virus particle concentration in BHK-21 cells infected with wild type or mutant TMEV, against time. It was thought that the ability of the various mutant TME viruses to induce CPE in BHK-21 cells might be indicative of their replication proficiency.

A preliminary investigation on the effect of the engineered specific point mutations on the subcellular localisation of the TMEV 2C protein was performed through the

transient expression of the mutant 2C proteins in BHK-21 cells. To determine the localisation of the expressed viral proteins, cells were stained with primary antibodies against the V5 epitope expressed on the C-terminus of the 2C mutant proteins as well as primary antibodies against marker proteins for the ER and Golgi apparatus. Secondary staining was performed with fluorophore-conjugated secondary antibodies and cells were examined either by laser scanning confocal microscopy or by epifluorescence microscopy.

## 3.2 AIMS AND OBJECTIVES

The fundamental goal of this component of the study was to identify highly conserved specific amino acid residues in the N-terminal domain of the TMEV 2C protein and to assess the importance of these amino acids with respect to the replication proficiency of TMEV in host cells and the localisation of the TMEV 2C protein. The specific objectives were as follows:

1. The identification of highly conserved amino acid residues in the N-terminal domain of the TMEV 2C protein by multiple alignment analysis of picornavirus 2C amino acid sequences.
2. The creation of amino acid substitutions in the TMEV 2C coding sequence.
3. An assessment of the effect of these amino acid substitution mutations on the replication proficiency of TMEV by the *in vitro* transcription of wild type and mutant TMEV cDNA and transfection of BHK-21 cells with infectious viral RNA.
4. A quantitative analysis of the effect of the engineered amino acid substitutions on the replication kinetics of TMEV by measuring virus yield at different time points.
5. An investigation of the host range of TMEV by the exposure of different mammalian cell cultures to TMEV.
6. The insertion of the coding sequences for the mutant TMEV 2C proteins into the mammalian expression vector pcDNA3.1/V5-His© TOPO®.
7. The expression of the mutant TMEV 2C proteins in BHK-21 cells through the transfection of this cell line with recombinant DNA encoding the proteins.

8. The immunolocalisation of the mutant TMEV 2C proteins in BHK-21 cells by the immunostaining of cells and either laser scanning confocal microscopy or epifluorescence microscopy.

## 3.3 METHODS AND MATERIALS

### 3.3.1 Identification of conserved residues in picornavirus 2C proteins

With the aim of identifying specific residues that are particularly highly conserved, the N-terminal 30 amino acids of a number of picornavirus 2C proteins were subjected to multiple alignment analysis using Blastp internet-based software (NCBI, 2006). This software program aligns the amino acid sequences of the various proteins and denotes a degree of conservation to each amino acid with respect to the sequences represented.

### 3.3.2 Creation of amino acid substitution mutations in the cDNA of TMEV

Amino acid substitution mutations were created in the cDNA of TMEV, encoded by the recombinant vector pGDVII-WT (see Appendix A, kind gift of Dr M Ryan, University of St Andrews, UK) where an alanine residue was substituted at amino acid residues 4, 8, 14, 18, 23 and 29 by overlap PCR. Figure 3.3.1 is a diagrammatic representation of the overlap PCR procedure. Alanine was chosen as the substitute amino acid as its small size and neutral charge was unlikely to have a significant effect on the tertiary structure of the 2C and 2BC proteins.

The pGDVII-WT recombinant vector comprises the cDNA genome of the GDVII strain of TMEV (Pubmed accession number: 2251141) inserted into the pBlueScript® II Phagemid Vector (Stratagene). Prior to this study overlap PCR was performed as described in Figure 3.3.1 by Dr Caroline Knox to create recombinant vectors encoding the cDNA genome of TMEV with amino acid substitution mutations at amino acid positions 4, 8, 18, 23 and 29 in the 2C protein (detailed in Table 3.3.1) (See Appendix C for primers used). The same overlap PCR procedure was performed

by Ms Cassandra Olds in this laboratory to create an amino acid substitution mutation at amino acid 14 in the 2C protein (See Appendix C for primers used).

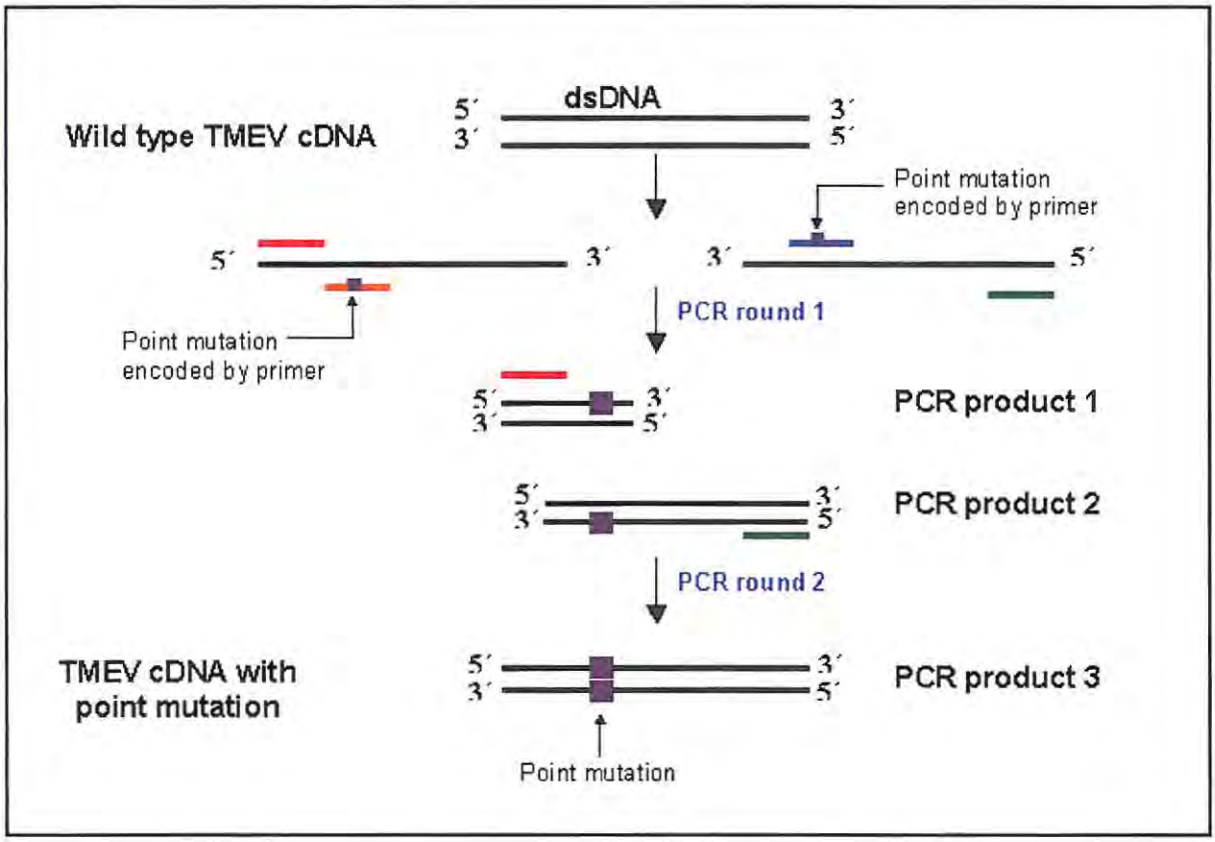


**Figure 3.3.1** Diagrammatic representation of the overlap PCR procedure used to engineer specific point mutations into the cDNA genome of TMEV. Two forward primers are designed: one that binds at the 5′ end of the positive strand (red) and the other that binds over the nucleotides to be mutated on the negative strand (blue). Likewise, two reverse primers are designed: the first of which binds at the 3′ end of the negative strand (green) and the second that binds over the nucleotides to be mutated on the positive strand (orange). The first round of PCR reactions involves two distinct reactions involving different sets of forward and reverse primers, as indicated above, and results in two different PCR products, each of which encode the engineered point mutation on one strand of the PCR product. The second round of PCR uses both PCR products from the first round as template molecules and only the two primers that bind at the 5′ end of the positive strand (red) and the 3′ end of the negative strand (green), resulting in a full length PCR product that encodes the engineered point mutation on both strands.

Subsequent to purification with the Wizard SV Gel and PCR Clean-up System (Promega) according to manufacturers instructions, overlap PCR products underwent restriction digestion with *Acc* III (Fermentas) and *Eco* N1 (Fermentas), as did the pBlueScript® II Phagemid vector. Following a second purification step, overlap PCR products were inserted into the linearised pBlueScript® II Phagemid vector using T4 DNA ligase (Promega). Figure 3.3.2 is a schematic representation of the insertion of the various overlap PCR products into the pBlueScript® II Phagemid vector.

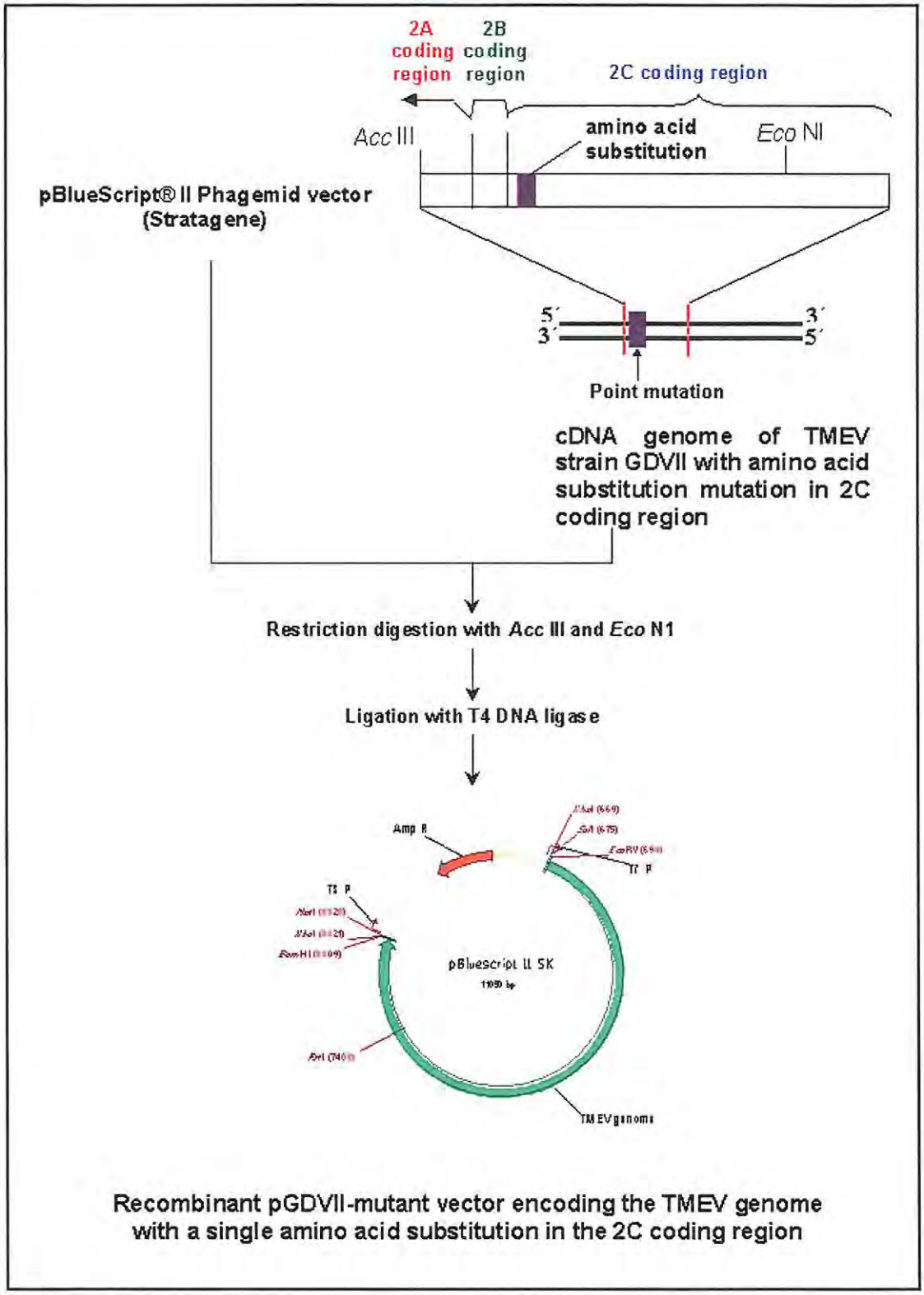


**Figure 3.3.2** Insertion of cDNA genomes of TMEV strain GDVII into the pBlueScript® II Phagemid vector subsequent to the creation of single amino acid substitution mutations in the 2C coding region by overlap PCR. Overlap PCR products comprising the TMEV strain GDVII cDNA genome with a single amino acid substitution mutation engineered into the 2C coding region, and the pBlueScript® II Phagemid vector were subjected to restriction digestion with Acc III and Eco N1. Following a purification step, the overlap PCR products were inserted into the linearised vector using T4 DNA ligase.

The presence of the correct mutation in the 2C coding sequence was confirmed by chain-termination-based sequencing (performed by Inqaba Biotechnical Industries (Pty) Ltd). All constructs described in Table 3.3.1 were sequenced between the *Acc* III (located at 3929 bp on TMEV sequence) and *Eco* N1 (located at 5537 bp on TMEV sequence) restriction enzyme recognition sequences in the 2A and 2C coding sequences, respectively, to confirm that no further mutations occurred in this region during the overlap PCR procedure, thus ensuring that the specific point mutation engineered into the cDNA genome of TMEV was the only difference between the wild type and mutant TMEV genomes. See Appendix B for details of sequencing primers.

**Table 3.3.1. Construction of recombinant vectors encoding specific point mutations in the coding region of the 2C protein in the cDNA genome of TMEV**

| Construct | Position of amino acid substitution mutation in 2C coding sequence (amino acid) | Amino acid substitution mutation |
|---|---|---|
| pGDVII-WT | None | None |
| pGDVII-mt4 | 4 | Arginine → Alanine |
| pGDVII-mt8 | 8 | Glutamate → Alanine |
| pGDVII-mt14 | 14 | Lysine → Alanine |
| pGDVII-mt18 | 18 | Tryptophan → Alanine |
| pGDVII-mt23 | 23 | Isoleucine → Alanine |
| pGDVII-mt29 | 29 | Tryptophan → Alanine |

### 3.3.3 Production of infectious wild type and mutant TMEV RNA by *in vitro* transcription of viral cDNA

As the RNA of all positive sense ssRNA viruses including Picornaviruses is infectious, viral RNA transcribed *in vitro* from the cDNA genome can be transfected into host cell cultures to produce replicating virus. The cDNA of the wild type and mutant TMEV genomes encoded by the constructs described in Table 3.3.1 provided the template required for this reaction.

The template plasmids were linearised by restriction digestion with *Bam* H1 at 37°C for 1 hour 30 minutes before being purified using the Wizard SV Gel and PCR Clean-up System (Promega) as per manufacturer's instructions. 1μg of each linearised template molecule was transcribed *in vitro* using the T7 Transcription Kit (Fermentas) for 2 hours at 37°C, as per manufacturer's instructions. As a positive control *in vitro* transcription was performed on the control template provided in the T7 transcription kit. RNA samples were stored at –80°C until further use.

### 3.3.4 Examining the replication proficiency of wild type and mutant TME viruses in BHK-21 cells

*(i) Transfection of BHK-21 cells with wild type and mutant TMEV RNA*

Transfection mixtures comprising 100 μl 150 mM NaCl, 1 μg wild type or mutant viral RNA and 3.3 μl ExGen reagent were made up in sterile eppendorf tubes and incubated for 1 hour at room temperature (RT), vortexing at 5-minute intervals. A negative control reaction comprising 100 μl 150 mM NaCl, 1 μg control RNA (*Section3.3.3*) and 3.3 μl ExGen reagent was made up in the same way.

Medium was aspirated from a 100% confluent monolayer of BHK cells grown overnight in a 24-well plate as described in *Section 2.3.5*. 400 μl DMEM (5% FCS, 1% PSF) was aliquoted into each well. The transfection mixtures were added drop wise to their respective wells and the 24-well plate was incubated at 37°C and 5% $CO_2$. After 4 hours incubation the medium and transfection reagents were aspirated off the cells and 500 μl of DMEM (5% FCS, 1% PSF) was added to each well and incubation continued for a further 92 hours to allow viral replication.

Cytopathic effect (CPE) can be described as the visible evidence of viral replication in the form of host cells that round up, detach from the growth surface and later lyse. The quantification of CPE is achieved through a visual estimation of the approximate percentage of cells in the monolayer that have detached from the growth surface. BHK-21 cells transfected with wild type and mutant TMEV RNA were observed for

CPE over a 120-hour period. The % CPE after 12, 24, 48, 72, 96 and 120 hours was noted.

Transfection of BHK-21 cells with RNA of the different mutant TME viruses was performed in separate 24-well plates to prevent possible cross-contamination of the different viruses. In all such plates one well of 100% confluent BHK cells was transfected with the negative control transfection mixture. Transfection of cells with the wild type and mutant TMEV RNAs occurred in the same experiment so the replication proficiency of the wild type and different mutant TME viruses could be directly compared.

It was necessary to confirm that the appearance of CPE, or the lack thereof, on transfected cells was due to virus replication or the inability of the mutant TME viruses to replicate, respectively. To this end, growth medium was aspirated off cells 120 hours post-transfection irrespective of whether CPE had been observed or not. This growth medium was aliquoted onto fresh BHK-21 cells grown to a 100% confluent monolayer overnight. Once again, three wells of 100% confluent BHK cells acted as negative controls in each 24-well plate. The appearance of CPE in this experiment was taken to indicate that replication had taken place.

BHK-21 cells were transfected with wild type and mutant TMEV RNAs, in triplicate, on three separate occasions and on all three occasions the pattern of CPE development was similar for each virus.

*(ii) Preparation of wild type and mutant virus stocks*

Growth medium aspirated from cells displaying 90-100% CPE as a result of infection with wild type or mutant TME viruses was aliquoted onto BHK-21 cells grown to 100% confluency in 25 $cm^3$ flasks as detailed in *Section 2.3.4.* Cells were incubated at 37°C, shaking at 50 rpm for 2 hours to allow virus adsorption. Cells were washed with serum-free DMEM and incubated 37°C and 5% $CO_2$ with 7 ml DMEM (5% FCS, 1% PSF) until 100% CPE was observed. At this point growth medium was aspirated from the flasks and centrifuged at 1 000 rpm for 2 minutes to pellet cell

debris. Supernatants were stored in 1 ml aliquots at –80°C and will be referred to as virus stocks from this point forward. From this point forward mutant viruses will be referred to according to the point mutation created in the 2C coding sequence, e.g. TMEV mutant 4 has a point mutation at amino acid 4 on the 2C protein.

*(iii) Confirmation that the appearance of CPE in BHK-21 cells was due to viral replication*

It was necessary to show that the CPE observed in cells transfected with wild type and mutant TMEV RNA was a result of viral replication and not a side effect of RNA transfection. To this end, the presence of nascent viral RNA in cells transfected with viral RNA produced *in vitro* was detected as described below.

BHK-21 cells were grown to 100% confluency in the wells of a 6-well plate (Sarstedt) as detailed in *Section 2.3.4*, except 5.00 x $10^5$ trypsinised cells were seeded into each well of the 6-well plate, as opposed to a 24-well plate, prior to overnight incubation at 37°C and 5% $CO_2$. Cells were transfected with RNA encoding wild type or mutant TME virus genomes as described above except that all ingredients of the transfection mixtures were in 7× the quantity to compensate for the larger number of cells. Two hours post transfection, mixtures were aspirated and cells were washed with 1 × PBS (pH 7.4) to remove remaining untransfected viral RNA. Cells were incubated with 7ml DMEM (5% FCS, 1% PSF) at 37°C and 5% $CO_2$ until the initial stages of CPE were observed. Specifically, the initiation of visible CPE was observed as the appearance of many rounded cells and the formation of small zones of clearance. At this point all medium was aspirated and cells were covered with 500 µl ice-cold Buffer RLN (50 mM Tris-HCl pH 8.0, 140 mM NaCl, 1.5 mM $MgCl_2$, 0.5% NP40, 100 U/ml RNase inhibitor, 1 mM DTT). Cells were scraped from wells, aliquoted into ice-cold 1.5 ml eppendorf tubes and incubated on ice for 5 minutes to lyse cells. Total cytoplasmic RNA was isolated using the Qiagen RNeasy® Mini Kit (Qiagen) as per manufacturer's instructions.

The total cytoplasmic RNA was used as a template for the RT-PCR amplification of the coding region of the TMEV 2BC protein. Successful RT-PCR amplification of this coding region indicates the presence of nascent viral RNA in infected cells.

RT-PCR was performed using the Qiagen OneStep RT-PCR Kit (Qiagen) as per manufacturer's instructions using 1μg of each isolated total cytoplasmic RNA sample as template RNA and the 2BF and 2CR primers (see Appendix C). It was found that of the two protocols described by the QIAGEN® OneStep RT-PCR Kit handbook, the one entailing the use of Q-solution gave a remarkably higher yield of PCR product. RT-PCR products were subjected to chain-termination-based sequencing (performed by Inqaba Biotechnical Industries (Pty) Ltd) using the 2Bfseq primer (see Appendix B).

*(iv) Confirmation that the absence of CPE in BHK-21 cells transfected with mutant TMEV RNA was not due to failed transfection*

It was necessary to prove that absence of CPE in BHK-21 cells transfected with mutant TMEV RNAs was in fact due to an inability of the mutant viruses to replicate and not due to failed transfection of the RNA. To this end, BHK-21 cells were grown to 100% confluency in the wells of a 24-well plate as described in *Section 2.3* and transfected with the mutant TMEV RNAs shown to not cause CPE, as described above.

Four hours post transfection growth medium and transfection mixtures were aspirated of cells and total cytoplasmic RNA was isolated as described above. RT-PCR was performed on isolated RNA, also as described above. Successful amplification of a PCR product the size of the coding region of the TMEV 2BC protein would indicate the presence of viral RNA in the cells, thus indicating that transfection was successful. It is possible that successful PCR amplification of a fragment the size of the 2BC protein coding sequence is the result of residual untransfected RNA on the surface of the cells, however this is unlikely as the cells were washed twice with 1 × PBS (pH 7.4) prior to the RNA isolation procedure.

### 3.3.5 Titration of replicating wild type and mutant TME virus stocks by plaque assay

The concentration of virus particles in the virus stocks of the replicating wild type and mutant TME viruses was determined as plaque forming units (p.f.u.)/ ml of virus stock by plaque assay as described below. BHK-21 cells were grown to a 100% confluent monolayer in the wells of a 6-well plate in DMEM (5% FCS, 1% PSF) at 37°C and 5% $CO_2$.

Eight ten-fold dilutions of wild type and mutant virus stocks were made in serum-free DMEM. Following compete aspiration of growth medium off cells, 1.5ml of virus stock dilutions between $1 \times 10^{-3} - 1 \times 10^{-8}$ were aliquoted into each well and virus adsorption occurred at 37°C, shaking at 50 rpm for 1 hour 30 minutes. Diluted virus stocks were aspirated, cells were washed with serum-free DMEM and overlayed with 3 ml overlay solution (50% DMEM, 1.25% Methocel (Fluka), 60 mM NaCl in sterile water). Plaque assays were incubated at 37°C, 5% $CO_2$ until plaques (zones of clearance) were clearly visible in the cell monolayer. At this point cells were washed with 1 × PBS (pH 7.4) and fixed with 4% paraformaldehyde in 1 × PBS at room temperature for 10 minutes. Fixed cells were washed with 1 × PBS and stained with Coomassie staining solution (45% methanol, 45% water, 10% glacial acetic acid, 0.002% wt/vol Coomassie Brilliant Blue [Saarchem]) for 5 minutes at room temperature. The number of plaques was counted and the titre of each virus stock was calculated in terms of p.f.u./ ml of original virus stock, taking the dilution factor into account.

### 3.3.6 Estimating virus yield for wild type and replicating mutant TME viruses

The rate at which the replicating mutant 4, 14 and 23 TME viruses were able to cause CPE in a BHK-21 cell monolayer appeared inhibited compared with that of the wild type TMEV. It was thus necessary to quantify the inhibitory effect of these specific point mutations on the replication proficiency of TMEV.

BHK-21 cells were grown to a 100% confluent monolayer in the wells of a 24-well plate in DMEM (5% FCS, 1% PSF) at 37°C and 5% $CO_2$. Following the aspiration of all growth medium, cells were infected with wild type or mutant 4, 14 or 23 TMEV stock at a multiplicity of infection (m.o.i.) of 3. Multiplicity of infection is defined as the number of virus particles present per cell in a particular sample. Viral adsorption occurred at 37°C, shaking at 50 rpm for 1 hour 30 minutes after which the virus was aspirated off cells and replaced with 500 µl DMEM (5% FCS, 1% PSF). Infection of BHK-21 cells with the wild type and the different mutant TME viruses was carried out in separate 24-well plates to prevent cross-contamination of the viruses. In all 24-well plates three wells of 100% confluent BHK-21 cells remained uninfected as negative controls. Following infection, cells were incubated at 37°C and 5% $CO_2$.

The growth medium covering the cells was removed at specific time points, i.e. at 1, 7, 13, 20, 24, 27 and 30 hours post infection (h.p.i.). Growth medium covering one well of BHK-21 cells infected with each of the wild type and replicating mutant TME viruses was aliquoted into a sterile eppendorf tube, centrifuged at 1 000 rpm for 2 minutes to remove cell debris and stored at –80°C for further analysis. The virus samples collected at the various time points post infection were titrated by plaque assay as described in *Section 3.3.5*. The ability of the various specific point mutations to inhibit the replication proficiency of TMEV was expressed as viable virus particles produced (p.f.u./ ml) against h.p.i.

### 3.3.7 Investigating the host range of TMEV in mammalian cell culture

BHK-21 cells have been previously established as a host system for TMEV replication in cell culture (Kong *et al*, 1994, van Pesch *et al*, 2001). A brief study was conducted to determine the ability of the wild type TMEV virus used throughout this research to replicate in other mammalian cell types in use in the tissue culture facility at Rhodes University, namely NIH-3T3 cells, Cos-7 cells and HeLa cells.

Different cell lines were grown to 100% confluency in the wells of a 24-well plate in DMEM (5% FCS, 1% PSF) at 37°C and 5% $CO_2$ as shown in Figure 3.3.3. Growth medium was aspirated off the cells in alternate wells and replaced with wild type TMEV stock at a multiplicity of infection (m.o.i.) of 1.

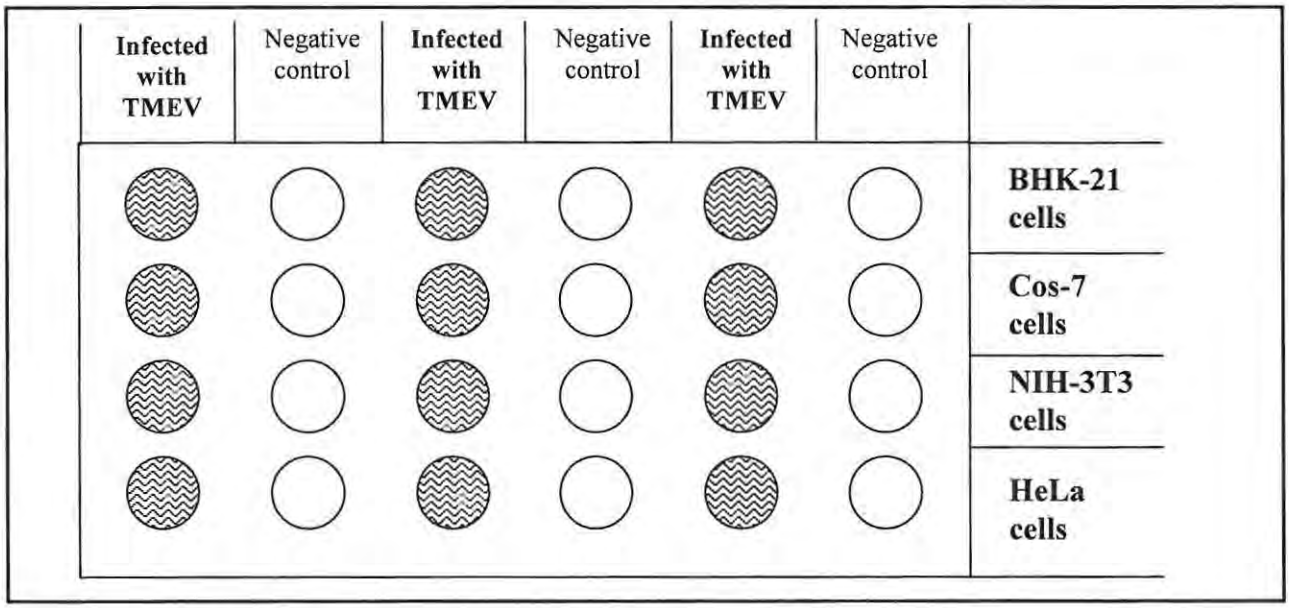


**Figure 3.3.3** Schematic diagram of study conducted to investigate the host range of wild type TMEV in cell culture. Different mammalian cell cultures were infected with wild type TMEV at an m.o.i. of 1 and observed for the development of CPE for 96 hours.

Cells in wells not infected with TMEV acted as negative controls in the experiment. Virus adsorption occurred at 37°C, shaking at 50 rpm for 1 hour 30 minutes. Virus stocks were aspirated off the cells and replaced with DMEM (5% FCS, 1% PSF). Incubation proceeded at 37°C and 5% $CO_2$ and cells were observed for the development of CPE over 120 hours.

In order to show that any CPE observed in cells other than BHK-21 cells was due to TMEV replication, growth medium was aspirated from cells showing CPE and used to infect fresh cells of both the cell type in question and BHK-21 cells. This second infection step was performed using cells gown to 100% confluency in the wells of a 24-well plate. The time taken for 100% CPE to be observed was recorded.

### 3.3.8 Construction of recombinant vectors for the expression of mutant TMEV 2C coding regions in mammalian cells

Subsequent to the quantification of the effect of amino acid substitution mutations in the N-terminal domain of the 2C protein on the replication proficiency of TMEV, the effect of these same point mutations on the subcellular localisation of the TMEV 2C protein was investigated. This involved the transient expression of the mutant 2C protein in host cells followed by immunolocalisation studies. In order to transiently express the mutant TMEV 2C proteins in host cells the coding regions for these proteins were subcloned into the mammalian expression vector pcDNA3.1/V5-His TOPO®.

The construction of recombinant vectors encoding the mutant 2C proteins was performed in exactly the same manner as described for the wild type 2C protein in *Section 2.3.1*. The cDNA template molecules used to PCR-amplify the coding regions for these proteins and the names of the recombinant vectors are recorded in Table 3.3.2. (See Appendix A for vector maps).

| Table 3.3.2. Recombinant vectors constructed by inserting cDNA regions encoding mutant TMEV 2C proteins into the pcDNA3.1/V5-His TOPO® mammalian expression vector | | | | | |
|---|---|---|---|---|---|
| **Name** | **Fwd primer** | **Rvs primer** | **Insert Size (bp)** | **Amino acid position on 2C protein** | **Amino acid substitution mutation** |
| pLMT2C4 | 2C4F | 2CR | 978 | 4 | Arginine → Alanine |
| pLMT2C8 | 2C8F | 2CR | 978 | 8 | Glutamate → Alanine |
| pLMT2C14 | 2CF | 2CR | 978 | 14 | Lysine → Alanine |
| pLMT2C18 | 2CF | 2CR | 978 | 18 | Tryptophan → Alanine |
| pLMT2C23 | 2CF | 2CR | 978 | 23 | Isoleucine → Alanine |
| pLMT2C29 | 2CF | 2CR | 978 | 29 | Tryptophan → Alanine |

The presence of the correct insert in the recombinant vectors shown in Table 3.3.2 was confirmed by restriction analysis and later by chain-termination-based sequencing (see *Section 2.3.1*)

### 3.3.9 Transient expression and indirect immunofluorescent localisation of mutant TMEV 2C proteins in BHK-21 cells

To achieve transient expression of the mutant TMEV 2C proteins, BHK-21 cells were transfected with the recombinant vectors shown in Table 3.3.1 as described in *Section 2.3.4*. Transfected BHK-21 cells expressing mutant 2C proteins were subjected to indirect immunofluorescent staining as described in *Section 2.3.5*.

Immunostained BHK-21 cells transiently expressing mutant TMEV 2C proteins were examined using either the Zeiss LSM 510 Meta confocal microscope at the Electron Microscopy Unit at the University of Kwazulu-Natal, Petermaritzburg as described in *Section 2.3.6*, or the Olympus BX-61 epifluorescence microscope in the Rhodes University Botany Department, Grahamstown. Cells that were imaged using the Olympus BX-61 epifluorescence microscope and AnalySIS B software were examined under the 60× oil immersion objective. Red fluorescence was emitted by the Texas Red® fluorophore (Excitation/Emission: 596 nm/615 nm) conjugated to the anti-mouse IgG and green fluorescence was emitted by the Alexa Fluor® fluorophore

(Excitation/Emission: 495 nm/519 nm) conjugated to the anti-rabbit IgG when cells were examined under the UMWIY2 (Excitation/Emission: 596 nm-615 nm) and UMWIB2 (Excitation/Emission: 390 nm-525 nm) filter cubes, respectively.

## 3.4 RESULTS AND DISCUSSION

### 3.4.1 Identification of conserved residues in picornavirus 2C proteins

Multiple alignment analysis (Figure 3.4.1) was performed on the N-terminal amino acid sequences of several picornavirus 2C proteins to gain an indication of which amino acid residues are particularly highly conserved in this region of the protein. The purpose of this exercise was to determine the effect of mutating conserved amino acid residues in the 2C protein on the subcellular localisation of 2C and the replication proficiency of TMEV.

As the N-terminal domain of the picornavirus 2C protein is thought to be involved in the interaction of the protein with host membranes as well as negative-sense viral RNA during viral RNA replication (Paul *et al*, 1994, Echeverri and Dasgupta, 1995, Echeverri *et al*, 1998, Rodriguez and Carasco, 1995), it was expected that this region would be highly conserved throughout the *Picornaviridae*. Additionally it was expected that several amino acids within this region might be show a particularly high degrees of conservation, indicating a crucial role in either the tertiary structure of the 2C protein or in the actual interactions formed between the 2C protein and host membranes or viral RNA.

The multiple alignment analysis of picornavirus 2C proteins (Figure 3.4.1) revealed several amino acids with a degree of conservation of 50% or higher, with some showing up to 100% conservation. Six of these amino acids were selected (indicated by an asterisk in Figure 3.4.1) for substitution based on their high degree of conservation as well as their strong hydrophobicity/ hydrophilicity. Amino acids 4 (arginine), 8 (glutamate) and 14 (Lysine) in the TMEV 2C sequence are all

hydrophilic amino acids. Amino acids 18 (tryptophan), 23 (isoleucine) and 29 (tryptophan) in the TMEV 2C sequence are relatively large hydrophobic amino acids.

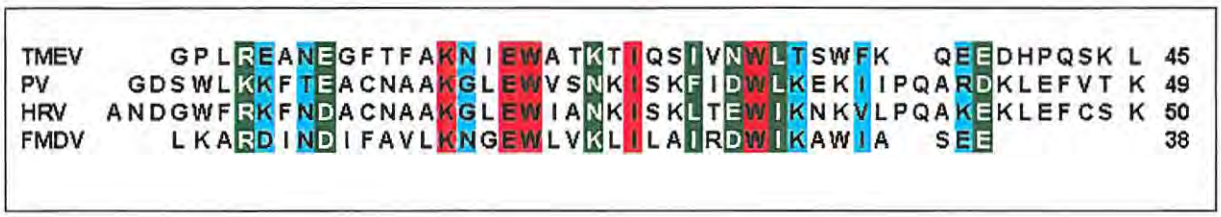


**Figure 3.4.1** Multiple sequence alignment of the N-terminal amino acids of various picornavirus 2C proteins using Blastp internet-based software (NCBI, 2006). A multiple alignment was performed on the N-terminal amino acids of the 2C proteins from the following picornaviruses: TMEV (strain GDVII) 2C protein (Accession number: NP_740431.1); PV (Sabin 1 strain) 2C protein (Accession number: NP_740473.1); HRV (strain B) 2C protein (Accession number: NP_740521.1); FMDV (strain O1K) 2C protein (Accession number: NP_740463.1). Red shading indicates 100% sequence homology, green shading indicates 50-75% sequence homology and blue shading indicates amino acids that do not display sequence homology but that have similar electrochemical properties. Asterisks indicate the amino acids 4, 8, 14, 18, 23 and 29 selected for mutagenesis in the TMEV (strain GDVII) 2C protein.

As mentioned in *Section 1.3.4*, the N-terminal amino acids of the 2C protein are thought to form a Class A amphipathic helix with a basic hydrophilic face that is exposed to the cytoplasm of host cells, and a hydrophobic face that is possibly inserted halfway into the phospholipid monolayer of membranes of the secretory pathway (Saier and McCaldon, 1988, Segrest *et al*, 1994). With this in mind it is most likely that the hydrophobic amino acids in this domain of the 2C protein are important for anchorage of the protein to host membranes, and thus subcellular localisation, at the site of the viral replication complex while acidic and basic amino acids aligned along the cytoplasmic surface of the replication complex are possibly more likely to be involved in the binding of negative-sense viral RNA during RNA replication (Saier and McCaldon, 1988, Segrest *et al*, 1994). Thus mutation of the large tryptophan and isoleucine residues would be likely to have a drastic effect on the secondary and/or tertiary structure of the 2C protein as well as the membrane binding abilities of the protein, while mutation of the acidic glutamate and basic arginine and lysine amino acid residues is more likely to interfere with the interaction of this protein with viral RNA.

### 3.4.2 Creation of amino acid substitution mutations in the cDNA of TMEV

Overlap PCR was used to engineer amino acid substitution mutations into the N-terminal domain of the cDNA coding sequence of the TMEV 2C protein substituting amino acid residues 4, 8, 14, 18, 23 and 29 of the 2C protein for alanine. Alanine was chosen to substitute these amino acid residues based on its small size and neutral charge. The constructs encoding the wild type and mutated TMEV genomes (Table 3.3.1.) were subjected to chain-termination-based sequencing to verify the presence of the engineered mutations. As expected the point mutations engineered into the mutant TMEV 2C coding sequences were all present. No further mutations were detected although it must be noted that only a small region (approximately 1700) of each of the pGDVII- constructs was sequenced due to the large size of the TMEV genome coding sequence and time constraints. It is possible that additional mutations existed outside of these regions.

Of the mutant TME viruses, mutants 8, 18 and 29 were unable to induce CPE indicating that the replication proficiency of these viruses was affected by the respective amino acid substitutions in the 2C coding sequence (see *Section 3.4.3.*). As the overlap PCR products were inserted into the TMEV cDNA between the *Acc* III restriction site at nucleotides 3929-3934 and the *Eco* N1 restriction site at nucleotides 5538-5547 of the TMEV cDNA (Figure 3.3.2) it was necessary to sequence this region of the genome to ensure that no additional mutations had occurred during the overlap PCR process.

Compared to the sequence of the GDVII strain of TMEV (Pubmed accession number: 2251141), a single Glu to Lys substitution mutation located at amino acid 69 on the 2B sequence was present in pGDVII-8, 18 and 29 sequences suggesting that this mutation was also present in the original wild type coding sequence (See Appendix B for summary of sequencing reactions). Aside from the engineered mutations present in the coding sequences of TMEV mutants 8 and 29 no additional mutations were detected. In contrast, several mutations were detected in the coding sequence for TMEV mutant 18. Substitution mutations were detected at the coding sequences for amino acids 74, 75 and 76 in the 2A protein and amino acids 14 and 30 in the 2B protein (See Appendix B for details). Accordingly, the altered replication proficiency

of this virus cannot conclusively be attributed to the engineered amino acid substitution mutation. Due to limited time the pGDVII-18 construct was not re-engineered, although this would be necessary to conclusively determine the effect of a point mutation at amino acid 18 of the 2C protein on TMEV replication.

### 3.4.3 Determining replication proficiency of wild type and mutant TME viruses in BHK-21 cells

*(i) Transfection of BHK-21 cells with wild type and mutant TMEV RNA*

In order to determine the effect of substitution mutations at amino acid residues 4, 8, 14, 18, 23 and 29 of the 2C protein on TMEV replication, BHK-21 cells were transfected with infectious RNA encoding wild type and mutant TME viruses. As described in *3.3.4*, BHK-21 cells were transfected with infectious RNA encoding wild type and mutant TME viruses in the same experiment and this experiment was repeated in triplicate. In all experiments untransfected BHK-21 cells acted as negative controls. Cells were observed for the development of CPE over a 120-hour period. The results of these experiments are shown in Table 3.4.1 below.

**Table 3.4.1. The proportion of BHK-21 cells displaying CPE subsequent to transfection with RNA encoding wild type or mutant TMEV RNA**

| Transfected TMEV RNA | Time (Hours) | | | | |
|---|---|---|---|---|---|
| | Onset of CPE | 20% CPE | 50% CPE | 80% CPE | 100% CPE |
| Wild type | 6 | 8 | 10 | 12 | 15 |
| Mutant 4 | 12 | 17 | 24 | 28 | 32 |
| Mutant 8 | - | - | - | - | - |
| Mutant 14 | 85 | - | 109 | 117 | 120 |
| Mutant 18 | - | - | - | - | - |
| Mutant 23 | 12 | 17 | 23 | 30 | 34 |
| Mutant 29 | - | - | - | - | - |
| No RNA | - | - | - | - | - |

CPE was not observed in the wells of BHK-21 cells transfected with transfection mixtures containing control RNA, indicating that the CPE observed in cells

transfected with RNA encoding TMEV wild type or mutants 4, 14 or 23 was not due to toxicity of any of the transfection components.

Wild type TMEV appeared to replicate at a significantly faster rate than the mutant 4, 14 and 23 TME viruses that were replicating. 100% CPE was observed in BHK-21 cells transfected with wild type TMEV RNA after only 15 hours while cells transfected with RNA encoding TMEV mutants 4 and 23 only showed 100% CPE after 32 and 34 hours, respectively (Table 3.4.1). These results suggest that point mutations at amino acids 4 and 23 in the TMEV 2C protein negatively effect but do not completely abolish viral replication.

The onset of apparent CPE in cells transfected with RNA encoding TMEV mutant 14 was only observed 85 hours post transfection. However after this point CPE advanced rapidly, with 100% CPE being observed at 120 hours post transfection. This result indicates that TMEV mutant 14 is able to replicate in BHK-21 cells, albeit at a severely attenuated rate. The rate at which CPE advanced between 85 and 120 hours suggests that this mutant virus may have evolved a mechanism to compensate for the engineered point mutation in some way and may be reverting to wild type TMEV. Very similar kinetics were observed in triplicate experiments where BHK-21 cells were transfected with TMEV mutant 14 RNA.

When the growth medium covering cells transfected with the wild type and various mutant TMEV RNAs was aliquoted onto fresh preparations of 100% confluent monolayers of BHK-21 cells, the appearance or absence of CPE occurred in the same trend as that recorded in Table 3.4.1 (Figure 3.4.2), confirming that CPE was a direct result of viral replication and not the transfection process.

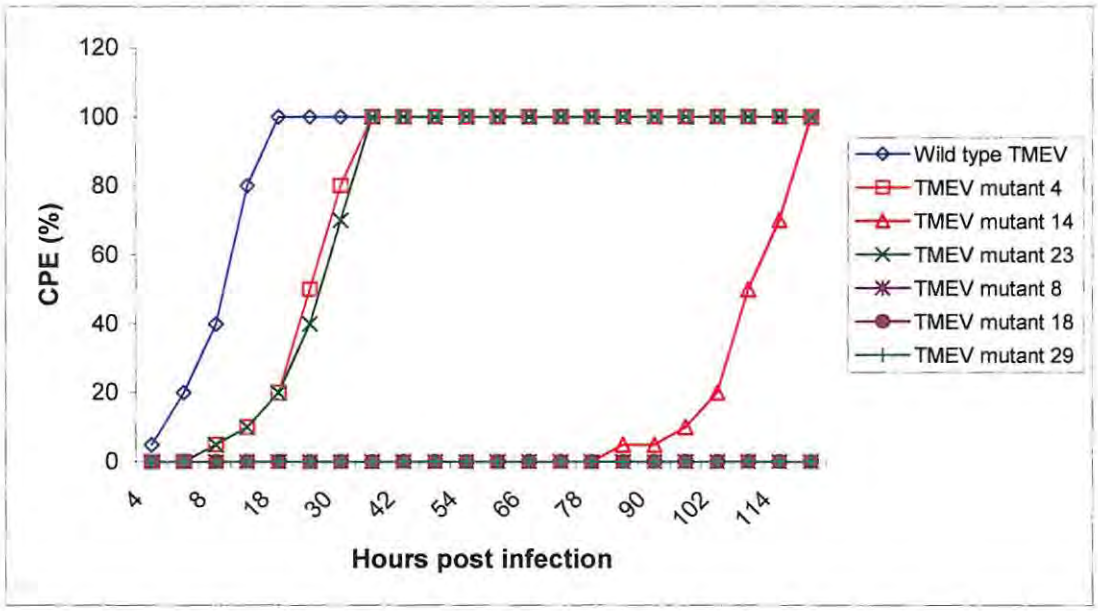


**Figure 3.4.2** The development of CPE over time in BHK-21 cells infected with wild type or TME viruses obtained from the growth medium covering BHK-21 cells previously transfected with wild type or mutant TMEV RNA. CPE was first observed in cells infected with wild type, mutant 4, mutant 14 and mutant 23 TME viruses 5, 8, 84 and 8 hours post infection, respectively. 100% CPE was observed in cells infected with wild type, mutant 4, mutant 14 and mutant 23 TME viruses 18, 36, 120 and 36 hours post infection, respectively.

However, when the cell lysate from the wells showing 100% CPE from TMEV mutant 14 was aliquoted onto a 100% confluent monolayer of BHK-21 cells and observed for a further 120-hour period, the development of CPE was repeatedly similar to that recorded in Table 3.4.1. This was unexpected as, if the rapid increase in CPE observed between 84 and 120 hours post transfection was due to a reversion of the mutant virus to wild type TMEV, the progression of CPE in BHK-21 cells infected with the virus in cell supernatant would be expected to progress at a more rapid rate than that recorded in Figure 3.4.2.

Although uninfected control cells showed no CPE after 120 hours, close inspection revealed that cells were beginning to round up and after 144 hours approximately 25% of the cells had detached from the growth substrate but were not lysed. In all experiments where BHK-21 cells were either transfected with viral RNA or infected with wild type or mutant TME viruses, the appearance of CPE was distinguished from cell senescence as cells undergoing CPE were lysed and the cell debris accumulated in clumps. Cells undergoing senescence were rounded and detached from the growth substrate but were not lysed.

The lack of CPE observed in cells transfected with RNA encoding TMEV mutants 8 and 29 (Table 3.4.1) indicates that mutation of amino acids 8 and 29 alters the activity of the 2C protein in such a profound manner as to totally disable viral replication. This same conclusion cannot be drawn from the lack of CPE observed in cells transfected with RNA encoding TMEV mutant 18 (Table 3.4.1) because, as described in *Section 3.4.2*, the TMEV mutant 18 cDNA template possessed several additional substitution mutations aside from the engineered mutation at amino acid 18 on the 2C protein.

*(ii) Confirmation that the appearance of CPE in BHK-21 cells was due to viral replication*

In order to establish a link between the appearance of CPE and viral replication it was necessary to show the production of nascent viral RNA in BHK-21 cells transfected with RNA encoding wild type, mutants 4, 14 or 23 TME viruses. To this end total cytoplasmic RNA was isolated from BHK-21 cells transfected with wild type or mutant TMEV RNA. RT-PCR was performed on the cytoplasmic RNA isolate using primers used to PCR-amplify the coding sequence for the 2BC protein as described in *Section 2.3.2.* The successful amplification of a PCR product the same size as the 2BC protein coding sequence (Figure 3.4.3) indicated the presence of nascent viral RNA in the transfected cells, thus suggesting a link between the appearance of CPE and viral replication. However, this link must be proven in future studies by showing the presence of viral replication in cells infected with TME viruses capable of inducing CPE in BHK-21 cells, as discussed below.

Chain-termination-based sequencing of the RT-PCR products served to identify the presence of the amino acids substitution mutations in replicating mutant TME viruses and to detect the presence of any additional mutations that may have evolved in these viruses. Sequencing of the mutant 23 RT-PCR product confirmed the presence of the engineered mutation at amino acid 23 in the 2C protein coding sequence of progeny virions. No additional mutations were detected in the region sequenced suggesting that the mutant 23 TME virus did not develop further mutations in the 2C protein to compensate for the effect of the engineered mutations on the functioning of the 2C or

2BC proteins. It must be noted that sequencing the RT-PCR products only served to detect compensating mutations in the 2BC coding sequences of these mutant viruses. It is possible that other mutations had developed in other regions of the viral genome but due to the large size of the TMEV genome and time constraints this possibility was not explored.

Sequencing of the mutant 4 and 14 RT-PCR products was repeated twice and four times, respectively, and in all sequences both the arginine → alanine substitution mutation at amino acid 4 and the lysine → alanine substitution mutation at amino acid 14 on the 2C protein coding sequences had reverted back to the wild type coding sequences. No further mutations were detected in either of the RT-PCR sequences.

The reversion of the TMEV mutant 4 back to the wild type virus is not consistent with the replication kinetics shown in Table 3.4.1 and Figure 3.4.2 as the TMEV mutants 4 and 23 appeared to be replicating at similar rates. If the TMEV mutant 4 was reverting back to the wild type virus we would expect to see a slow initiation of CPE in BHK-21 cells transfected with RNA encoding TMEV mutant 4 while the mutant virus was mutating back to the wild type, followed by a rapid progression of CPE as the wild type virus replicated.

Furthermore, the development of CPE in BHK-21 cells infected with cell lysate from BHK-21 cells transfected with TMEV mutant 4 RNA would be expected to have kinetics similar to those of the wild type virus. This was not the case (Figure 3.4.2), indicating that it is possible that only some nascent mutant 4 RNA molecules are reverting to the wild type sequence producing a mixed population of mutant 4 and wild type TME viruses in infected BHK-21 cells and that the mutated 2C protein is acting as a dominant negative mutation on the wild type protein. A dominant negative mutation is defined by the University of Washington and Children's Health System as "a mutation whose gene product adversely affects the normal, wild-type gene product within the same cell" (Internet 3). Further studies will investigate whether there is a mixed population of mutant 4 and wild type TME viruses present in cell infected with mutant 4 TMEV and whether the substitution of amino acid 4 on the 2C protein is able to act as a dominant negative mutation, thus attenuating viral replication. The

discovery of such a mutation could aid in the development of novel disease treatments.

The reversion of the TMEV mutant 14 RT-PCR product back to the wild type sequence was not consistent with the replication kinetics reported in Figure 3.4.2 as, if the rapid development of CPE in cells transfected with RNA encoding TMEV mutant 14 between 85 and 120 hours (Table 3.4.1) was reflective of a reversion to wild type, the development of CPE in BHK-21 cells infected with the cell lysate from the cells transfected with RNA encoding TMEV mutant 14 would be expected to follow a similar trend to that observed with the wild type virus (Figure 3.4.2).

As with TMEV mutant 4, these results indicate that a lysine → alanine substitution mutation at amino acid 14 on the 2C protein may act as a dominant negative mutation by inhibiting the functioning of any wild type 2C or 2BC proteins present. However, the rapid development of CPE between 85 and 120 hours post transfection/ infection (Table 3.4.1, Figure 3.4.2) is not in keeping with the consistently slower development of CPE observed in cells infected with TMEV mutant 4. As mentioned above, control cells showed no CPE at 120 hours, at 144 hours approximately 25% of the cells had senesced and detached from the growth substrate. Taken together, this observation and the replication kinetics of the TMEV mutant 14 (Table 3.4.1, Figure 3.4.2) suggest firstly that the substitution mutation at amino acid 14 on the 2C protein may act as a dominant negative mutation which inhibits the functioning of any wild type 2C protein to a greater extent than a substitution mutation at amino acid 4. Secondly, the rapid increase in CPE between 85 and 120 hours post transfection/ infection is the result of the combined effects of depleted nutrients in the growth medium (contributing to cellular senescence) and replication of the mutant 14 TME virus.

In order to investigate the ability of the substitution mutations at amino acids 4 and 14 on the 2C protein to acts as dominant negative mutations, future studies will involve an investigation of the effect of the simultaneously infecting cells with both wild type and mutant viruses on the replication kinetics of the wild type TME virus.

As mentioned above, it must be noted that although BHK-21 cells were washed with PBS following transfection with wild type or mutant TMEV RNA, the RNA

originally transfected into the cells may have been isolated along with the total cytoplasmic RNA and would have thus provided a template for the subsequent RT-PCR reaction. Thus the production of a correctly sized RT-PCR product does not convincingly prove that RNA replication was occurring. However, the reversion of TMEV mutants 4 and 14 to wild type does conclusively demonstrate the incidence of viral RNA replication in cells infected with these viruses. An alternative method for detecting viral RNA replication involves labelling nascent viral RNA with Bromouridine triphosphate (BrUTP) and the immunofluorescent detection of the replicating viral RNA by staining with primary antibodies raised against BrUTP and fluorophore conjugated secondary antibodies. This procedure will be performed as part of future work.

*(iii) Confirmation that a lack of CPE in BHK-21 cells transfected with mutant RNA was not due to failed transfection*

To investigate whether the lack of CPE observed in BHK-21 cells transfected with TMEV mutants 8, 18 and 29 RNAs was in fact due to an inability of the mutant viruses to replicate and not due to failed transfection of the RNA, total cytoplasmic RNA was isolated from transfected cells and RT-PCR was performed on isolated RNA as described in *Section 3.4.4*, using primers used to PCR-amplify the coding sequence for the 2BC protein as described in *Section 2.3.2.* The successful amplification of a PCR product the same size as the 2BC protein coding sequence indicated the successful transfection of cells with viral RNA (Figure 3.4.3). However, this conclusion can only be reached through the assumption that all untransfected RNA was removed by extensively washing the transfected cells with 1 × PBS (pH 7.4) prior to RNA isolation.

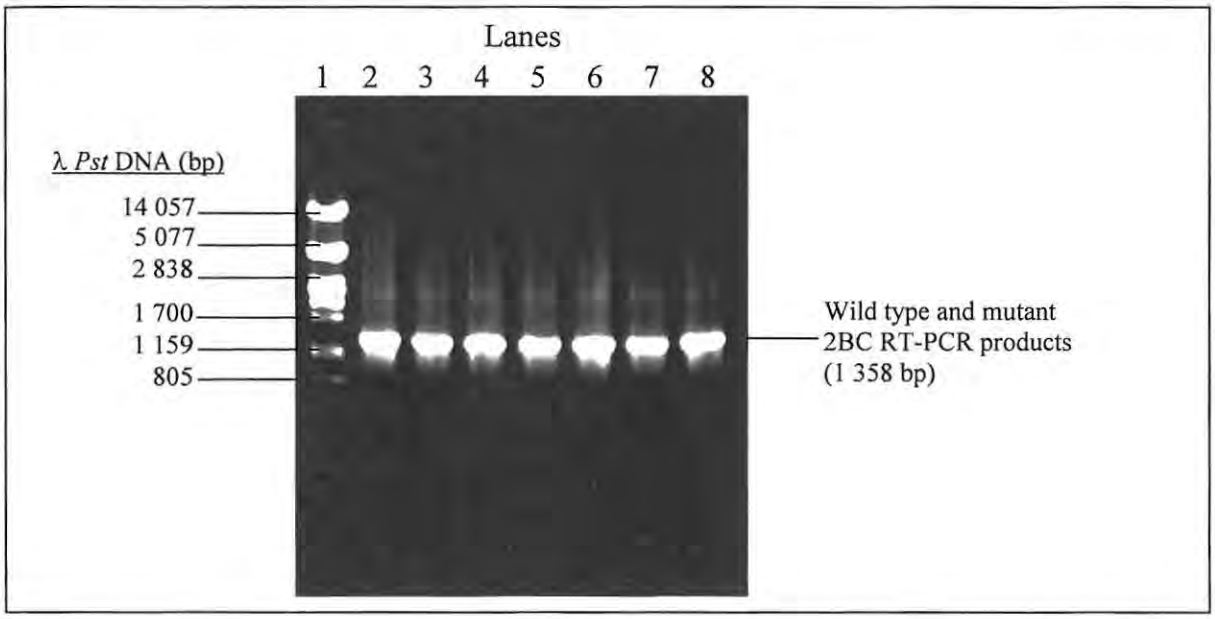


**Figure 3.4.3** BHK-21 cells were transfected with *in vitro* transcribed RNA encoding the TMEV genome with substitution mutations at amino acids 4, 8, 14, 18, 23 or 29 on the 2C protein. RT-PCR was performed on the total RNA isolated from transfected cells. RT-PCR amplification of a PCR product the same molecular weight as the TMEV 2BC protein coding sequence were electrophoresed through a 1% agarose gel (containing 0.16 μg/ml ethidium bromide) in 1× TAE buffer at 100V before being imaged under UV illumination. **Lane 1-** λ *Pst* PCR molecular weight ladder, **Lane 2-** wild type TMEV RT-PCR product, **Lane 3-** TMEV mutant 4 RT-PCR product, **Lane 4-** TMEV mutant 8 RT-PCR product, **Lane 5-** TMEV mutant 14 RT-PCR product, **Lane 6-** TMEV mutant 18 RT-PCR product, **Lane 7-** TMEV mutant 23 RT-PCR product, **Lane 8-** TMEV mutant 29 RT-PCR product.

### 3.4.4 Titration of replicating wild type and mutant TME virus stocks by plaque assay

The concentration of virus particles in the virus stocks of the replicating wild type and mutants 4, 14 and 23 TME viruses was determined as plaque forming units (p.f.u.) / ml of virus stock by plaque assays. At the start of the plaque assay procedure, when virus adsorption occurs, the BHK-21 cell monolayer is already 100% confluent. It was found that this confluent monolayer only survived under the methocel overlay solution during a plaque assay for a maximum of 96 hours before the cells began to senesce and detach from the growth surface. As CPE is only observed in cells infected with TMEV mutant 14 after 96 hours it must be noted that it was impossible to obtain an accurate titre of this virus stock by plaque assay. As discussed in *Section 3.4.3 (i)*, it was surprising that insufficient viable virus particles were present in the TMEV mutant 14 stock to be able to obtain a titre in three days before the cells senesced. It is

possible that although this mutant virus appears to be consistently reverting to the wild type, a large proportion of the nascent virus particles are defective. Virus stocks were titrated during three identical experiments and the average titre (Table 3.4.2) was calculated and used from this point forward.

**Table 3.4.2. Titration of replicating wild type and mutant TMEV stocks. The concentration of viable virus particles in wild type and mutant TMEV stocks was quantified by plaque assay whereby 100% confluent monolayers of BHK-21 cells in 6-well plates were infected with eight tenfold dilutions of each virus stock and observed for the formation of plaques.**

| TMEV stock | Titre (p.f.u./ ml) | | | |
|---|---|---|---|---|
| | 1 | 2 | 3 | Average |
| Wild type | $6.97 \times 10^6$ | $7.04 \times 10^6$ | $6.99 \times 10^6$ | **$7.00 \times 10^6$** |
| Mutant 4 | $17.82 \times 10^6$ | $18.13 \times 10^6$ | 18.18 | **$18.10 \times 10^6$** |
| Mutant 23 | $7.15 \times 10^6$ | $7.07 \times 10^6$ | $7.05 \times 10^6$ | **$7.09 \times 10^6$** |

### 3.4.5 Constructing replication curves for wild type and replicating mutant TME viruses

Observation of the percentage CPE, as indicated by the proportion of BHK-21 cells detached from the substrate, caused by the wild type and mutants 4, 14 and 23 TME viruses over time was not an accurate quantification of the effect of these point mutations on the replication proficiency of TMEV. A more accurate measure was obtained through the infection of BHK-21 cells with wild type and mutant TMEV virus stocks at an m.o.i. of 3. Samples of the growth medium covering the infected cells was removed at specific time points over 30 hours and titrated for virus concentration by plaque assay. The virus yield was then plotted against time to produce "virus yield curves" (Figure 3.4.4.).

Virus yield curves were successfully constructed for the wild type and mutants 4 and 23 TME viruses (Figure 3.4.4.). The difference in virus yield at the different time points between the wild type and mutant 4 and 23 TME viruses was significant. Consequently this experiment was only performed once as small differences in the

titres of the various time points that may occur during repeated experiments would not impact on the overall trends of the wild type and mutant TMEV replication kinetics. Additionally, the replication kinetics reflected in Figure 3.4.4 coincide with the repeated rates at which CPE was seen to develop in BHK-21 cells transfected with viral RNA encoding the same TME viruses (Table 3.4.1).

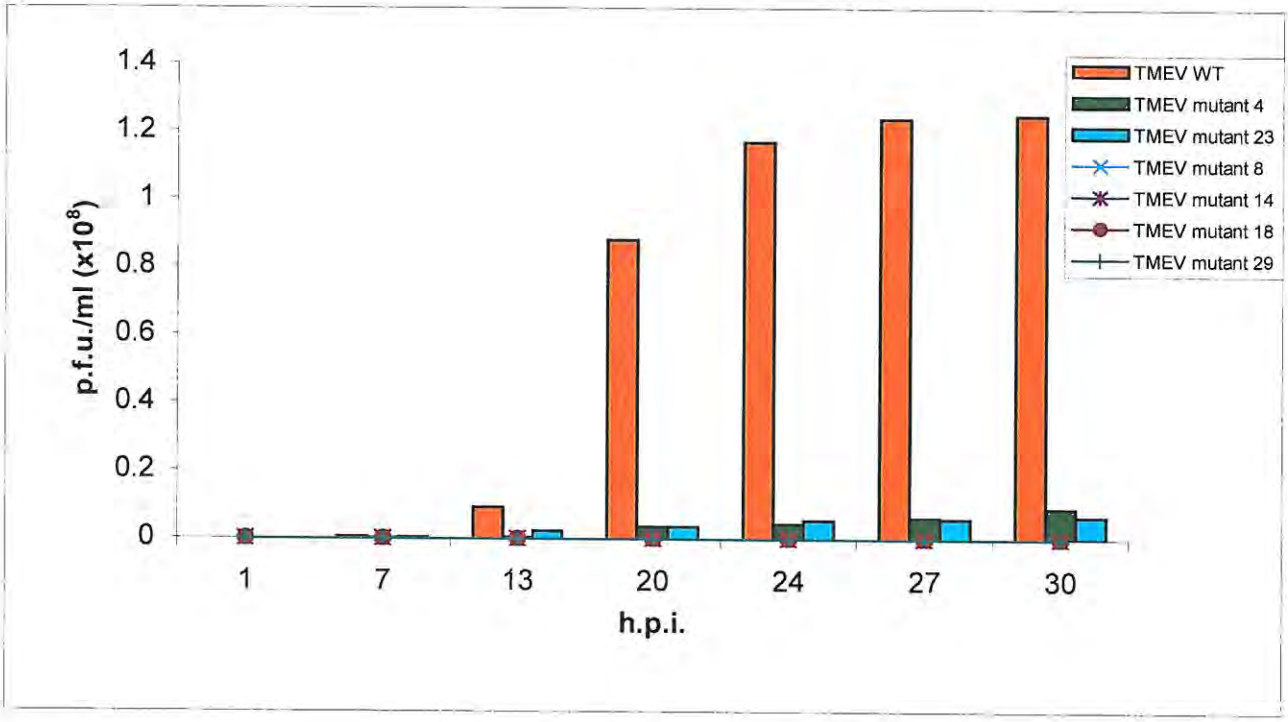


**Figure 3.4.4.** Quantitative analysis of the effect of specific point mutations in the N-terminal domain of the 2C protein on the replication proficiency of TMEV. 100% confluent HK-21 cells were infected with wild type and mutant TME viruses at an m.o.i. of 3. Samples of the growth medium covering the cells were taken over a 30-hour time period and titred for virus yield. No nascent virion production was observed for TMEV mutants 8, 14, 18 and 29. Compared to wild type TMEV, mutants 4 and 23 demonstrated extremely inhibited virus yield. Virus yield was expressed as plaque forming units (p.f.u.)/ ml at hours post infection (h.p.i.).

The mutant 4 and 23 TME viruses showed relatively similar levels of viable virus yield that were all radically lower than those recorded with wild type TMEV. Interestingly, although 100% CPE was observed in cells infected with these mutant viruses after 36 hours during this experiment the virus titre for both of these mutants never reached levels as high as those measured for the wild type TMEV samples (Figure 3.4.4.). Thus it appears that the substitution of amino acid residues 4 and 23 on the coding sequence for the 2C protein not only attenuates TMEV replication but also affects the amount of viable virus particles produced from infected cells.

Once again no CPE was observed in cells infected with mutant 14 during the 30-hour time period and no viable virions were detected in the time point samples taken from these infected cells (Figure 3.4.4.). However 100% CPE was observed in the same cells 120 hours post infection showing that virus replication was occurring. Further studies over a 120-hour time period would be needed to examine this mutant TME virus' replication kinetics and to characterise the reversion of the point mutation at amino acid 14 on the 2C protein to the wild type.

### 3.4.6 Investigating the host range of TMEV in mammalian cell culture

The ability of wild type TMEV GDVII to replicate in mammalian cell lines available at Rhodes University other than BHK-21 cells was investigated. NIH-3T3 cells (Kind gift of Professor G Blatch, Rhodes University, South Africa), Cos-7 cells (Kind gift of Professor R Hay, St Andrews University, UK) and HeLa cells (Kind gift of Dr M Ryan, St Andrews University, UK) were infected with wild type TMEV at an m.o.i. of 1 and observed for CPE over a 120 hour period. BHK-12 cells were infected in the same manner to act as a positive control. No CPE was observed in the "infected" or the negative control Cos-7 cells and HeLa cells. CPE was observed in the infected NIH-3T3 cells after 20 h.p.i. and 100% CPE occurred at 56 h.p.i. 100% CPE was observed in BHK-21 cells after 24 h.p.i, as indicated by all the cells detaching from the growth substrate. No CPE was observed in the uninfected negative control NIH-3T3 cells and BHK-21 cells.

The growth medium covering NIH-3T3 cells and BHK-21 cells was removed after 100% CPE was observed and aliquoted onto fresh 100% confluent NIH-3T3 cells and BHK-21 cells. The development of CPE in these cells proceeded at similar rates to those of the first round of infections with 100% CPE being observed at 50 h.p.i. in the NIH-3T3 cells and 20 h.p.i. in the BHK-21 cells. These results indicate that TMEV GDVII can replicate in both BHK-21 and NIH-3T3 cell lines and that the same virus isolate can be replicated on first one cell line then the other. However the replication of the virus on NIH-3T3 cells appears inhibited compared to that on BHK-21 cells. Further studies are necessary to determine the exact kinetics of this difference in

replication rate and to determine whether a lower virus titre is produced in NIH-3T3 cells.

The ability of a virus to infect a cell type (cell tropism) is determined by many factors including the presence of specific receptor molecules on the cell surface and specific metabolic characteristics of the cell type. The factors determining the cell tropism and specifically the cell surface receptor bound by TMEV prior to viral entry into the host cell, are not understood but are thought to involve a 34-kDa glycoprotein (Kilpatrick and Lipton, 1991) as well as sialic acid (Zhou *et al*, 1997). The extent and the nature of glycosylations might vary according to the cell type as demonstrated by Jnaoui *et al*, 2002 in their study where they adapted the GDVII strain of TMEV to infect CHO-K1 cells from BHK-21 cells. Such variations may be the cause of the attenuated ability of TMEV, initially raised in a BHK-21 cell line, to infect NIH-3T3 cells. Both BHK-21 and NIH-3T3 cells are rodent cell lines. BHK-21 cells are a fibroblastic cell line derived from hamster kidney tissue explants while NIH-3T3 cells are a mouse fibroblastic cell line. Thus the ability of TMEV to replicate in NIH-3T3 cells is not surprising given that mice are the natural host of the virus. Likewise, the inability of TMEV to replicate in HeLa or Cos-7 cells was expected as these cell lines are derived from a human cervical adenocarcinoma and African green monkey kidney tissue explants, respectively.

Further studies could explore the possibility that with repetitive rounds of replication on NIH-3T3 cells, TMEV GDVII may "adapt" to using this cell line as a host and in doing so viral replication kinetics may become comparable with those observed in BHK-21 cells.

### 3.4.7 Construction of recombinant vectors for the expression of mutant TMEV 2C coding regions in mammalian cells

*(i) Restriction analysis of recombinant vectors*

The coding regions for the mutant TMEV 2C proteins were subcloned into the mammalian expression vector pcDNA3.1/V5-His TOPO® as described in *Section 3.3.8*. Subsequent to purification from transformed *E. coli* JM109 cells, recombinant vectors underwent restriction analysis with *Bam* H1 and *Xba* 1 to confirm the presence of the correct insert. Figure 3.4.5 below is a digital image of agarose gel electrophoresis of the digested constructs.

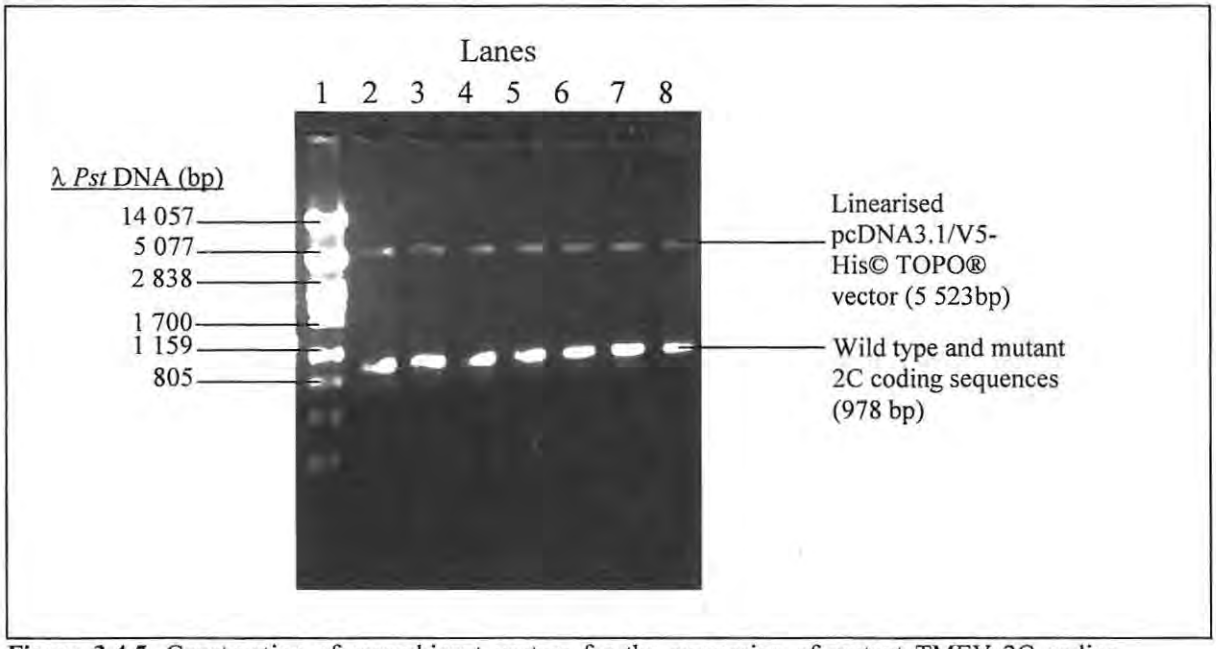


**Figure 3.4.5.** Construction of recombinant vectors for the expression of mutant TMEV 2C coding regions in mammalian cells. Coding sequences for the mutant TMEV 2C proteins were PCR amplified from the cDNA of the viral genome and inserted into the multiple cloning site of the mammalian expression vector pcDNA3.1/V5-His TOPO®. The presence of the correct coding sequence inserts in the recombinant vectors was confirmed via restriction analysis with *Bam* H1 and *Xba* 1. Digested vectors were electrophoresed through a 1% agarose gel (containing 0.16 μg/ml ethidium bromide) in 1× TAE buffer at 100V before being imaged under UV illumination. **Lane 1-** λ *Pst* DNA molecular weight ladder, **Lane 2-** pCOT2C containing an insert of the wild type 2C coding sequence, **Lane 3-** pLMT2C4 containing an insert of the 2C mutant 4 coding sequence, **Lane 4-** pLMT2C8 containing an insert of the 2C mutant 8 coding sequence, **Lane 5-** pLMT2C14 containing an insert of the 2C mutant 14 coding sequence, **Lane 6-** pLMT2C18 containing an insert of the 2C mutant 18 coding sequence, **Lane 7-** pLMT2C23 containing an insert of the 2C mutant 23 coding sequence, **Lane 8-** pLMT2C29 containing an insert of the 2C mutant 29 coding sequence. All inserts are 978 bp in size while the pcDNA3.1/V5-His TOPO® vector is 5523 bp in size.

*(ii) Chain-termination-based sequencing of recombinant vectors*

Chain-termination-based sequencing was performed on the recombinant vectors shown in Figure 3.4.4 using the T7 primer (Invitrogen) to ensure the presence of the engineered mutation in the mutant 2C coding sequences. All the mutant 2C coding sequences contained the desired substitution mutation and no other mutations were detected. It must be noted however, that sequencing of these recombinant vectors with the T7 primer only resulted in the sequencing of at most the first 700 nucleotides of the mutant 2C coding sequences. Thus further sequencing with the BGH reverse primer is necessary before the presence of other mutations can be ruled out completely.

### 3.4.8 Transient expression and indirect immunofluorescent localisation of mutant TMEV 2C proteins in BHK-21 cells

With the aim of characterising the subcellular distribution of TMEV 2C proteins with point mutations at amino acids 4, 8, 14, 18, 23 and 29 and thus to determine the effect of these mutations on 2C localisation in host cells, BHK-21 cells were transfected with recombinant mammalian expression vectors encoding these proteins. Following an expression window of 19 hours, cells were fixed and immunostained with primary antibodies recognising the V5 epitope on the C-terminus of the expressed viral proteins as well as primary antibodies raised against specific marker proteins of the ER or Golgi apparatus. Subsequent to secondary staining with fluorophore-conjugated secondary antibodies, cells were mounted on microscope slides and examined by either laser-scanning confocal microscopy or epifluorescence microscopy.

The TMEV 2C mutants 14, 18 and 23-V5 fusion proteins were all successfully expressed in BHK-21 cells at varying transfection efficiencies and cells were examined using the Zeiss LSM 510 Meta confocal microscope. Successful expression of TMEV mutant 2C-V5 fusion proteins in transfected and immunostained BHK-21 cells was indicated by the observation of red fluorescence when samples were excited with the 543nm laser line. Staining of organelle marker proteins was identified by green fluorescence when samples were excited with the 543nm laser line.

The TMEV 2C mutants 4, 8 and 18-V5 fusion proteins were also successfully expressed in BHK-21 cells and cells were examined using the Olympus BX-61 epifluorescence microscope. Expression of TMEV protein-V5 fusions was indicated by red fluorescence under the UMWIY2 cube due to the excitation of the Texas Red® fluorophore while green fluorescence resulting from the excitation of the Alexa Fluor® 488 fluorophore indicated the distribution of either the ERp60 ER marker protein or the β-COP Golgi apparatus marker protein.

A brief summary of the transfection efficiency of the constructs encoding the mutant 2C proteins as well as the subcellular localisation of the various 2C mutant proteins is given in Table 3.4.3.

**Table 3.4.3 Summary of the effect of amino acid substitution mutations in the TMEV 2C coding region on the replication proficiency of TMEV and the subcellular localisation of the 2C protein**

| Position of amino acid substitution on 2C protein | Transfection efficiency of mutant 2C protein (%) | Subcellular localisation of mutant 2C protein | Replication proficiency of mutant virus |
|---|---|---|---|
| 2C wild type | 1-5 | • Faint reticular stain partially overlapping with ERp60 stain<br>• At high levels of expression protein was concentrated in concentrated structures in the perinuclear region that overlap with β-COP<br>• Faint perinuclear localisation | Rapid development of CPE in BHK-21 cells with high virus yield |
| 4 | 1-5 | • Majority of the protein is distributed in a reticular stain, partially overlapping with ERp60<br>• At high levels of expression protein was concentrated in concentrated structures in the perinuclear region that overlap with β-COP<br>• Distinct perinuclear localisation | Retarded development of CPE in BHK-21 cells with an inhibited rate of virus yield |
| ** **14** | **0.05 - 0.10** | • **Majority of the protein shows a cytoplasmic distribution**<br>• **Faint perinuclear localisation** | |
| ** **23** | **1-5** | • **Small punctate structures that partially overlap with the stain of the ER marker protein ERp60**<br>• **Completely separate from β-COP stain**<br>• **No perinuclear stain** | |
| 8 | 1-5 | • Majority of the protein is distributed in a reticular stain, partially overlapping with ERp60<br>• At high levels of expression protein was concentrated in concentrated structures in the perinuclear region that overlap with β-COP<br>• Distinct perinuclear localisation | Does not cause CPE in BHK-21 cells |
| ** **18** | **1-5** | • **Majority of the protein shows a cytoplasmic distribution**<br>• **Faint perinuclear localisation** | |
| 29 | 1-5 | • Majority of the protein is distributed in a reticular stain, partially overlapping with ERp60<br>• At high levels of expression protein was concentrated in concentrated structures in the perinuclear region that overlap with β-COP<br>• Distinct perinuclear localisation | |

** Note: The highlighted mutant 2C proteins in Table 3.4.3 displayed subcellular localisation patterns distinctly different to that of the wild type 2C protein.

*(i) Transient expression of mutant 4, 8 and 29 TMEV 2C proteins in BHK-21 cells*

The TMEV 2C mutants 4, 8 and 29-V5 fusion proteins were successfully expressed in BHK-21 cells at approximately equivalent transfection efficiencies to that of the wild type 2C protein. As with the wild type 2C protein, the majority of the mutants 4, 8 and 29 2C proteins localised to a reticular stain that that partially overlapped with the ERp60 stain (Frames C, F, I and L, Figure 3.4.6). At higher levels of expression large structures in the perinuclear region that partially overlapped with the β-COP stain were also present (Frames C, F, I and L, Figure 3.4.7), however these structures were smaller and less numerous than those observed in cells expressing the TMEV 2C wild type protein. As with the 2C wild type protein, an approximately equal number of cells expressing the mutant 4, 8 and 29 2C proteins showed the two different protein distributions.

Despite the many similarities, there was a distinct difference between the subcellular localisation of the wild type 2C protein and that of the mutant 4, 8 and 29 2C proteins in that cells expressing the 2C wild type protein showed a faint perinuclear stain while those expressing any of the mutant 4, 8 and 29 2C proteins showed a concentrated perinuclear stain. This was particularly evident in BHK-21 cells expressing the mutant 29 2C protein. The subcellular localisation of the mutant 29 2C protein was also slightly different from that of the mutant 4 and 8 2C proteins as a slightly higher proportion of cells expressing the protein (60% as opposed to 50%) showed larger punctate structures in the perinuclear region, partially overlapping with the Golgi marker protein β-COP.

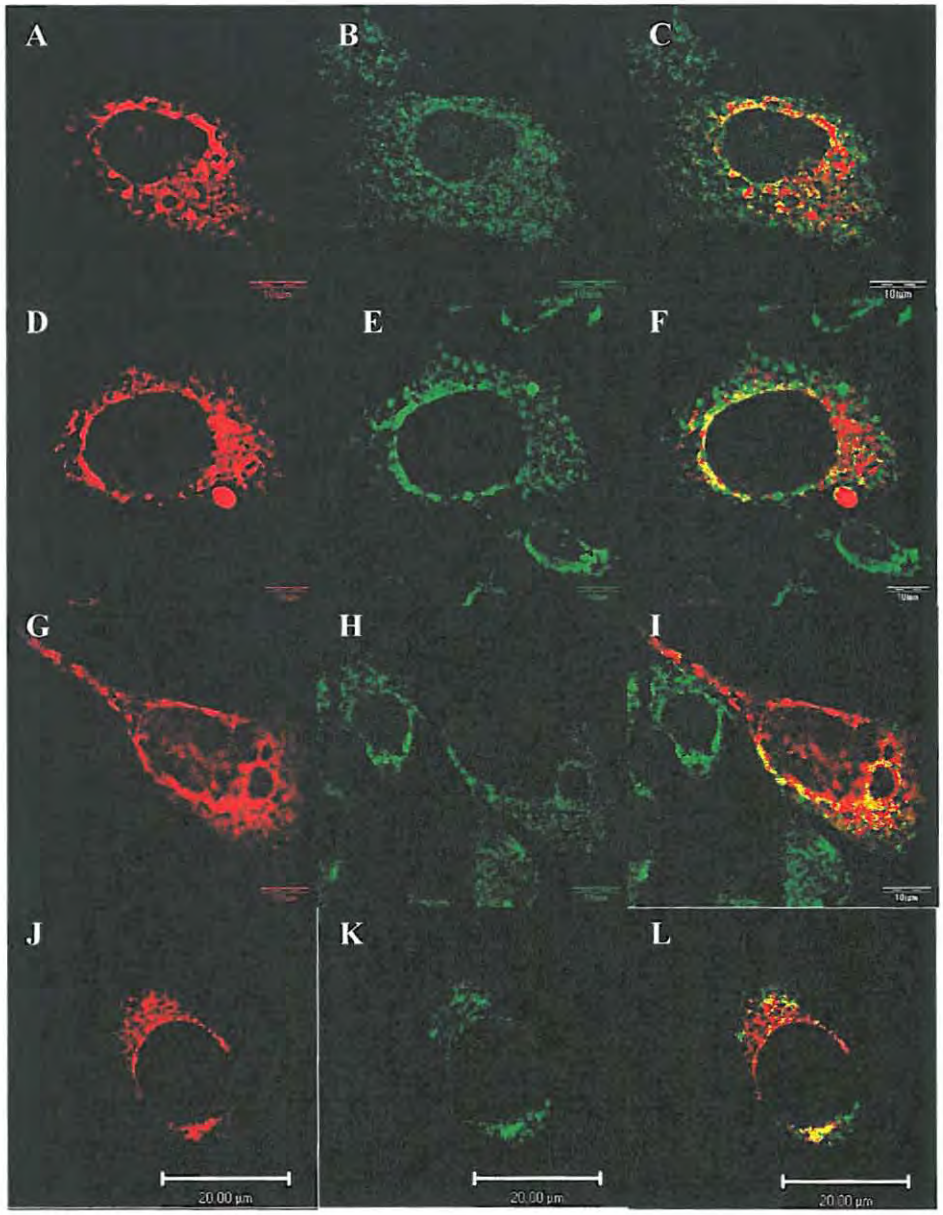


**Figure 3.4.6.** Subcellular localisation of TMEV mutant 4, 8 and 29 2C-V5 fusion proteins in BHK-21 cells. BHK-21 cells were transfected with pLMT2C mutant constructs and expressed the encoded 2C mutant proteins. Cells were imaged using an Olympus BX61 epifluorescence microscope and AnalySIS B software. Cells are immunostained with primary antibodies raised against the V5 tag and the ERp60 ER marker protein, as well as fluorophore-conjugate secondary antibodies. Red fluorescence indicates the position of the mutant or wild type 2C-V5 fusion protein (**Frames A, D, G and J**), green fluorescence indicates the ERp60 stain (**Frames B, E, H and K**) and yellow signal in the merged images (**Frames C, F, I and L**) indicates an overlap of red and green signals. The wild type and mutant 4, 8 and 29 2C proteins are localising to a reticular stain that partially overlaps with ERp60 as well as showing distinct perinuclear localisation with some larger punctate structures adjacent to the nucleus.

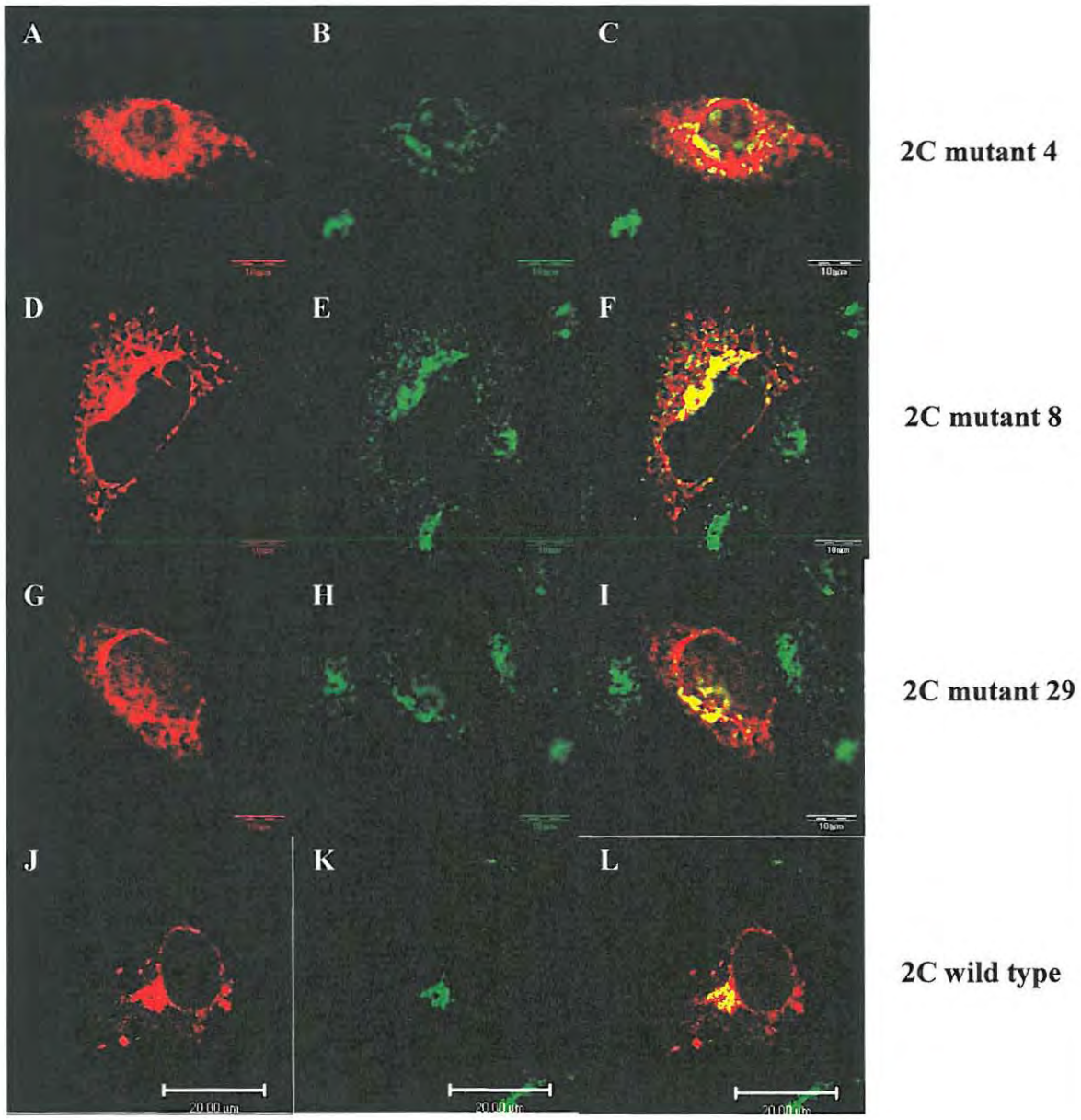


**Figure 3.4.7.** Subcellular localisation of TMEV mutant 4, 8 and 29 2C-V5 fusion proteins in BHK-21 cells. BHK-21 cells were transfected with pLMT2C mutant constructs and expressed the encoded 2C mutant proteins. Cells were imaged using an Olympus BX61 epifluorescence microscope and AnalySIS B software. Cells are immunostained with primary antibodies raised against the V5 tag and the β-COP Golgi marker protein, as well as fluorophore-conjugate secondary antibodies. Red fluorescence indicates the position of the mutant or wild type 2C-V5 fusion protein (**Frames A, D, G and J**), green fluorescence indicates the β-COP stain (**Frames B, E, H and K**) and yellow signal in the merged images (**Frames C, F, I and L**) indicates an overlap of red and green signals. The wild type and mutant 4, 8 and 29 2C proteins are localising to a reticular stain as well as showing distinct perinuclear localisation with some larger punctate structures adjacent to the nucleus that partially overlap with β-COP.

The similarities between the localisation of the wild type and mutant 4, 8 and 29 2C proteins in BHK-21 cells suggests that amino acid substitution mutations at amino acid residues 4, 8 and 29 on the 2C protein do not grossly alter the localisation of this protein in host cells. Interestingly, of these three mutations only the mutant 4 TME virus is able to replicate in BHK-21 cells, while the mutant 8 and 29 TME viruses are unable to cause CPE in this cell line (Figure 3.4.4). In order to confirm the effects of these mutations on the localisation of the 2C protein the different proteins, future studies will include the examination of BHK-21 cells transiently expressing the different proteins using the same laser-scanning confocal microscope, unlike this study which had to resort to the use of two different microscopy techniques due to equipment constraints.

Taken together, these results suggest that substitution mutations of amino acids 4, 8 and 29 on the 2C protein do alter the replication proficiency of TMEV but that this effect is not a result of an altered ability of the 2C protein to localise to host cell membranes. However, in order to confirm that the subcellular localisation characteristics of the 2C protein is not altered by these mutations future studies will include membrane fractionation studies whereby BHK-21 cells, transiently expressing the wild type or mutant 4, 8 and 29 2C proteins, will be subjected to a membrane fractionation procedure followed by detection of the proteins in the different fractions by SDS-PAGE and Western analysis.

*(ii) Transient expression of mutant 14, 18 and 23 TMEV 2C proteins in BHK-21 cells*

The TMEV 2C mutants 18 and 23-V5 fusion proteins were successfully expressed in BHK-21 cells at approximately equivalent transfection efficiencies (1-5 %) to that of the wild type 2C protein. In contrast, the TMEV 2C mutant 14-V5 fusion protein was only expressed at extremely low transfection efficiencies with approximately 0.05-0.10 % of the total cells present expressing the protein. These three mutant proteins all displayed subcellular localisation patterns that were distinctly different to that of the wild type TMEV 2C protein (Table 3.4.3).

The mutant 18 2C protein showed an even cytoplasmic distribution with a very faint perinuclear stain in all cells expressing this protein (frame D, Figures 3.4.8 and 3.4.9).

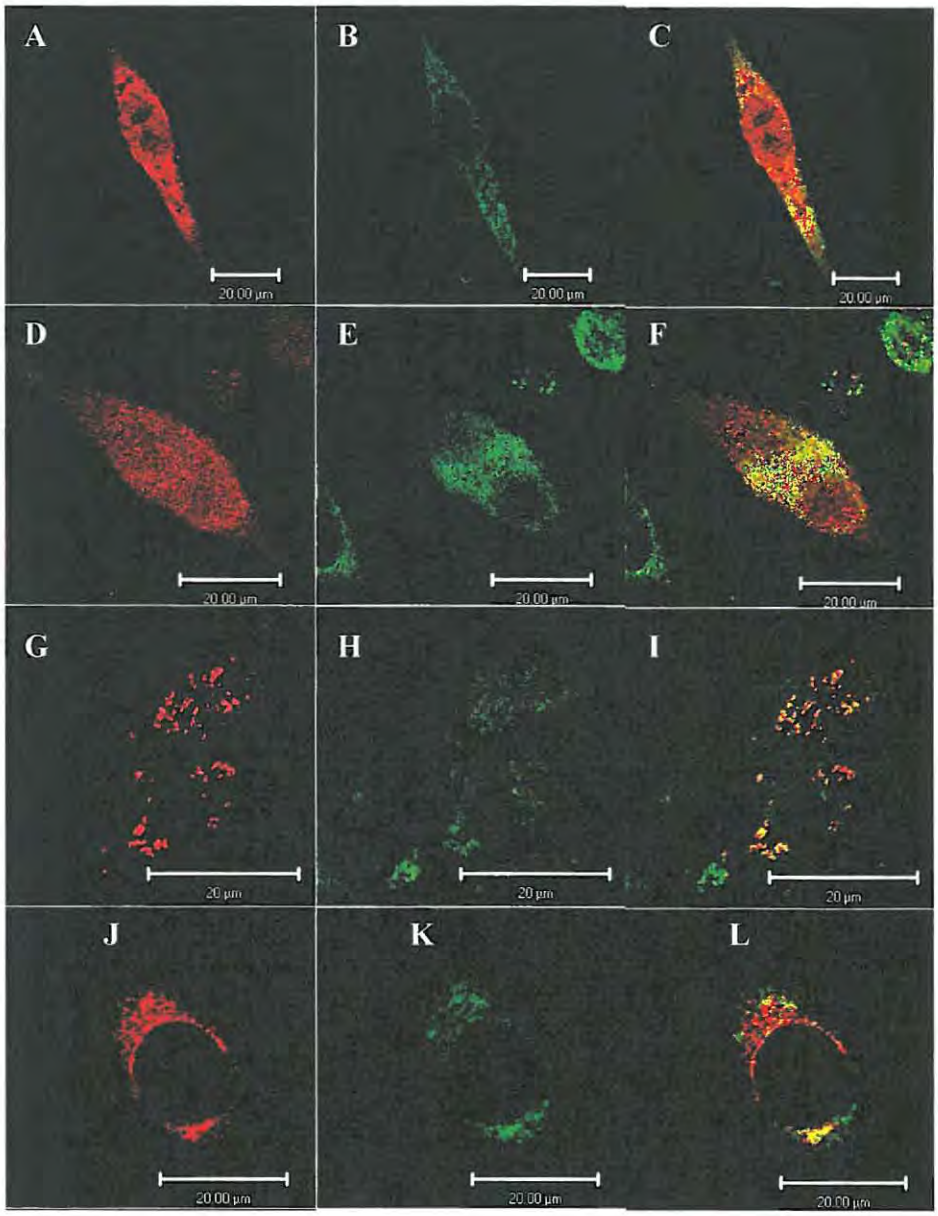


**Figure 3.4.8.** Subcellular localisation of TMEV mutant 14, 18 and 23 2C-V5 fusion proteins in BHK-21 cells. BHK-21 cells transfected with pLMT2C mutant constructs or pCOT2C and expressing either a TMEV mutant 2C-V5 fusion protein or the wild type 2C-V5 fusion protein, respectively, and imaged using a Zeiss LSM 510 Meta confocal microscope and LSM 510 software. Cells are immunostained with primary antibodies raised against the V5 tag and the ERp60 ER marker protein, as well as fluorophore-conjugate secondary antibodies. Red fluorescence indicates the position of the mutant or wild type 2C-V5 fusion protein (**Frames A, D, G and J**), green fluorescence indicates the ERp60 stain (**Frames B, E, H and K**) and yellow signal in the merged images (**Frames C, F, I and L**) indicates an overlap of red and green signals. The mutant 14 and 18 2C proteins displayed and even cytoplasmic localisation with a very faint perinuclear stain. The mutant 23 2C protein localised to small distinct punctate structures that partially overlapped with the ERp60 stain. The localisation patterns of these mutant 2C protein were different from that of the wild type 2C protein that localised to a reticular stain as well as showing distinct perinuclear localisation with some larger punctate structures adjacent to the nucleus.

The substitution mutation at amino acid residue 18 converted a tryptophan residue to an alanine residue. Tryptophan is a large negatively charged amino acid compared to the neutral, small alanine and thus it is possible that such a gross change in the properties of the amino acid sequence would alter the tertiary structure of the 2C protein, thus affecting its ability to localise to host membranes.

Like the mutant 18 2C protein, the mutant 14 2C protein showed an even cytoplasmic distribution with a very faint perinuclear stain in all cells expressing this protein (frame A, Figures 3.4.8 and 3.4.9). The replication proficiency of TMEV was inhibited by this same mutation (Figure 3.4.3) although mutant 14 TMEV was seen to revert back to the wild type virus after a significant time period following infection. Taken together, these results suggest that a substitution mutation at amino acid residue 14 on the 2C protein affects the ability of this protein to associate with host membranes in a manner that severely inhibits viral RNA replication. Once again, the ability of this mutation to affect the membrane association characteristics of the TMEV 2C protein will be investigated through membrane fractionation studies.

The 2C mutant 23 protein localises to small punctate structures that partially overlap with the stain of the ER marker protein ERp60 (frame G, Figure 3.4.8) but are completely separate from the stain of the peripheral Golgi marker protein β-COP (frame G, Figure 3.4.9). Additionally, in approximately 50% of cells expressing the 2C mutant 23 protein the ERp60 stain was extremely faint while the same stain in the remaining 50% of expressing cells was more punctate than reticular unlike cells not expressing the protein. The localisation of the 2C mutant 23 protein differed from that of the wild type 2C protein which was seen to localise to a faint reticular structures as well as to large structures adjacent to the nucleus, partially overlapping both the ERp60 and β-COP stains. Taken together these observations suggest that the 2C mutant 23 protein may be associating with and modifying the ER membranes in some way but is not associated with the membranes of the peripheral Golgi apparatus. In view of the fact that TMEV mutant 23 is able to replicate at an inhibited rate, the significance of the altered localisation of the 2C mutant 23 protein suggests that another virus protein is able to compensate for any altered functioning of the 2C protein.

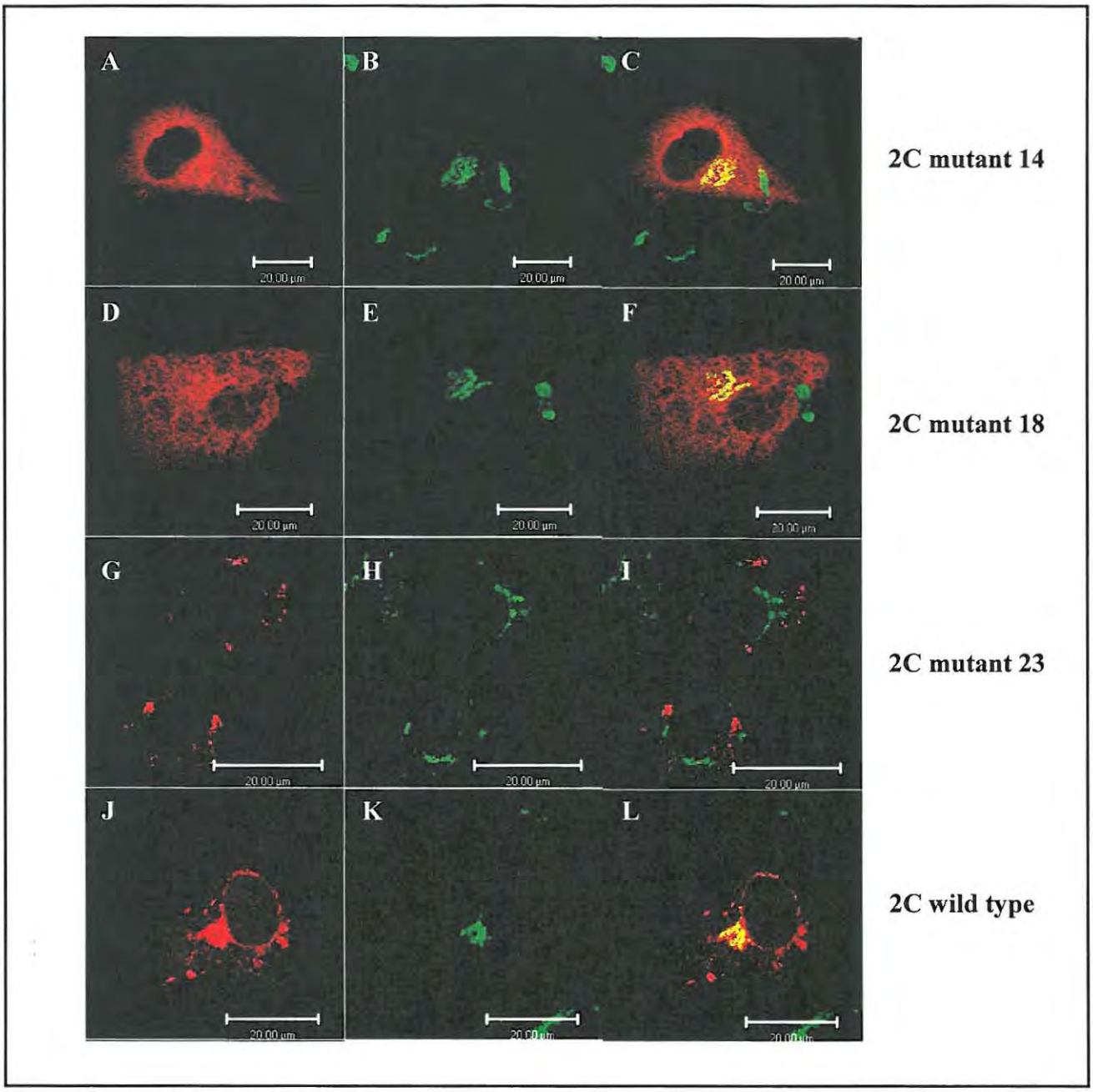


**Figure 3.4.9.** Subcellular localisation of TMEV mutant 14, 18 and 23 2C-V5 fusion proteins in BHK-21 cells. BHK-21 cells transfected with pLMT2C mutant constructs or pCOT2C and expressing either a TMEV mutant 2C-V5 fusion protein or the wild type 2C-V5 fusion protein, respectively, and imaged using a Zeiss LSM 510 Meta confocal microscope and LSM 510 software. Cells are immunostained with primary antibodies raised against the V5 tag and the β-COP Golgi marker protein, as well as fluorophore-conjugate secondary antibodies. Red fluorescence indicates the position of the mutant or wild type 2C-V5 fusion protein (**Frames A, D, G and J**), green fluorescence indicates the β-COP stain (**Frames B, E, H and K**) and yellow signal in the merged images (**Frames C, F, I and L**) indicates an overlap of red and green signals. The mutant 14 and 18 2C proteins displayed and even cytoplasmic localisation with a very faint perinuclear stain. The mutant 23 2C protein localised to small distinct punctate structures that were completely separate from the β-COP stain. The localisation patterns of these mutant 2C protein were different from that of the wild type 2C protein that localised to a reticular stain as well as showing distinct perinuclear localisation with some larger punctate structures adjacent to the nucleus.

The biological significance of the altered localisation of the 2C mutant proteins with respect to the role of the 2C protein in viral replication is not clear. In order to link the ability of point mutations in the N-terminal domain of the 2C protein to attenuate, and in some cases completely abolish, TMEV replication a loss of function in either the 2C or 2BC proteins must be demonstrated. To this end future studies would firstly involve the localisation of transiently expressed 2BC mutant proteins followed by the characterisation of the membrane binding abilities of both the mutant 2C and 2BC proteins compared with those of the wild type 2C and 2BC proteins. Further investigations could compare the ability of the mutant and wild type TMEV 2C proteins to bind negative sense viral RNA and to exhibit ATPase/GTPase activity.

## 3.5 CONCLUSIONS

Point mutations were successfully created at highly conserved amino acid residues in the N-terminal domain of the 2C protein. The following conclusions were reached regarding the effect of these mutations on the ability of TMEV to replicate in BHK-21 cells and on the subcellular localisation of the 2C protein:

1. Amino acids 4, 8, 14, 18, 23 and 29 at the N-terminal domain of the TMEV 2C protein are highly conserved throughout the picornavirus family. Amino acid substitution mutations were successfully created at these amino acid residues in the cDNA genome of TMEV, inserted into the pBlueScript® II Phagemid Vector.

2. Amino acid substitution mutations at amino acids 4, 14 and 23 attenuate but do not completely abolish TMEV replication. The point mutation at amino acid 23 is retained in the replicating mutant TME virus. In contrast repeated chain-termination based sequencing revealed that the point mutations at amino acids 4 and 14 both revert to the wild type sequence in a portion of the viable virus particles present.

3. The replication kinetics of TMEV mutant 23 differ to that of wild type TMEV. The rate of TMEV mutant 23 nascent virions produced over time and the uppermost concentration of virions produced when 100% of the infected BHK-21 cells had succumbed to CPE were both drastically lower than that of the wild type virus.

4. The retarded replication kinetics of TMEV mutant 4 closely resembled those of TMEV mutant 23. In view of the reversion of the engineered mutation to the wild type sequence this suggests that a mixed population of wild type and mutant virions are present and that the TMEV mutant 4 replication may dominate that of the wild type virus.

5. The replication kinetics of TMEV mutant 14 indicate that although a portion of the virus particles present in BHK-21 cells infected with this virus may have reverted to wild type TMEV, the substitution mutation at amino acid 14 on the 2C protein as a dominant negative mutation to any wild type 2C or 2BC proteins present to a greater extent than the mutation at amino acid 4.

6. Point mutations at amino acids 8, 29 and possibly amino acid 18 of the 2C protein completely abolish the ability of TMEV to replicate in BHK-21 cells indicating that these mutations dramatically alter the ability of the 2C or 2BC proteins to interact with negative sense viral RNA and host cell membranes possibly preventing the assembly of the viral replication complex and viral RNA replication.

7. In addition to BHK-21 cells, TMEV strain GDVII is able to infect NIH-3T3 cells in tissue culture but is unable to infect HeLa or Cos-7 cells. The development of TMEV-induced CPE in NIH-3T3 cells is retarded compared to that in BHK-21 cells but it is unknown whether repeated rounds of infection of the virus in NIH-3T3 cells would enable the virus to "adapt", adjusting the replication kinetics of the virus in this cell line.

8. The localisation of transiently expressed mutant 4, 8 and 29 TMEV 2C proteins in BHK-21 cells was similar to that of the wild type 2C protein. This suggested

that the altered ability of the mutant 4, 8 and 29 TME viruses to induce CPE in BHK-21 cells was not a symptom of an altered localisation of the 2C protein in host cells. Further studies would investigate whether the altered ability of the mutant 4, 8 and 29 TME viruses to cause CPE in BHK-21 cells was linked to an altered membrane-association ability, a reduced ATP/GTPase activity or altered ability of these proteins to bind the negative strand of viral RNA during viral replication.

9. Transiently expressed mutant 14 and 18 TMEV 2C proteins showed an even cytoplasmic distribution with a faint perinuclear stain. The contrast of this localisation pattern with that of the wild type 2C protein suggests that these proteins have an altered ability to localise in host cells and that this may be the cause for the altered ability of mutant 14 and 18 TME viruses to induce CPE in BHK-21 cells

10. Transiently expressed TMEV mutant 23 protein localised to small punctate structures that partially overlap with the stain of the ER marker protein ERp60 but are completely separate from the stain of the peripheral Golgi marker protein β-COP. As previously mentioned, the wild type 2C protein localises to a faint reticular stain and/ or large structures adjacent to the nucleus and partially overlaps with both the ERp60 and β-COP stains. These contrasting localisations suggest that the mutant 23 2C protein localises to regions of the secretory pathway in a dissimilar manner to that of the wild type 2C protein.

11. Further studies would investigate the effect of the specific point mutations engineered into the 2C protein in this study on the membrane association characteristics of both the mutant 2Cand 2BC proteins. This would be followed by an investigation of the effect of the point mutations on the ability of the 2C protein to bind negative sense viral RNA and to exhibit ATPase/GTPase activity.

# 4 General discussion and future studies

## 4.1 GENERAL DISCUSSION AND FUTURE WORK

Primarily, this study sought to increase the general understanding of the interactions formed between picornavirus non-structural proteins and host cell components with the broader aim of expanding knowledge to allow the development of novel strategies for the control of picornavirus infections.

The localisation of the TMEV non-structural 2B, 2C, 2BC and 3A proteins in BHK-21 cells was compared to that of the corresponding FMDV and PV proteins. Despite the highly conserved genome organisation of the *Picornaviridae*, notable differences in the localisation of the FMDV and PV non-structural proteins in host cells have been reported (Doedens and Kirkegaard, 1995; Moffat *et al*, 2005; Aldabe and Carasco, 1995; Bienz *et al*, 1987; Bienz *et al*, 1990; Bienz *et al*, 1992; Cho *et al*, 1994; Schlegel *et al*, 1996; Rust *et al*, 2001; Doedens *et al*, 1997, Neznanov *et al*, 2001).

The distribution of transiently expressed TMEV 2B protein in a reticular stain in BHK-21 cells resembled that of the FMDV 2B protein (Moffat *et al*, 2005). However, there was some apparent colocalisation with the Golgi marker protein β-COP, suggesting that the localisation of the TMEV 2B protein may also imitate that of the PV 2B protein which localises exclusively to the Golgi (Doedens and Kirkegaard, 1995). Similarly, the localisation of the TMEV 2C protein most closely mimicked that of the FMDV 2C protein and not that of the PV 2C protein, as discussed in *Section 2.4.2*.

The TMEV 2BC protein appeared to locate exclusively to the Golgi. This distribution was distinct from that of both the PV and FMDV 2BC proteins which have been shown to associate with the membranes of the ER (Moffat *et al*, 2005; Rust *et al*, 2001). The TMEV 3A protein localised to the ER as well as the peripheral Golgi. The former observation, together with the distorted swelling of ER cisternae, resembled the localisation of both the PV and FMDV 3A proteins to an extent (Moffat *et al*, 205;

Doedens *et al*, 1997; Neznanov *et al*, 2001). Thus the comparison of the distributions of the transiently expressed 2B, 2C, 2BC and 3A proteins in host cells with the FMDV and PV proteins served only to demonstrate the diverse manner in which corresponding picornavirus proteins interact with host cell components while highlighting the involvement of secretory pathway membranes in picornavirus replication.

Future studies will involve an investigation of the membrane association characteristics of these TMEV proteins in order to gain a more complete understanding of their interaction with host membranes. This will involve the transient expression of the TMEV proteins in BHK-21 cells, followed by a differential fractionation procedure and coimmunoprecipitation of the TMEV proteins and the various organelle marker proteins from membrane fractions pertaining to specific organelles.

Following the description of the localisation of the non-structural TMEV proteins, the effect of these proteins on the ultrastructure of the same host cells will be investigated to determine which, if any, of the 2B, 2C, 2BC or 3A proteins are able to induce the disassembly of the Golgi complex and/ or the formation of vesicles. This will be performed through the examination of BHK-21 cells transiently expressing viral proteins by transmission electron microscopy. Following this, protein transport assays will be conducted to identify whether these proteins are able to disrupt protein trafficking through the exocytic pathway.

A more complete understanding of the roles played by the various picornavirus non-structural proteins in the assembly of the virus replication complex on the surface of modified host membranes is dependent on the identification of the mechanism through which these proteins interact with the host membranes in question. Interaction with host membranes must either occur directly or be mediated through the interaction of viral proteins with host membrane proteins. Picornavirus proteins may also form additional viral protein-host protein interactions during other stages of the virus replication cycle. Identification and understanding of these interactions would greatly enhance the general understanding of picornavirus replication as well as possibly providing targets for therapeutic drugs. Future studies will endeavour to identify and

describe interactions between TMEV non-structural proteins and host proteins through the coimmunoprecipitation of viral and host proteins using protein pull-down assays.

The detection of the TMEV 2B, 2C, 2BC and 3A proteins by Western analysis during membrane fractionation procedures or protein pull-down assays as well as the localisation of these proteins in transiently expressing host cells by electron microscopy is reliant on the availability of antibodies against these proteins. To this end, this study sought to express and purify a hydrophilic, antigenic region of the 2C protein in fusion with an N-terminal GST-tag. This was successfully achieved and future studies will involve the large-scale expression and purification of the GST-2C178 fusion peptide and the production of antibodies against this peptide, which will recognise both the TMEV 2C and 2BC proteins. The expression, purification and raising of antibodies against the 2B and 3A proteins may also be performed in future.

Various amino acid substitution mutations in the highly conserved N-terminal domain of the TMEV 2C protein affected the localisation of this protein in BHK-1 cells as well as the overall replication proficiency of the TME virus to different extents. The mutation of amino acids 14, 18 and 23 caused the mutant 2C proteins to localise in a manner distinct from that of the wild type 2C protein, while the localisation of the 2C protein was less dramatically altered by the mutation of amino acids 4, 8 and 29. In contrast, mutation of amino acids 8, 18 and 29 on the 2C protein completely inhibited the ability of TMEV to induce CPE in BHK-21 cells, while TME viruses with amino acid substitution mutations at amino acids 4, 14 and 23 showed an inhibited ability to induce CPE in BHK-21 cells.

In order to discern whether the altered ability of the mutant TME viruses to cause CPE in BHK-21 cells is a direct consequence of an altered membrane association ability of the mutant 2C proteins, the association of these mutant proteins with host cell membranes will be investigated by the comparative coimmunoprecipitation of the mutant and wild type 2C proteins with various organelle marker proteins from membrane fractions pertaining to specific organelles.

## 4.2 CONCLUSION

In conclusion, this study has described the localisation of the TMEV 2B, 2C, 2BC and 3A proteins in BHK-21 cells and the effect of introducing amino acid substitution mutations at highly conserved residues in the N-terminal domain of the 2C protein on the localisation of this protein as well as the overall replication proficiency of TMEV. Additionally the research reported here has prepared an extensive platform from which future research activities will be able to greatly increase our understanding of the varied interactions formed between host cell components and the proteins of different picornaviruses.

# 5 References


1. **Aldabe R., Carasco, L.** (1995). Induction of membrane proliferation by poliovirus proteins 2C and 2BC. *Biochem. Biophs. Res. Commun.* **206:** 64-76.
2. **Aldabe R., Barco, A. and Carasco, L.** (1996). Membrane permeabilisation by poliovirus proteins 2B and 2BC. *J. Biol. Chem.* **271:** 23134-23137.
3. **Alexandersen, S., Zhang, Z. and Donaldson, A.I.** (2002). Aspects of the persistence of foot-and-mouth disease virus in animals- the carrier problem. *Microbes Infect.* **4:** 1099-1110.
4. **Andino, R., Reickhof, G.E. and Baltimore, D.** (1990). A functional ribonucleoprotein complex forms around the 5' end of poliovirus RNA. *Cell* **63:** 369-380
5. **Andino, R., Reickhof, G.E., Achacoso, P.L. and Baltimore, D.** (1993). Poliovirus RNA synthesis utilises an RNP complex formed around the 5' end of viral RNA. *EMBO J.* **12:** 3587-3598.
6. **Banerjee, R. and Dasgupta, A.** (2000). Specific Interaction of Hepatitis C Virus Protease/Helicase NS3 with the 3'-Terminal Sequences of Viral Positive- and Negative-Strand RNA. *J. Virol.* **75:** 1708-1721
7. **Banerjee, R., Echeverri, A. and Dasgupta, A.** (1997). Poliovirus encoded 2C polypeptide specifically binds to the 3'-terminal sequences of viral negative-strand RNA. *J. Virol.* **71:** 9570-9578.
8. **Banerjee, R., Weidman, M.K., Echeverri, A., Kundu, P. and Dasgupta, A.** (2004). Regulation of Poliovirus 3C protease by the 2C polypeptide. *J. Virol.* **78:** 9243-9256.
9. **Barco, A. and Carasco, L.** (1995). A human virus protein, poliovirus protein 2BC, induces membrane proliferation and blocks the exocytic pathway in the yeast *Saccharomyces cerevisiae. EMBO J.* **14:** 3349-3364.
10. **Barco, A. and Carasco, L.** (1998). Identification of regions of poliovirus 2BC protein that are involved in cytotoxicity. *Virol.* **72:** 3560-3570.
11. **Barlowe, C., Orci, L., Yeung, T., Hosobuchi, M., Hamamoto, S., Salama, N., Rexach, M.F., Ravazzola, M, Amherdt, M. and Schekman, R.** (1994). COPII: a membrane coat formed by Sec proteins that drive vesicle budding from the endoplasmic reticulum. *Cell* 77: 895-907.

12. **Barton, D.J. and Flanegan, J.B.** (1997). Synchronous replication of poliovirus RNA: initiation of negative-strand RNA synthesis requires the guanidine-inhibited activity of protein 2C. *J. Virol.* **71:** 8482-8489.
13. **Beard, C.W. and Mason, C.W.** (2000). Genetic determinants of altered virulence of Taiwanese foot-and-mouth disease virus. *J. Virol.* **74:** 987-991.
14. **Bedard, K.M. and Semler, B.L.** (2004). Regulation of Picornavirus gene expression. *Micro. Infect.* **6:** 702-713.
15. **Beneduce, F., Pisane, G., Divizia, M., Pana, A. and Morace, G.** (1995). Complete nucleotide sequence of a cytopathic hepatitis A virus strain isolated in Italy. *Virus Res.* **36:** 299-309.
16. **Bernstein, H., Sarnow, P. and Baltimore, D.** (1986). Genetic complementation among poliovirus mutants derived from an infectious cDNA clone. *J. Virol.* 60: 1040-1049.
17. **Bienz, K., Egger, D. and Pasamontes, L.** (1987). Association of polioviral proteins of the P2 genomic region with the viral replication complex and virus-induced membrane synthesis as visualised by electron microscopic immunocytochemistry and autoradiography. *Virology* **160:** 220-226.
18. **Bienz, K., Egger, D., Troxler, M. and Pasamontes, L.** (1990). Structural organisation of poliovirus RNA replication is mediated by viral proteins of the P2 genomic region. *J. Virol.* **64:** 1156-1163.
19. **Bienz, K., Egger, D., Pfister, T. and Troxler, M.** (1992). Structural and functional characterisation of the poliovirus replication complex. *J. Virol.* **66:** 2740-2747.
20. **Bienz, K., Egger, D., Pfister, T.** (1994). Characteristics of the poliovirus replication complex. *Arch. Virol.* **9**(Suppl)**: 147-157.**
21. **Carasco, L.** (1995). Modification of membrane permeability by animal viruses. *Ad. Vir. Res.* **45:** 61-112.
22. **Cho, M.W., Teterina, N., Egger, D., Bienz, K. and Ehrenfeld, E.** (1994). Membrane rearrangement and vesicle induction by recombinant poliovirus 2C and 2BC in human cells. *Virology* **202:** 129-145.
23. **Choe, S.S., Dodd, D.A. and Kirkegaard, K.** (2005). Inhibition of cellular protein secretion by picornaviral 3A proteins. *Virology* **337:** 18-29.
24. **Constans, A.** (2002). Protein Purification II: Affinity Tags. *The Scientist* **16:** 37

25. **Cuconati, A., Moller, A. and Wimmer, E.** (1998). Brefeldin A inhibits cell free, de novo synthesis of poliovirus. *J. Virol.* **72:** 6456-6464

26. **Deitz, S.B., Dodd, D.A., Cooper, S., Parham, P. and Kirkegaard, K.** (2000). MHC-I dependent antigen presentation is inhibited by poliovirus protein 3A. *Proc. Natl. Acad. Sci. U.S.A.* **97:** 137-90-13795.

27. **de Jong, A.S., Schrama, I.W.J., Willems, P.H.G.M., Galama, J.M.D., Melchers, W.J.G. and van Kuppeveld, F.J.M.** (2002). Multimerization reactions of coxsackievirus proteins 2B, 2C and 2BC: a mammalian two-hybrid analysis. *J. Gen. Virol.* **83:** 783-793.

28. **Dodd, D.A., Giddings Jr, T.H. and Kirkegaard, K.** (2001). Poliovirus 3A protein limits interleukin-6 (II-6), il-8 and interferon-beta secretion during viral infection. *J. Virol.* **75:** 8158-8165.

29. **Doedens, J.R. and Kirkegaard, K.** (1995). Inhibition of cellular protein secretion by poliovirus proteins 2B and 3A. *EMBO J.* **14:** 894-907.

30. **Doedens, J.R., Giddings Jr., T.H., and Kirkegaard, K.** (1997). Inhibition of endoplasmic reticulum-to-Golgi traffic by poliovirus protein 3A: genetic and ultrastructural analysis. *J. Virol.* **71:** 9054-9064.

31. **Duden, R., Griffiths, G., Frank, R., Argos, P. and Kreis, T.E.** (1991). Beta-COP, a 110 kd protein associated with the non-clathrin-coated vesicles and the Golgi complex, shows homology to beta-adaptin. *Cell* **64:** 649-665.

32. **Egger, D., Pasamontes, L., Bolton, R., Boyko, V. and Bienz, K.** (1996). Reversible dissociation of the poliovirus replication complex: functions and interactions of its components in viral RNA synthesis. *J. Virol.* **70:** 8675-8683.

33. **Echeverri, A. and Dasgupta, A.** (1995). Amino terminal regions of poliovirus 2C protein mediate membrane binding. *Virology* **208:** 540-553.

34. **Echeverri, A., Banerjee, R. and Dasgupta, A.** (1998). Amino-terminal region of poliovirus 2C protein is sufficient for membrane binding. *Vir. Res.* **54:** 217-223.

35. **Flanegan, J.B. and Baltimore, D.** (1977). Poliovirus-specific primer-dependent RNA polymerase able to copy poly(A). *Proc. Natl. Acad. Sci. USA* **74:** 3677-3680.

36. **Fujiwara, T., Oda, K., Yokota, S., Takasuki, A. and Ikehara, Y.** (1988). Brefeldin A causes disassembly of the Golgi complex and accumulation of

secretory proteins in the endoplasmic reticulum. *J. Biol. Chem.* **263:** 18545-18552.

37. **Gasteiger E., Hoogland C., Gattiker A., Duvaud S., Wilkins M.R., Appel R.D., Bairoch A.**; Protein Identification and Analysis Tools on the ExPASy Server; Accessed 2006/09/02, (In) John M. Walker (ed): The Proteomics Protocols Handbook, Humana Press (2005). 571-607.
38. **Giachetti, C. and Semler, B.L.** (1991). Role of a viral membrane polypeptide in strand-specific initiation of poliovirus RNA synthesis. *J. Virol.* **65:** 2647-2654.
39. **Giachetti, C., Hwang, S.S. and Semler, B.L.** (1992). *cis*-acting lesions targeted to the hydrophobic domain of a poliovirus membrane protein involved in RNA replication. *J. Virol.* **66: 6045-6057.**
40. **Guinea, R. and Carasco, L.** (1990). Phospholipid biosynthesis and poliovirus genome replication: two coupled phenomena. *EMBO J.* **9:** 2011-2016.
41. **Haenni, A. and Kadare, G.** (1997). Virus-encoded helicases. *J. Virol.* **71:** 2583-2590.
42. **Harris, K.S., Hellen, C.U.T., and Wimmer, E.** (1990). Proteolytic processing in the replication of picornaviruses. *Virol.* **1:** 323-333.
43. **Harris, K.S., Xiang, W., Alexander, L., Lane, W.S., Paul, A.V. and Wimmer, E.** (1994). Interaction of poliovirus polypeptide with $3CD^{pro}$ with 5' and 3' termini of the poliovirus genome. Identification of viral and cellular co-factors needed for efficient binding. *J. Biol. Chem.* **269:** 27004-27014.
44. **Invitrogen** (2004). pcDNA3.1/V5-His© TOPO® TA Expression Kit instruction manual, Version H.
45. **Irurzun, A., Perez, L., Carasco, L.** (1992). Involvement of membrane traffic in the replication of the poliovirus genomes: effects of Brefeldin A. *Virology* **191:** 166-175.
46. **Jnaoui, K., Minet, M. and Michiels.** T. (2002). Mutations That Affect the Tropism of DA and GDVII Strains of Theiler's Virus In Vitro Influence Sialic Acid Binding and Pathogenicity. *J. Virol.* **76:** 8138-8147
47. **Johnson, K., Sarnow, P.** (1991). Three poliovirus 2B mutants exhibit noncomplementable defects in viral RNA amplification and display dosage-dependent dominance over wild-type poliovirus. *J. Virol.* **65:** 4341-4349.

48. **Kilpatrick, D. R., and H. L. Lipton.** 1991. Predominant binding of Theiler's virus to a 34-kilodalton receptor protein on susceptible cell lines. J. Virol. **65:**5244–5249

49. **Knox, C., Ali, S., Ryan, M. and Wileman, T.** (2005). Foot and mouth disease virus replication complexes form within the Golgi apparatus but exclude host membrane components. *J. Gen. Virol.* **86:** 687-696

50. **Kolaskar, A.S. & Tongaonkar, P.C.** (1990). A semi empirical method for prediction of antigenic determinants on protein antigens, *FEBS* **276:** 172-174

51. **Kong, W.-P., Ghadge, G.D. and Roos, R.P.** (1994). Involvement of Cardiovirus leader in host-restricted virus expression. *Proc. Natl. Acad. Sci. U.S.A.* **91:** 1796-1800.

52. **Li, J.P., and Baltimore, D.** (1988). Isolation of poliovirus 2C mutants defective in viral RNA synthesis. *J. Virol.* **62:** 4016-4021.

53. **Li, J.P., and Baltimore, D.** (1990). An intragenic revertant of poliovirus 2C mutant has an uncoating effect. *J. Virol.* **64;** 1102-1107.

54. **Lippincott-Schwartz, J., Donaldson, J.G., Schweizzer, A., Berger, E.G., Hauri, H.P., Yuan, I.C. and Klausner, R.D.** (1990). Microtubule-dependent retrograde transport of proteins into the ER in the presence of Brefeldin A suggests an ER recycling pathway. *Cell* **60:** 821-836.

55. **Mackenzie, J.M., Jones, M.K. and Westaway, E.G.** (1999). Markers for *trans*-Golgi Membranes and the Intermediate Compartment Localize to Induced Membranes With Distinct Replication Functions in Flavivirus-Infected Cells. *J. Virol.* **73**: 9555-9567.

56. **Magliano, D., Marshall, J.A., Bowden, D.S., Verdaxis, N., Meanger, J and Lee, J.Y.** (1998). Rubella virus replication complexes are virus-modified lysosomes. *Virology.* **240**: 57-63.

57. **Maynell, L.A. Kirkegaard, K. and Klymkowsky, M.W.** (1992). Inhibition of poliovirus RNA synthesis by Brefeldin A. *J. Virol.* **66:** 1985-1994.

58. **Miller, D.J. and Ahlquist, P.** (2002). Flock House Virus RNA polymerase is a transmembrane protein with amino-terminal sequences sufficient for mitochondrial localisation and membrane insertion. *J. Virol.* **76**: 9856-9867.

59. **Mirzayan, C. and Wimmer, E.** (1992). Genetic analysis of an NTP-binding motif in poliovirus peptide 2C. *Virology* **189:** 547-555.

60. **Mirzayan, C. and Wimmer, E.** (1994). Biochemical studies on poliovirus polypeptide 2C: evidence for ATPase activity. *Virology* **199:** 176-187.

61. **Moffat, K., Howell, G., Knox, C., Belsham, G.J., Monaghan, P., Ryan, M.D. and Wileman, T.** (2005). Effects of foot-and-mouth disease virus nonstructural proteins on the structure and function of the early secretory pathway: 2BC but not 3A blocks endoplasmic reticulum-to-Golgi transport. *J. Virol.* **79:** 4382-4395.

62. **Monaghan, P., Cook, H., Jackson, T., Ryan, M. and Wileman, T.** (2004). The ultrastructure of the developing replication site in foot-and-mouth disease virus-infected BHK-38 cells. *J. Gen. Virol.* **85:** 933-946.

63. **Monteyne, P., Bureau, J.F. and Brahic, M.** (1997). The infection of mouse from Theiler's virus: from genetics to immunology. *Immunol. Rev.* **159:** 163-176.

64. **National Centre for Biotechnology Information (NCBI)** (Last revised 27th September 2006). http://www.ncbi.nlm.nih.gov/

65. **Neznanov, N.A., Kondratova, A., Chumakov, K.M., Angres, B., Zhumabayeva, B., Agol, V.I. and Gudkov, A.V.** (2001). Poliovirus protein 3A inhibits tumor necrosis factor (TNF)-induced apoptosis by eliminating the TNF receptor from the cell surface. *J. Virol.* **75:** 10409-10420.

66. **Nunez, J.I., Baranowski, E., Molina, N., Ruiz-Jarabo, C.M., Sanchez, C., Domingo, E. and Sobrino, F.** (2001). A single amino acid substitution in non-structural protein 3A can mediate adaptation of foot-and-mouth disease virus to the guinea pig. *J. Virol.* **75:** 3977-3983.

67. **O'Donnel, V.K., Pacheco, J.M., Henry, T.M. and Mason, P.W.** (2001). Subcellular distribution of the foot-and-mouth disease virus 3A protein in cells infected with viruses encoding wild-type and bovine attenuated forms of 3A. *Virology* **287:** 151-162.

68. **Paul, A.V., Molla, A. and Wimmer, E.** (1994). Studies of a putative amphipathic helix in the N-terminus of poliovirus protein 2C. *Virology* **199:** 188-199.

69. **Pelletier, J. and Sonenberg, N.** (1988). Internal initiation of translation of eukaryotic mRNA directed by a sequence derived from poliovirus RNA. *Nature* **334:** 320-325.

70. **Pevear, D.C., Borkowski, J., Calenoff, M., Oh, C.K., Ostrowski, B. and Lipton, H.L.** (1988). Insight into Theiler's virus neurovirulence based on a genomic comparison of the neurovirulent GDVII and less virulent BeAn strains. *Virology* **165:** 1-12.

71. **Pfister, T., Pasamontes, L., Troxler, M., Egger, D. and Bienz, K.** (1992). Immunocytochemical localisation of capsid-related particles in subcellular fractions of poliovirus infected cells. *Virology* **188:** 676-684.

72. **Pfister, T. and Wimmer, E.** (1999). Characterisation of the nuceoside triphosphatase activity of poliovirus protein 2C reveals a mechanism by which guanidine inhibits poliovirus replication. *J. Biol. Chem.* **274:** 6992-7001.

73. **Pfister, T., Jones, K.W. and Wimmer, E.** (2000). A cysteine-rich motif in poliovirus protein $2C^{ATPase}$ is involved in RNA replication and binding zinc *in vitro*. *J. Virol.* **74:** 334-343.

74. **Rodriguez, P.L. and Carasco, L.** (1993). Poliovirus protein 2C has ATPase and GTPase activities. *J. Biol. Chem.* **268:** 8105-8110.

75. **Rodriguez, P.L. and Carasco, L.** (1995). Poliovirus protein 2C contains two regions involved in RNA binding activity. *J. Biol. Chem.* **270:** 10105-10112.

76. **Rust, R.C., Landmann, L., Gosert, R., Tang, B.L., Hong, W., Hauri, H. -P., Egger, D. and Bienz, K.** (2001). Cellular COPII proteins are involved in production of the vesicles that form the poliovirus replication complex. *J. Virol.* **75:** 9808-9818.

77. **Saier, M.H.J. and McCaldon, P.** (1988). Statistical and functional analysis of viral and cellular proteins with N-terminal amphipathic alpha-helices with large hydrophobic moments importance to macromolecular recognition and organelle targeting. *J. Bacteriol.* **170:** 2296-2300.

78. **Sandoval, I.V. and Carasco, L.** (1997). Poliovirus infection and expression of the poliovirus protein 2B provoke the disassembly of the Golgi complex, the organelle target for the antipoliovirus drug Ro-090179. *J. Virol.* **71:** 4679-4693.

79. **Sanz-Para, A., Sobrino, F. and Ley, V.** (1998). Infection with foot-and-mouth disease virus results in a rapid deduction in MHC class 1 surface expression. *J. Gen. Virol.* **79:** 43-436.

80. **Savolainen, C., Blomqvist, S., Mulders, M.N. and Hovi, T.** (2002) Genetic clustering of all 102 human rhinovirus prototype strains: serotype 87 is close to human enterovirus 70. *J. Gen. Virol.* **83:** 333–340

81. **Schlegel, A.T.H., Giddings, Jr, T.H., Ladinsky, M.S. and Kirkegaard, K.** (1996). Cellular origin and ultrastructure of membranes induced during poliovirus infection. *J. Virol.* **70:** 6576-6588.

82. **Schmidt-Mende, J., Bieck, E., Hugle, T., Penin, F., Rice, C.M., Blum, H.E. and Moradpour, D.** (2001). Determinants for membrane association of the Hepatitis C virus RNA-dependent RNA polymerase. *J. Biol. Chem.* **276**: 44052-44063.

83. **Segrest, J.P., Garber, D.W., Brouillete, C.G., Harvey, S.C. and Anantharamaiah, G.M.** (1994). The amphipathic α helix: a multifunctional a structural motif in plasma apolipoproteins. *Adv. Protein Chem.* **45:** 303-369.

84. **Silverman, L.R., Phipps, A.J., Montgomery, A., Ratner, L. and Lairmore, M.D.** (2004). Human T-Cell Lymphotropic Virus Type 1 Open Reading Frame II-Encoded $p30^{II}$ Is Required for In Vivo Replication: Evidence of In Vivo Reversion. *J. Virol.* **78:** 3837-3845

85. **Strauss, D.M., Glustrom, L.W. and Wuttke, D.S.** (2003). Towards an understanding of the poliovirus replication complex: the solution structure of the soluble domain of the poliovirus 3A protein. *J. Mol. Biol.* **330:** 225-234.

86. **Suhy, D.A., Giddings, Jr, T.H., and Kirkegaard, K.** (2000). Remodelling the endoplasmic reticulum by poliovirus infection and by individual viral proteins: an autophagic-like origin for virus-induced vesicles. *J. Virol.* **74:** 8953-8965.

87. **Teterina, N.L., Kean, K.M., Gorbalenya, A.E., Agol, V.I. and Girard, M.** (1992). Analysis of the functional significance of amino acid residues in the putative NTP-binding pattern of the poliovirus 2C protein. *J. Gen. Virol.* **73:** 1977-1986.

88. **Teterina, N.L., Bienz, K., Egger, D., Gorbalenya, A.E. and Ehrenfeld, E.** (1997). Induction of intracellular membrane rearrangements by HAV proteins 2C and 2BC. *Virology* **237:** 66-77.

89. **Teterina, N.L., Gorbalenya, A.E., Egger, D., Bienz, K. and Ehrenfeld, E.** (1997). Poliovirus 2C protein determinants of membrane binding and rearrangements in mammalian cells *J. Virol.* **71:** 8962-8972.

90. **Tolley, N.D., Tsunoda, I. and Fujinami, R.S.** (1999). DNA Vaccination against Theiler's Murine Encephalomyelitis Virus Leads to Alterations in Demyelinating Disease. *J Virol.* **73:** 993–1000.

91. **Troxler, M., Egger, D., Pfister, T. and Bienz, K.** (1992). Intracellular localisation of poliovirus RNA by *in situ* hybridisation at the ultrastructural level using single-stranded riboprobes. *Virology* **191:** 687-697.

92. **Tuschall, D.M., Hiebert, E. and Flanegan, J.B.** (1982). Poliovirus RNA-dependent RNA polymerase synthesises full-length copies of poliovirion RNA, cellular mRNA and several plant virus RNAs *in vitro*. *J. Virol.* **44:**209-216.

93. **Vance, L.M., Moscufo, N., Chow, M. and Heinz, B.A.** (1997). Poliovirus 2C region functions during encapsidation of viral RNA. *J. Virol.* **71:** 8759-8765.

94. **Van Dyke, T.A. and Flanegan, J.B.** (1980). Identification of poliovirus polypeptide p63 as a soluble RNA-dependent RNA polymerase. *J. Virol.* **35:** 732-740.

95. **Van Dyke, T.A., Rickles, R.J. and Flanegan, J.B.** (1982). Genome-length copies of poliovirion RNA are synthesised *in vitro* by the poliovirus RNA-dependent RNA polymerase. *J. Biol. Chem.* **257:** 4610-4617.

96. **van Kuppeveld, F.J., Melchers, W.J., Kirkegaard, K. and Doedens, J.R.** (1997). Structure-function analysis of coxsakie B3 virus protein 2B. *Virology* **227:** 111-118.

97. **van Pesch, V., van Eyll, O. and Michiels, T.** (2001). The leader protein of Theiler's virus inhibits immediate early alpha/beta interferon production. *K. Virol.* **75:** 7811-7817.

98. **Wimmer, E., Helen, C.U.T. and Cao, X.** (1993). Genetics of poliovirus. *Annu. Rev. Genet.* **27:** 353-436.

99. **World Health Organization** (2002). The global poliomyelitis eradication initiative: number of endemic countries at lowest ever. *Wkly Epidemiol Rec.* **77:**414-5.

100. **Xiang, W., K. S. Harris, L. Alexander, and E. Wimmer.** (1995). Interaction between the 5'-terminal cloverleaf and 3AB/3CD$^{pro}$ of poliovirus is essential for RNA replication. *J. Virol.* **69:**3658-3667.

101. **Ypma-Wong, M.F., Dewalt, P.G., Johnson, V.H., Lamb, J.G. and Semler, B.L.** (1998). Protein 3CD is the major poliovirus proteinase responsible for cleavage of the Pi capsid precursor. *Virology* **166:** 265-270.

102. **Zhou, L., X. Lin, T. J. Green, H. L. Lipton, and M. Luo.** 1997. Role of sialyloligosaccharide binding in Theiler's virus persistence. J. Virol. **71:**9701–9712.

## Internet references


1. Yin-Murphy, M. and Almond, J.W. (Accessed 28/07/06). Picornaviruses. *http://www.gsbs.utmb.edu/microbook/ch053.htm*
2. U.S. Department Of Health (2006). Accessed: 21/07/2006. http://www.kidsource.com/health/the.common.cold.html
3. http://ghr.nlm.nih.gov/ghr/glossary/dominantnegativemutation, Genetics Home Reference, October 2006


# Appendix A Vector Maps

### A.1 Commercial vectors

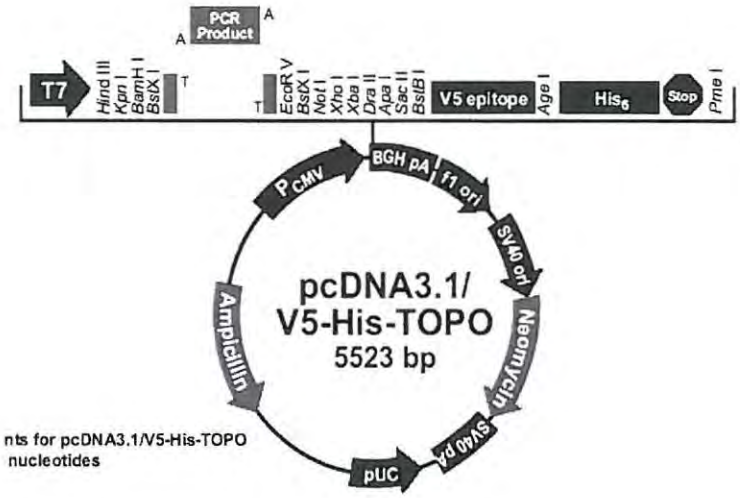


**Figure A.1** The pcDNA3.1/V5-His© TOPO® mammalian expression vector (Invitrogen)

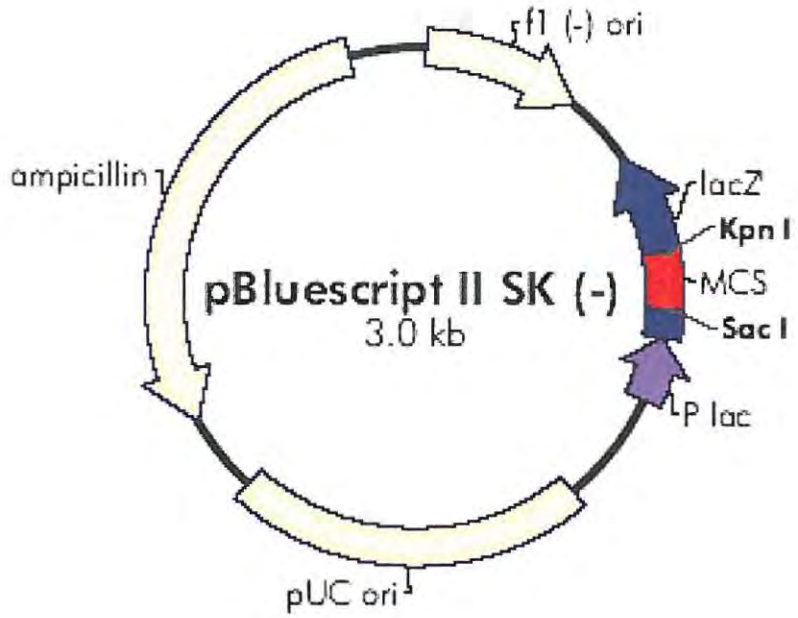


**Figure A.2** The pBlueScript® II Phagemid Vector (Stratagene)
http://www.stratagene.com/products/displayProduct.aspx?pid=267


**Figure A.3** The pGEX-2T bacterial expression vector (Amersham)
http://www5.amershambiosciences.com/aptrix/upp01077.nsf/Content/Products?OpenDocument&ModuleId=38859&hometitle=E-tech%20Support

## A.2 Recombinant vectors with pcDNA3.1/V5-His© TOPO® as the parent vector

The insert shown in the recombinant vector below represents the coding sequence for any one of the TMEV proteins shown in Table A.1.

**Table A.1 Recombinant vectors and corresponding inserts represented by Figure A.4**

| Recombinant vector | TMEV protein coding sequence | Insert size (bp) | Recombinant vector size (bp) |
|---|---|---|---|
| pLMT2B | 2B | 380 | 5 903 |
| pCOT2C | 2C | 978 | 6 501 |
| pLMT2C4 | 2C mutant 4 | 978 | 6 501 |
| pLMT2C8 | 2C mutant 8 | 978 | 6 501 |
| pLMT2C14 | 2C mutant 14 | 978 | 6 501 |
| pLMT2C18 | 2C mutant 18 | 978 | 6 501 |
| pLMT2C23 | 2C mutant 23 | 978 | 6 501 |
| pLMT2C29 | 2C mutant 29 | 978 | 6 501 |
| pLMT2BC | 2BC | 1 358 | 6 881 |
| pLMT3A | 3A | 264 | 5 787 |
| pLMT2C60 | 2C60 | 180 | 5 703 |
| pLMT2BC60 | 2BC60 | 560 | 6 083 |

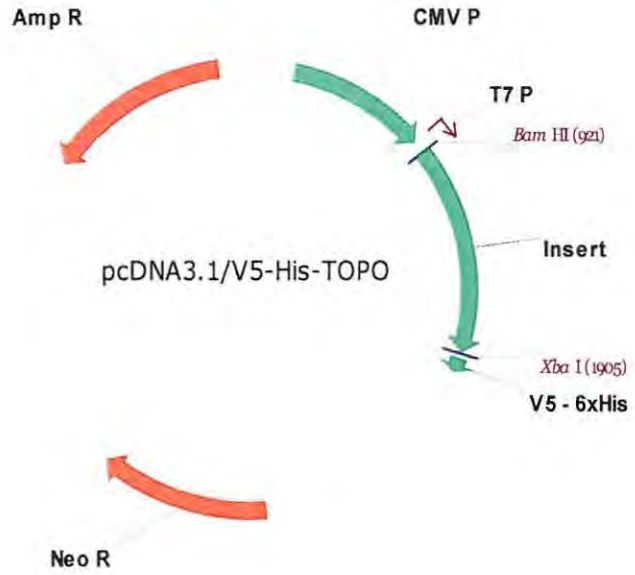


**Figure A.4** A representative of the recombinant vectors created through the insertion of the wild type 2B, 2C, 2BC and 3A, truncated 2C and 2BC and mutant 2C TMEV coding sequences into the mammalian expression vector pcDNA3.1/V5-His© TOPO®. The insert in this recombinant vector represents any one of these coding sequences.

## A.3 Recombinant vector constructed by inserting the coding sequence of the TMEV genome into the pBlueScript® II Phagemid Vector

| Table A.2 Recombinant vectors and corresponding inserts represented by Figure A.4 | |
|---|---|
| **Recombinant vector** | **TMEV genomic sequence** |
| pGDVII-WT | Wild type |
| pGDVII-mt4 | Substitution mutation at amino acid 4 on 2C protein |
| pGDVII-mt8 | Substitution mutation at amino acid 8 on 2C protein |
| pGDVII-mt14 | Substitution mutation at amino acid 14 on 2C protein |
| pGDVII-mt18 | Substitution mutation at amino acid 18 on 2C protein |
| pGDVII-mt23 | Substitution mutation at amino acid 23 on 2C protein |
| pGDVII-mt29 | Substitution mutation at amino acid 29 on 2C protein |

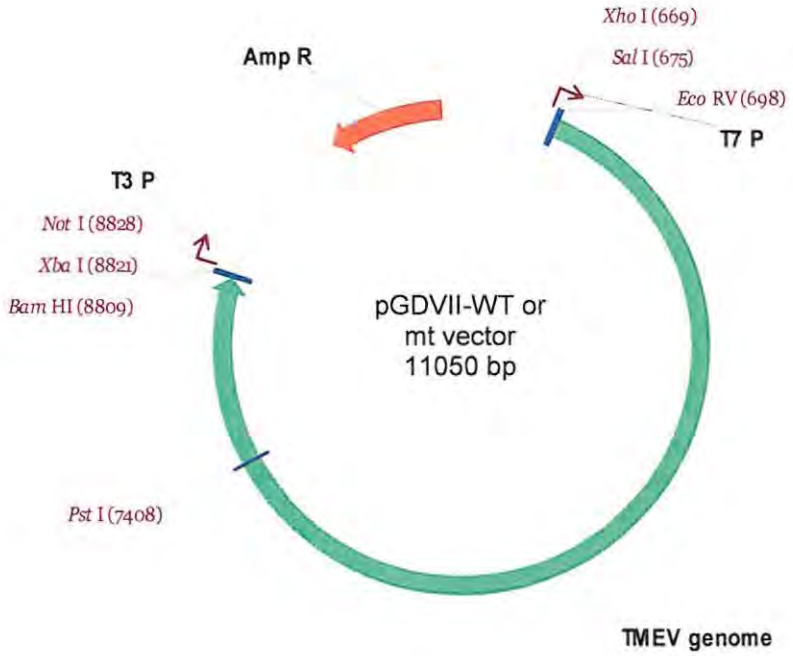


**Figure A.5** A representative of the recombinant vectors named pGDVII-WT or pGDVII-mt, created through the insertion of the wild type or mutant TMEV genomic sequences into the pBlueScript® II Phagemid Vector.

## A.2 pLMG2T2C178 recombinant vector

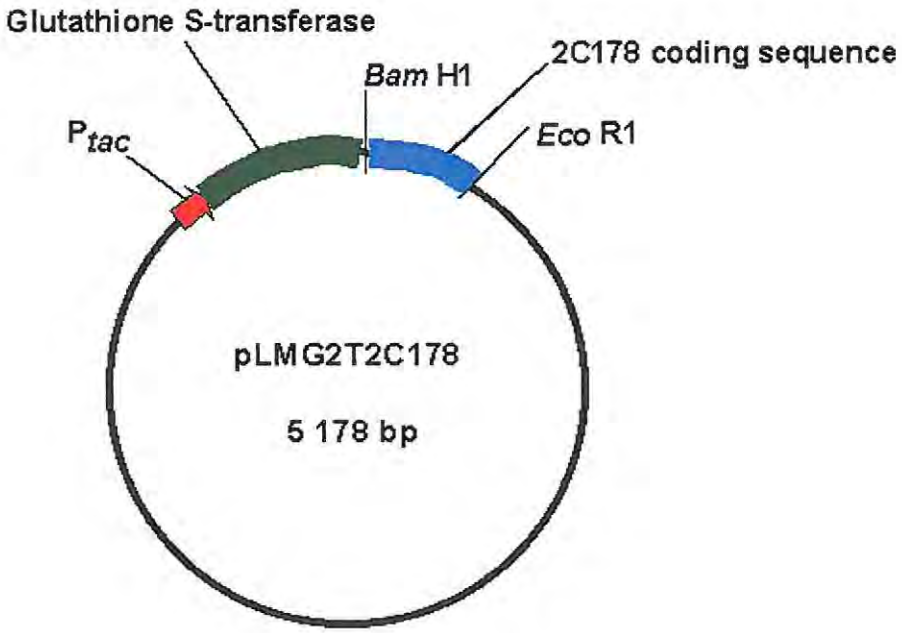


**Figure A.6** The pLMG2T2C178 recombinant vector created through the insertion of the 2C178 peptide into the bacterial expression vector pGEX-2T.

# Appendix B Sequence data

## B.1 Coding regions for the wild type and truncated TMEV P2 and 3A proteins subcloned into the pcDNA3.1/V5-His TOPO mammalian expression vector

The constructs resulting from the subcloning of the TMEV 2B, 2C, 2BC and 3A coding regions into the mammalian expression vector pcDNA3.1/V5-His TOPO® were sequenced using T7 forward and BGH reverse sequencing primers (Invitrogen).

| Recombinant vector | TMEV Protein Encoded | Sequencing Primers | Protein in frame | Undesirable mutations |
|---|---|---|---|---|
| pLMT2B | 2B | T7 & BHG | Yes | Single substitution (Glu to Lys) present at amino acid 69. Present in pGD7 templates |
| pCOT2C | 2C | T7 & BHG | Yes | None |
| pLMT2BC | 2BC | T7 & BHG | Yes | Single substitution (Glu to Lys) present at amino acid 69. Present in pGD7 templates |
| pLMT3A | 3A | T7 | Yes | None |
| pLMT2C60 | Truncated 2C | T7 | Yes | None |
| pLMT2BC60 | Truncated 2BC | T7 | Yes | None |

## B.2 Coding regions for mutant TMEV 2C proteins subcloned into the pcDNA3.1/V5-His TOPO mammalian expression vector

The constructs resulting from the subcloning of the mutant TMEV 2C coding regions into the mammalian expression vector pcDNA3.1/V5-His TOPO® were sequenced using T7 forward and BGH reverse sequencing primers (Invitrogen).

| Recombinant vector | Position of amino acid substitution | Sequencing Primers | Protein in frame | Undesirable mutations |
|---|---|---|---|---|
| pLMT2C4 | 4 | T7 | Yes | None |
| pLMT2C8 | 8 | T7 | Yes | None |
| pCOT2C14 | 14 | T7 | Yes | None |
| pCOT2C18 | 18 | T7 | Yes | None |
| pLMT2C23 | 23 | T7 | Yes | None |
| pLMT2C429 | 29 | T7 | Yes | None |

### B.3 Recombinant pLMG2T2C4 vector

| Recombinant vector | Coding region | Sequencing Primers | Peptide in frame | Undesirable mutations |
|---|---|---|---|---|
| pLMG2T2C4 | 2C178 peptide | pGEX 3' sequencing primer | Yes | None |

The sequence of the pGEX 3' sequencing primer is as follows:
5'-CCGGGAGCTGCATGTGTCAGAGG-3'

### B.4 Wild type and mutant TMEV genome sequences inserted into the pBlueScript® II Phagemid Vector

| Recombinant vector | Sequencing primer | Desired mutation present | Undesirable mutations |
|---|---|---|---|
| pGDVII-mt4 | 2Bf | Yes | None |
| pGDVII-mt8 | 2Bf | Yes | None |
| pGDVII-mt14 | 2Bf | Yes | None |
| pGDVII-mt18 | 2Bf | Yes | None |
| pGDVII-mt23 | 2Bf | Yes | None |
| pGDVII-mt29 | 2Bf | Yes | None |

The sequence of the 2Bf sequencing primer is as follows:
5'-CCTGTGCAGTCGGTTTTTCAGCC -3'

### B.5 Replicating TMEV mutants 4 and 23 RT-PCR products

| RT-PCR product | Sequencing Primers | Desired mutation present |
|---|---|---|
| TMEV mt 4 RT-PCR | 2Bf | No |
| TMEV mt 14 RT-PCR | 2Bf | No |
| TMEV mt 23 RT-PCR | 2Bf | Yes |

**B.6 Non-replicating TMEV mutants 8, 18 and 29 sequenced between the *Acc* III and *Eco* NI sites overlayed with the sequences in point 5 above**

| Recombinant vector | Sequenced | Sequencing Primers | Desired mutation present | Undesirable mutations |
|---|---|---|---|---|
| pGDVII-mt8 | Yes | AccIII fwd<br>AccIII rev | Yes | • Substitution mutation at amino acid 69 in the 2B protein. Present in all pGD-7sequences. |
| pGDVII-mt18 | Yes | AccIII fwd<br>AccIII rev | Yes | • 3 substitution mutations at amino acids 74, 75, 76 in the 2A protein.<br>• 2 substitution mutations at amino acids 14&30in the 2B protein.<br>• Substitution mutation at amino acid 69 in the 2B protein. Present in all pGD-7 sequences. |
| pGDVII-mt29 | Yes | AccIII fwd<br>AccIII rev | Yes | • Substitution mutation at amino acid 69 in the 2B protein. Present in all pGD-7sequences. |

The sequence of the AccIII forward sequencing primer is as follows:
5'-CCCGCTTCTCTCTACCGC -3'

The sequence of the AccIII reverse sequencing primer is as follows:
5'-CCTGTCTGGTGGGGACTGGGC -3'

# Appendix C Primers for PCR amplification

| Table C.1 Primers used for PCR amplification of TMEV protein coding sequences | | |
|---|---|---|
| **PCR product** | **Forward primer (5' - 3')** | **Reverse primer (5' - 3')** |
| **2B** | **2BF:** TTTGGATCCACCATGCCTGTGCAGTCGTTTTTCAG | **2BR:** CTGAGGTTGCATGACATTGG |
| **2C** | **2CF:** TTTGGATCCACCATGGGGCCTCTACGCGAGG | **2CR:** GGGCCCTCTAGACTCTGGGCAACCAAGCTGTTC |
| **2BC** | **2BF** | **2CR** |
| **3A** | **3AF:** TTTGGATCCACCATGTCCCCACCAGACTGGCAAC | **3AR:** GGGCCCTCTAGACTCTGTTCGCCCTCAGAGAGC |
| **2C60** | **2CF** | **2C60R:** CCCGGGTCTAGACTAGGGAATTCCATAAGC |
| **2BC60** | **2BCF** | **2C60R:** CCCGGGTCTAGACTAGGGAATTCCATAAGC |
| **2C178** | **ASqeF:** CCCGGATCCACTAGCTGGTTCAAGCAGG | **ASqeR:** CCCAAGCTTTCAGCTAGAGGTGAAAGGGGT |

| Table C.2 Primers used for the overlap PCR amplification of mutant TMEV genome coding sequences | | | |
|---|---|---|---|
| **Overlap PCR product** | **Round 1 (reaction 1)** | **Round 1 (reaction 2)** | **Round 2** |
| **TMEV GDVII mutant 4** | TME28CF | R4AF | TME28CF |
| | R4AR | TME28CR | TME28CR |
| **TMEV GDVII mutant 8** | TME28CF | E8AF | TME28CF |
| | E8AR | TME28CR | TME28CR |
| **TMEV GDVII mutant 14** | TME28CF | K14AF | TME28CF |
| | K14AR | TME28CR | TME28CR |
| **TMEV GDVII mutant 18** | TME28CF | W18AF | TME28CF |
| | W18AR | TME28CR | TME28CR |
| **TMEV GDVII mutant 23** | TME28CF | I23AF | TME28CF |
| | I23AR | TME28CR | TME28CR |
| **TMEV GDVII mutant 29** | TME28CF | W29AF | TME28CF |
| | W29AR | TME28CR | TME28CR |

| Table C.2 Sequences of primers used for overlap PCR reactions | |
|---|---|
| **Primer name** | **Sequence (5' - 3')** |
| TME28CF | GTG CTC ACC TTC CGG ATT CCA GGC TTC GGT CTG |
| TME28CR | CCA TTT TCA CAA CCT GTT GAA GGT TGT AGA C |
| R4AF | GCC TCT AGC CGA GGC CAA TG |
| R4AR | CAT TGG CCT CGG CTA GAG GC |
| E8AF | CGA GGC CAA TGC CGG TTT TAC |
| E8AR | GGT AAA ACC GGC ATT GGC C |
| K14AF | ACC TTT GCC GCC AAT ATT GAA TGG |
| K14AR | CCA TTC AAT ATT GGC GGC AAA GG |
| W18AF | GAA TAT TGA AGC CGC CAC GAA AAC C |
| W18AR | GGT TTT CGT GGC GGC TTC AAT ATT C |
| I23AF | ACG AAA ACC GCC CAG TCC ATT G |
| I23AR | CAA TGG ACT GGG CGG TTT TCG T |
| W29AF | CCA TTG TCA ATG CCC TTA CTA GC |
| W29AR | GCT AGT AAG GGC ATT GAC AAT GG |